

嘉南藥理科技大學
環境工程與科學系

碩士論文

五種不同複合式幾丁質吸附劑應用於砷(V)去除
之研究

Assessing Adsorption Performance of As(V) on
Adsorbents Prepared via Embedding Chitosan on
Various Carriers

指導教授：萬孟瑋 老師

共同指導：陳煜斌 老師

研 究 生：黃于亘

中華民國 101 年

嘉南藥理科技大學環境工程與科學系

Department of Environmental Engineering and Science

Chia-Nan University of Pharmacy and Science

碩士論文

Thesis for the Degree of Master

五種不同複合式幾丁質吸附劑應用於砷(V)去除之研究

Assessing Adsorption Performance of As(V) on
Adsorbents Prepared via Embedding Chitosan on Various
Carriers

指導教授(Advisor)：萬孟瑋 (Prof. Meng-Wei Wan)

共同指導(Co Advisor)：陳煜斌 (Prof. I-Pin Chen)

研究生(Master student)：黃于亘 (Yu-Shen Huang)

中華民國 101 年

2012

嘉南藥理科技大學
碩士學位考試委員會審定書

本校環境工程與科學系碩士班_____黃于亘_____君

所提論文不同幾丁聚醣複合式吸附劑應用於砷(V)去除之
研究

合於碩士資格水準，業經本委員會評審認可。

考試委員：_____楊惠玲_____萬連璋_____

_____林秀雄_____陳煜文_____

指導教授：_____萬連璋_____

系主任（所長）：_____余光昌_____

中華民國 101 年 7 月

嘉南藥理科技大學碩士紙本論文授權書

本論文為本人（即著作權人）黃于亘於嘉南藥理科技大學
環境工程研究所 所 100 學年度第 2 學期取得碩士學位之論文。

論文題目：五種不同複合式幾丁質吸附劑應用於砷(V)去除之研究

指導教授： 萬孟瑋

☒ 同意立即開放

■紙本論文延後公開年限

☐一年 ☐二年 ☐三年 ☐四年 ☐五年

■延後公開原因：

☐ 申請專利(申請專利文號: _____)

☐ 準備申請專利

☐其他：

【以上各項延後公開期限，依教育部 97 年 7 月 23 日台高通字第 0970140061 號函文規定，需訂定合理期限，不超過研究生畢業次日起 5 年】

以非專屬、無償授權嘉南藥理科技大學圖書館和國家圖書館。基於推動「資源共享、互惠合作」之理念，於回饋本校與社會作為學術研究目的之用，得不限地域、時間與次數，以紙本、光碟、學位論文全文系統、網路或其他各種方法收錄、重製、與發行，或再授權他人以各種方法重製與利用，以提供讀者基於個人非營利性質之線上檢索、閱覽、下載或列印。

學 號： G9906024

研究生：黃子玉 (親筆簽名)

指導教授： 黃 玉 瑞 (親筆簽名)

中 華 民 國 101 年 07 月 31 日

說明：

- (1) 本授權書請填寫並親筆簽名後，裝訂於各紙本論文封面後之次頁。
- (2) 讀者基於非個人營利性質之線上檢索、閱覽、下載或列印上列論文，應依著作權法有關規定辦理。

Acknowledgements

First, I have to say thanks to my advisor Dr. Meng-Wei Wan who spent two years to teach me lessons in my field and even in life. Also for letting me understand that I have to be serious with my studies and in whatever I do every time. I always have a problem in my studies and I am thankful to Professor who always supports me.

The completion of this dissertation is also thanks to Professor Lin and Professor Yang. They give me many advices which helped in the completion of my thesis.

I also would like to thank my family. They push me a lot to succeed in life and always tell me to look forward to my future. So, I want to make all of you to feel pleased and proud of me.

I would also like to thank Cybelle, Mayzonee, Carlo, Adrian, Gelo and all foreign students for teaching me about my thesis and for helping me improve my English. Thank you for always pushing me when I do not feel good and bothered.

Yu-Shen (Jack) CNU 2012/9/14

Abstract

In recent years, chitosan (β -(1-4)-N-acetyl-D- glucosamine) is a very popular and well known polymer owing to its many advantages, such as biocompatibility, biodegradability, renewability, bioactivity, and non-toxicity. Chitosan is a polysaccharide formed by the deacetylation of chitin, and chitosan is the second most abundant natural polymer, which is obtained from shrimps, crabs, and fungi. Many literatures have indicated that chitosan was excellent in removing heavy metal ions and dyes. However, pure chitosan is very expensive. Lowering the cost of chitosan is recommended in future application. To support chitosan, the usage of different carriers such as bentonite, kaolinite, and quartz sand were applied to reach the goal of this study.

In this experiment, small amount of chitosan was coated on the bentonite, kaolinite and quartz sand to form Chitosan coated bentonite (CCB), Chitosan coated kaolinite (CCK), and Chitosan coated sand (CCS). BET, TGA, and FT/IR analysis were firstly implemented to characterize the adsorbents. Effect of adsorbing time (0.5, 1, 2, 4, 6, 12, 24 hours), initial concentration (50, 100, 500, 1000 ppb), and temperature (25, 35, 45, 55°C) were evaluated. Kinetic studies (pseudo-first order, pseudo-second order, and intraparticle diffusion models),

equilibrium studies (Langmuir, Freundlich, and Dubinin-Radushkavich isotherm), and thermodynamic studies were executed and confirmed the research results.

This research indicates the equilibrium time of different adsorbents at different initial concentrations was about 12 hours. The kinetic study exhibits all adsorbents approximately follow pseudo-second order, with the R^2 ranges as follows: Active Carbon (AC) ($0.9064 < R^2 < 0.9987$), pure chitosan ($0.9213 < R^2 < 0.98$), CCB ($0.9575 < R^2 < 0.9988$), CCK ($0.9916 < R^2 < 0.998$), and CCS ($0.794 < R^2 < 0.9991$). Langmuir isotherm of the different adsorbents has best R^2 ($0.94 \sim 0.99$). The maximum adsorption capacity of adsorbents (AC, pure chitosan, CCB, CCK and CCS) are $11.416 \mu\text{g/g}$, $23.310 \mu\text{g/g}$, $67.114 \mu\text{g/g}$, $68.966 \mu\text{g/g}$, and $16.779 \mu\text{g/g}$ respectively. Moreover, the n of all adsorbents in the Freundlich isotherm are all greater than 1 which verifies that all adsorbents follow physical sorption. Thermodynamic studies determined that AC and pure chitosan are non-spontaneous, CCK and CCB are spontaneous, but the CCB is non-spontaneous at 35°C ; CCS is spontaneous when the temperature is 25°C but becomes non-spontaneous at higher temperatures.

Keyword: Adsorption, As (V), Chitosan, Biopolymer

摘要

近年來，幾丁聚醣(β -(1-4)-N-acetyl-D- glucosamine)是廣泛受到矚目與多元運用的生物聚合物，並且具有：生物相容性、生物降解性、再生性，生物活性及無毒性等特點；此外，幾丁聚醣為幾丁質去乙醯化之多醣體，而幾丁質含量為全球僅此次於纖維素之聚合物，可由蝦蟹及菌類中提煉出；眾多文獻指出：幾丁聚醣對於重金屬離子及染料具有良好的吸附能力。但是，若單純使用幾丁聚醣應用於汙染物之去除，其價格昂貴，不符實場應用之經濟效益，所以，本研究為降低其應用成本，利用了自然界、易取得之不同載體，如：膨潤土、高嶺土及石英砂等，作為幾丁聚醣之吸附載體，使之達到降低成本的目的。

本研究利用少量的幾丁聚醣與膨潤土、高嶺土及石英砂參合，形成：幾丁聚醣固化於膨潤土（CCB）、幾丁聚醣固化於高嶺土（CCK）及幾丁聚醣固化於石英砂（CCS）等吸附劑，對五價砷進行吸附。此外，本研究先以 BET、TGA 及 FT/IR 等分析了解吸附物的特性，並探討在不同反應時間（0.5, 1, 2, 4, 6, 12, 24 小時），不同起始濃度（50, 100, 500, 1000 ppb）及不同溫度下（25, 35, 45, 55°C）各吸附劑之吸附效益；此外，進一步探討動力吸附（pseudo-first order、pseudo-second order and intraparticle diffusion models），等溫吸附（Langmuir、Freundlich 及 Dubinin-Radushkevich）及吸附熱力學

等模式演算。

結果顯示：不同吸附劑皆在 12 小時達到達吸附平衡；在動力吸附方面，所有吸附劑皆遵循擬二階動力模式，各吸附物之 R^2 值依序如下：活性碳（AC）（ $0.9064 < R^2 < 0.9987$ ）、純幾丁聚醣（ $0.9213 < R^2 < 0.98$ ）、CCB（ $0.9575 < R^2 < 0.9988$ ）、CCK（ $0.9916 < R^2 < 0.998$ ）及 CCS（ $0.794 < R^2 < 0.9991$ ）。此外，在等溫吸附方面：各吸附物在 Langmuir 模式下具有較高的 R^2 值（ $0.94 \sim 0.99$ ），而各吸附物的最大吸附能力分別為 AC（ $11.41553 \mu\text{g/g}$ ），純幾丁幾丁聚醣（ $23.31002 \mu\text{g/g}$ ），CCB（ $67.11409 \mu\text{g/g}$ ），CCK（ $68.96552 \mu\text{g/g}$ ）及 CCS（ $16.77852 \mu\text{g/g}$ ）；再者，Freundlich 模式中的 n 值皆大於 1，表示各個吸附劑皆遵循物理吸附。在吸附熱力學方面：活性碳及純幾丁聚醣皆為非自發性反應、CCB 和 CCK 為自發性；但 CCB 在 35°C 時為非自發性，而 CCS 在 25°C 時為自發性隨著溫度的升高轉變成非自發性。

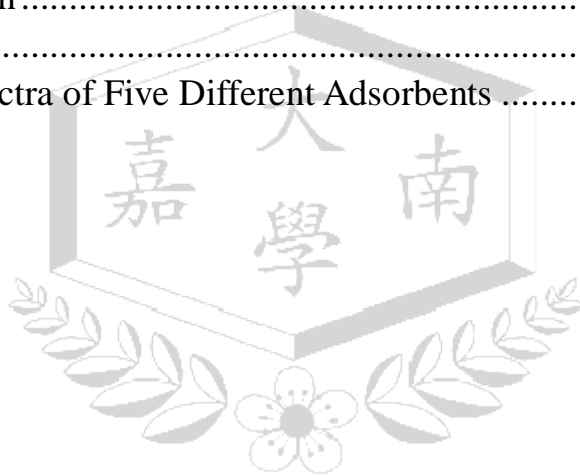
關鍵字：吸附，五價砷，幾丁聚醣，生物聚合物

Contents

Abstract.....	I
摘要	I
Contents	VI
List of Tables.....	VI
List of Figures	VIII
Chapter 1 Introduction	1
1.1 Background of the Study	1
1.2 Significance of the study.....	4
1.3 Objectives.....	5
Chapter 2 Literature Review	7
2.1 Elemental Arsenic Contamination.....	7
2.2 Current Remediation Technologies.....	10
2.3 Adsorption.....	12
2.3.2 Adsorption Mechanism	12
2.3.3 Batch Adsorption Studies - Adsorption Capacity.....	13
2.3.4 Adsorption Kinetic Study	14
2.3.5 Adsorption Isotherm Study.....	16
2.3.6 Adsorption Thermodynamic Study.....	18
2.4 Practical Adsorbents for Heavy Metal Removal from Aqueous Solution.....	19
2.4.1 Chitin and Chitosan.....	19
2.4.2 Modification of chitosan	22
2.4.3 Interaction of pristine chitosan with metal ions	23
2.5 Adsorbent	24
2.5.1 Kaolinite	24
2.5.2 Bentonite.....	26
2.5.3 Sand	28

2.5.4 Activated carbon	30
2.6 Brunauer, Emmett, and Teller Analysis	31
2.7 Thermogravimetric Analysis	31
2.8 Fourier Transform Infrared Analysis	32
2.9 Permeable Reactive Barrier System	33
Chapter 3 Materials and Methods	35
3.1 Experimental Procedure	35
3.2 Chemicals and Reagents	37
3.3 Instrumentation	37
3.4 Preparation of the CCK, CCB and CCS	38
3.5 Preparation of Stock Solutions and Reagents	41
3.5.1 Arsenic (V) Aqueous Solution (Stock Solution)	41
3.5.2 Standard Solutions and Reagents for ICP-OES Analysis	42
3.6 Batch Adsorption Studies	43
3.7 Adsorption kinetic studies	47
3.8 Adsorption isotherm studies	47
3.9 Adsorption thermodynamics study	48
Chapter 4 Results and Discussion	49
4.1 Characteristic analysis of the Adsorbents	49
4.1.1 BET Analysis	49
4.1.2 TGA Analysis	51
4.2 Effect of contact time on adsorption capacity using different adsorbents and concentration	54
4.3 Adsorption Kinetics studies	59
4.3.1 Pseudo- first order model	59
4.3.2 Pseudo-second order model	63

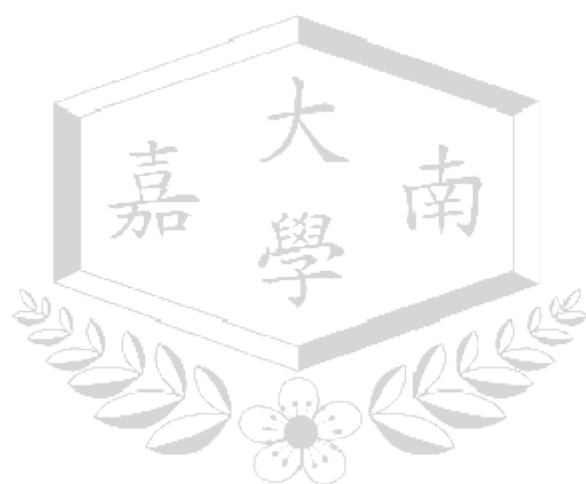
4.3.3 Intraparticle Diffusion Model.....	67
4.3.4 Analysis Summary of Three Kinetic Models	71
4.4 Adsorption isotherm studies.....	72
4.4.1 Freundlich model	73
4.4.2 Langmuir model.....	77
4.4.3 Dubinin-Radushkevich model	83
4.5 Fourier Transformation-Infrared Analysis	87
4.6 Adsorption Thermodynamic studies.....	92
4.7 Adsorption mechanism of As(V) and chitosan	100
Chapter 5 Conclusion	101
References.....	103
Appendix: FTIR spectra of Five Different Adsorbents	110



List of Tables

Table 1. Percentage of Chitin Present in the Bodies of the Crustacean and Insect Species	21
Table 2. Adsorption Capacity of Different Chitosan to Support Material Ratio	38
Table 3. Preliminary Experiment: Effect of Different Adsorbents weight on the Equilibrium Concentration	44
Table 4. BET Analysis of Different Adsorbents	50
Table 5. Equilibrium Adsorption Capacity of Different Initial Concentration using Different Adsorbents.....	58
Table 6. Kinetic Parameters for the Pseudo-first Order Model of Different Adsorbents at Different initial Concentrations.....	62
Table 7. Kinetic Parameters for the Pseudo-second Order Model of Different Adsorbents at Different Initial Concentrations	66
Table 8. Kinetic Constants for the Intraparticle Diffusion Model of Different Adsorbents at Different Initial Concentrations	71
Table 9. Freundlich Constants under Different Adsorbents	76
Table 10. Langmuir Constants under Different Adsorbents	81
Table 11. R_L of Adsorbents from Langmuir Isotherm.....	83
Table 12. Contacts of D-R Model Using Different Adsorbents	86
Table 13. FT/IR of Activated Carbon.....	88
Table 14. FT/IR of Pure Chitosan	89
Table 15. FT/IR of Chitosan Coated on Bentonite	90
Table 16. FT/IR of Chitosan Coated on Kaolinite	91
Table 17. FT/IR of Chitosan Coated on Sand.....	92
Table 18. Thermodynamic of Arsenic Using Different Adsorbents	93

Table 19. Adsorption Capacity of Different Temperature	94
Table 20. Thermodynamic Parameters of the Different Adsorbents Using 500 ppb of As(V) Initial Concentration	99



List of Figures

Figure 1. Potential-pH Diagram for The Arsenic-Water System	2
Figure 2. Skin Diseases Caused By Arsenic.....	7
Figure 3. Arsenic Concentration in Taiwan.....	9
Figure 4. Structures of Cellulose, Chitin And Chitosan.....	22
Figure 5. Chitosan Derived From Chitin.....	23
Figure 6. Structure of Kaolinite	26
Figure 7. Chemical Structure of Bentonite.....	27
Figure 8. Scanning Electron Microscopy image of Sand	29
Figure 9. Illustration of Curved Carbon Fragments, Containing Pentagonal and Heptagonal Rings	30
Figure 10. Curve of (a) Isothermal Thermogravimetry (b) Quasi-Isothermal Thermogravimetry (c) Dynamic Thermogravimetry.....	32
Figure 11. Groundwater Treated by a Permeable Reactive Barrier	34
Figure 12. Experiment Procedure	36
Figure 13. Preparation of Chitosan Coated on Kaolinite	39
Figure 14. Preparation of Chitosan Coated on Bentonite	40
Figure 15. Preparation of Chitosan Coated on Sand.....	41
Figure 16. Batch Adsorption Studies	45
Figure 17. Batch Adsorption Experiment.....	46
Figure 18. TG Analysis of Chitosan Coated on Bentonite.....	52
Figure 19. TG Analysis of Chitosan Coated on Kaolinite	52
Figure 20. TG Analysis of Chitosan Coated on Sand	53

Figure 21. Adsorption Capacity of Activated Carbon.....	55
Figure 22. Adsorption Capacity of Pure Chitosan	55
Figure 23. Adsorption Capacity of Chitosan-Coated Bentonite.....	56
Figure 24. Adsorption Capacity of Chitosan-Coated Kaolinite	56
Figure 25. Adsorption Capacity of Chitosan-Coated Sand	57
Figure 26. Pseudo-First Order Model of Activated Carbon.....	60
Figure 27. Pseudo-first Order Model of Pure Chitosan	60
Figure 28. Pseudo-first Order Model of CCB	61
Figure 29. Pseudo-first Order Model of CCK	61
Figure 30. Pseudo-first Order of CCS	62
Figure 31. Pseudo-second Order Model of Activated Carbon	63
Figure 32. Pseudo-second Order Model of Pure Chitosan.....	64
Figure 33. Pseudo-second Order Model of CCB	64
Figure 34. Pseudo-second Order Model of CCK	65
Figure 35. Pseudo-second Order Model of CCS	65
Figure 36. Intraparticle Diffusion Model of Activated Carbon.....	68
Figure 37. Intraparticle Diffusion Model of Pure Chitosan	68
Figure 38. Intraparticle Diffusion Model of CCB	69
Figure 39. Intraparticle Diffusion Model of CCK	69
Figure 40. Intraparticle Diffusion Model of CCS.....	70
Figure 41. Freundlich Isotherm of Activated Carbon	74
Figure 42. Freundlich Isotherm of Pure Chitosan	74
Figure 43. Freundlich Isotherm of Chitosan-Coated Bentonite	75
Figure 44. Freundlich Isotherm of Chitosan-Coated Kaolinite.....	75
Figure 45. Freundlich Isotherm of Chitosan-Coated Sand	76

Figure 46. Langmuir Isotherm of Activated Carbon.....	78
Figure 47. Langmuir Isotherm of Pure Chitosan.....	79
Figure 48. Langmuir Isotherm of Chitosan -Coated Bentonite.....	79
Figure 49. Langmuir Isotherm of Chitosan-Coated Kaolinite	80
Figure 50. Langmuir Isotherm of Chitosan-Coated Sand	80
Figure 51. Dubinin-Radushkavich Isotherm of Activated Carbon.....	84
Figure 52. Dubinin-Radushkavich Isotherm of Pure Chitosan	84
Figure 53. Dubinin-Radushkavich Isotherm of Chitosan-Coated Bentonite	85
Figure 54. Dubinin-Radushkavich Isotherm of Chitosan-Coated Kaolinite	85
Figure 55. Dubinin-Radushkavich Isotherm of Chitosan-Coated Sand	86
Figure 56. Adsorption Capacity of Activate Carbon	96
Figure 57. Adsorption Capacity of Pure Chitosan.....	96
Figure 58. Adsorption Capacity of Using Chitosan-Coated Kaolinite	97
Figure 59. Adsorption Capacity of Chitosan -Coated Bentonite.....	97
Figure 60. Adsorption Capacity of Chitsan-Coated Sand	98
Figure 61. Thermodynamic Study of the Five Adsorbents	99
Figure 62. Adsorption mechanism of As(V) and chitosan.....	100
Figure 63. FTIR Spectra of AC Before And After Adsorption	110
Figure 64. FTIR Spectra of Pure Chitosan Before And After Adsorption.....	111
Figure 65. FTIR Spectra of CCB Before And After Adsorption.....	112
Figure 66. FTIR Spectra of CCK Before And After Adsorption.....	113
Figure 67. FTIR Spectra of CCS Before And After Adsorption	114

Chapter 1 Introduction

1.1 Background of the Study

Arsenic (As) in the water system mainly comes from mineral dissolution, industrial waste discharges, and use of arsenic pesticides in agriculture (Altundogan, et al., 2001). Arsenic is dangerous for the human health owing to the damage effect of the nervous system, heart, skin, and stomach, which causes cancer and will eventually lead to death (Pontoni and Fabbicino, 2012). Arsenic pollution has been reported recently in the USA, China, Chile, Bangladesh, Taiwan, Mexico, Argentina, Poland, Canada, Hungary, New Zealand, Japan, and India (Mohana, Pittman 2007).

Arsenic contamination in the environment is one of the major problems in the world. The World Health Organization (WHO) set a standard of As as 0.01 mg/L (WHO, 2011). The U.S. Environmental Protection Agency (USEPA) also issued the same standard of arsenic for drinking water (USEPA, 2012).

Arsenic has two types: these are As (III) and As (V). As (III), arsenite, is found to be more toxic than the As (V), arsenate (Goldberg, 2002). The removal of arsenite is more difficult than arsenate, because it has a neutral charge in pH 4

to 10 (Maji, Pal, and Pal, 2007). Arsenites and arsenate would change with respect to pH and E (Lorenzen, van Deventer and Landi, 1995). As shown in Figure 1, arsenate is present as H_2AsO_4^- between the ranges of pH 3 to 6, whilst for natural drinking water with the pH ranging from 6.5 to 7.5, it is present as HAsO_4^{2-} (Gerente, et al., 2010).

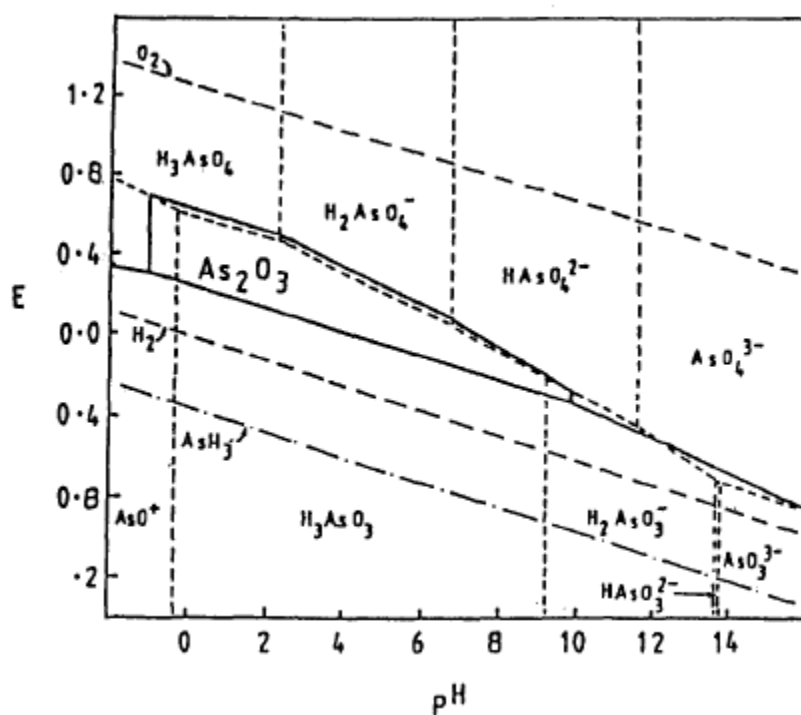


Figure 1. Potential-pH Diagram for The Arsenic-Water System

Removal methods of arsenate includes precipitation/coprecipitation, ion exchange, aeration stripping, coagulation sedimentation granular filtration, lime softening, membrane processes, activated carbon adsorption, biosorbents adsorption, and adsorption onto activated alumina and bauxite (Chang, 2010;

Lorenec et al., 1994; Crittenden et al., 2005). The removal of arsenite by aeration stripping is seen to be of low efficiency (0-20%). Coagulation sedimentation granular media filtration has a high removal rate (90-100%). However, the drawback of this process is that it would be more expensive and would take a longer reaction time. On the other remove technology, removal rate of lime softening ranges from 20-100%. The rate of ion exchange ranges from 90-100%, but this would be more expensive. Moreover, membrane processes have an efficiency removal rate ranging from 20-100%, which are costly and have complicated operations compared to other process. The removal rate of chemical oxidation is from 0-20%. Adsorption could reach almost the same removal rate as the ion exchange, but less cost. (Crittenden et al., 2005) This is the reason that adsorption is chosen as an investigation technology in this study.

This research focuses on the adsorption process using chitosan, a derivative from chitin. Chitin is the second most abundant natural polymer. It is obtained from shrimps, crabs, or fungi (Wan Ngah, Teong, Hanafiah, 2011). Chitosan has many advantages such as biocompatibility, biodegradability, renewability, bioactivity, and non-toxicity (Wan, Kan, Rogel, Dailda, 2009). It also contains amino and hydroxyl groups that can get the heavy metals (Dalida et al., 2011). However, chitosan is very expensive; hence, lowering the cost of chitosan would

be considered. Synthesizing it by adding a different type of carrier materials is thus investigated.

This experiment used chitosan as coating on sand, bentonite, and kaolinite. Clays, such as bentonite and kaolinite, have many anions and cations for ion exchange and adsorption which is advantageous for this study. The anions and cations that are present in the clays are Ca^{2+} , Mg^{2+} , H^+ , NH_4^+ , Na^+ , and SO_4^{2-} , Cl^- , PO_4^{3-} , and NO_3^- . These ions can be interchange with other ions (Bhattacharyya and Gupta, 2008). Sand is also chosen due to the three dimensional structure of the adsorbent (Wan Ngah, Teong, Hanafiah, 2011). This reflects to this study that chose sand, bentonite, and kaolinite to be the supported materials for the chitosan.

1.2 Significance of the study

Arsenic is very toxic for the human health. Taiwan has higher concentration of arsenic in groundwater compared to other countries. People will become sick through the arsenic contamination from surface or subsurface water environment. The arsenic concentration has to be properly monitored. Therefore, this research provided additional information to lower the effect of arsenic in our environment by using the adsorption technology.

Numerous studies of metal ion adsorption by chitosan have been undertaken in recent years, such as the removal of metal ions from aqueous solution but were stalled for their practical application due to certain considerations. Moreover, the procedure of contaminated waste stream remediation would be costly if chitosan were to be used alone. Filters must be constructed along the stream requiring large quantities of material but much lower amounts are needed if chitosan is immobilized on low-cost material. Notably, the overall metal adsorption capacity may not be affected (Wan et al., 2004). Unfortunately, there are limited references to adsorption studies that provide readily available support for chitosan in spite of its inherent practical advantages.

The adsorbents in this study are low cost and can be applied to Permeable Reactive Barrier (PRB) system, where arsenic removal from groundwater, drinking water, and even the waste water can be achieved.

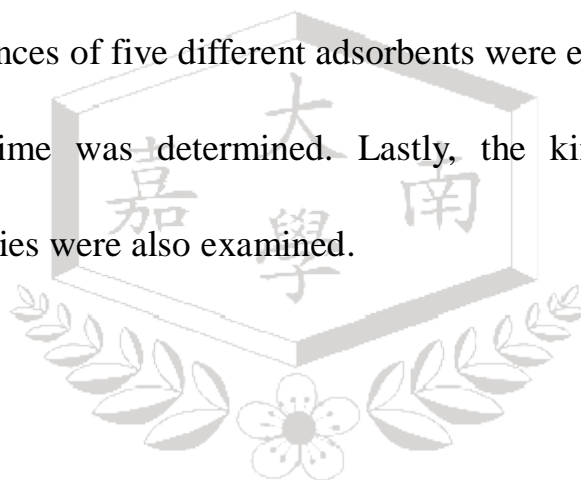
1.3 Objectives

In this context, the utilization of an appropriate immobilization technique is crucial for the success of chitosan in industrial applications. The provision of

physical backing is deemed vital in enhancing metal binding sites' accessibility.

The importance of this study rests on the evaluation of chitosan, activated carbon (AC), chitosan-coated bentonite (CCB), chitosan-coated kaolinite (CCK), and chitosan-coated sand (CCS) in the removal of heavy metals from subsurface water sources. Of note is the adsorption of arsenic (V) ions as adsorbates onto five different adsorbents.

To achieve this, the following specific objectives are determined. First, the adsorptive performances of five different adsorbents were evaluated. Second, the effect of contact time was determined. Lastly, the kinetic, isotherm, and thermodynamic studies were also examined.



Chapter 2 Literature Review

2.1 Elemental Arsenic Contamination

Arsenic pollution is prevalent in China, Vietnam, Nepal, and even in Taiwan. High concentrations of arsenic greatly affect human's health. It can cause cancer of the skin, lung, and bladder. The skin will have pathological changes, such as change of color. The hands and feet will also have keratosis, as seen in figure 2C.

(Ng, Wang, Shraim, 2003)

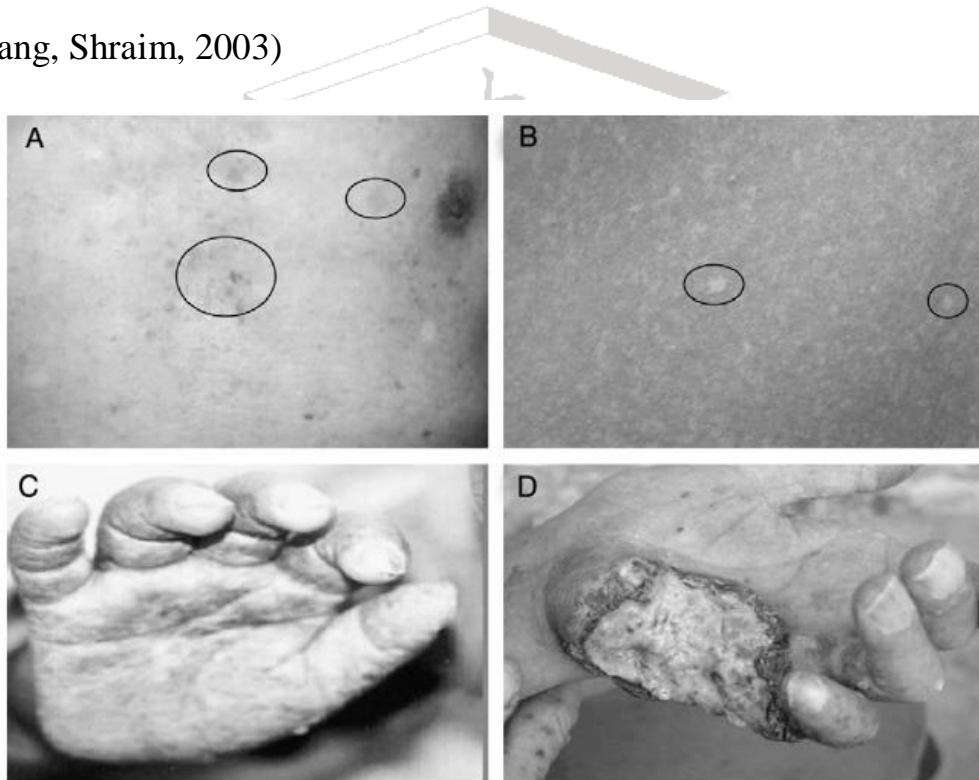


Figure 2. Skin Diseases Caused By Arsenic: (A) Hyperpigmentation, (B)Hypopigmentation, (C)Keratosis, (D)Skin cancer (Ng, Wang, Shraim, 2003)

The World Health Organization (WHO) has set the arsenic standards for drinking water to 0.01 mg/L (Lorenzen, van Deventer and Landi, 1995). US Environmental Protection Agency (USEPA) also issued a new standard of arsenic to 10 ppb in 2001 (USEPA, 2001). A study was conducted in Taiwan regarding arsenic exposure after periods of time. After 5 years of being exposed to As, 76.3% people survived. Within 10 and 15 years, the rate went down to 63.3% and 52.2% respectively (Department of Medicine, National Taiwan University, College of Medicine, Taipei, Taiwan, 1997). These fatality rates show the importance of arsenic removal.

The groundwater in Taiwan has high arsenic concentration. The places with the highest concentration of arsenic are in Yunlin (0.05-0.5 ppm), Tainan (> 0.5 ppm), Kaohsiung (> 0.5 ppm), Ilan (0.05-0.5 ppm), and Ping-tung (0.05-0.5 ppm). Figure 3 shows the groundwater concentration of As(V) in Taiwan, which includes the above mentioned locations. Groundwater has many applications which have the following percentages; agriculture (45%), aquaculture (32%), industry (14%), and tap water (9%), which is almost used to produce food. Arsenic will stay in the food, which will make people sick.

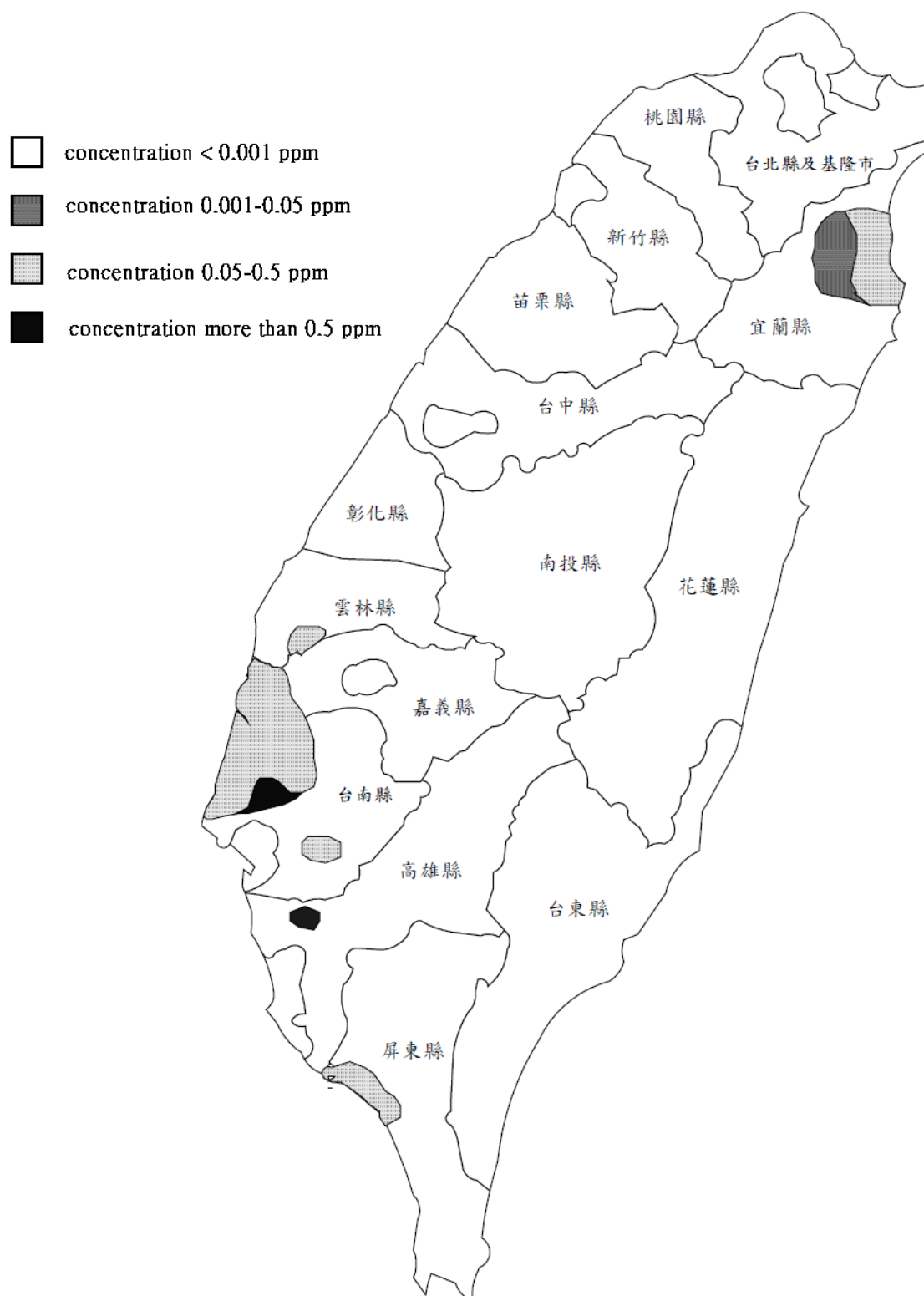


Figure 3. Arsenic Concentration in Taiwan (Lin, et al., 1999)

2.2 Current Remediation Technologies

Several methods of removal of heavy metal in the water and wastewater stream have already been investigated which include reverse osmosis, electrodialysis, ultrafiltration, phytoremediation, ions exchange, chemical precipitation, aeration stripping, lime softening, and adsorption. However, some methods have disadvantages in removing heavy metal from groundwater.

Reverse osmosis is a very effective process in removing both organic and inorganic contaminants. However, it is an expensive process resulted in high capital and operating cost. In electrodialysis, the ions are separated by permeable membranes. During the exchange of electrons between electrodes, the ions pass through the membranes which will leave a dilute concentration of ions on the membrane. This will cause a formation of metal hydroxides, which will clog the membrane. Ultrafiltration process produces sludge which will cause fouling in the membrane while the phytoremediation process has to spend a very long time to remove heavy metal ions. (Ahalya, Ramachandra, Kanamadi 2003) Aeration stripping has poor removal percentages, ion exchange, on the other hand, is expensive and sophisticated, and chemical precipitation yields a large amount of sludge (Bhattacharyya et al., 2008; Crittenden, et al., 2005). The cost and operation are factors to be considered.

The adsorption is a favorable process among the processes mentioned above because it can recycle wastes to become the adsorbents. This lowers the capital cost and helps solve the problem of pollution. Fly ash, chitin, chitosan, agricultural wastes and banana pith are examples of adsorbents from recycled wastes. (Popuri, et al., 2009)

2.3 Adsorption

Adsorption has two types; one is physical adsorption, and the other is chemical adsorption. For the physical adsorption or physisorption, Van der Waals force and dipole-dipole attraction are the ones that usually connect the adsorbate on the adsorbent. Physisorption has the following points: adsorption can be done at low temperature; the heat of adsorption is lower than 10(kcal/mole); the intermolecular forces have Van der Waals; and it can be related to the surface area of the adsorbent. Desorption can be applied for this type of adsorption. Chemical adsorption or chemisorption uses chemical bonds, such as covalent and ionic, in chelating the ions on the adsorbent. Chemisorption requires higher temperatures for easier removal and the heat of adsorption is higher than 10(kcal/mole). The intermolecular structure of the adsorbent and adsorbate have chemical bonds, hence; desorption cannot be applied.

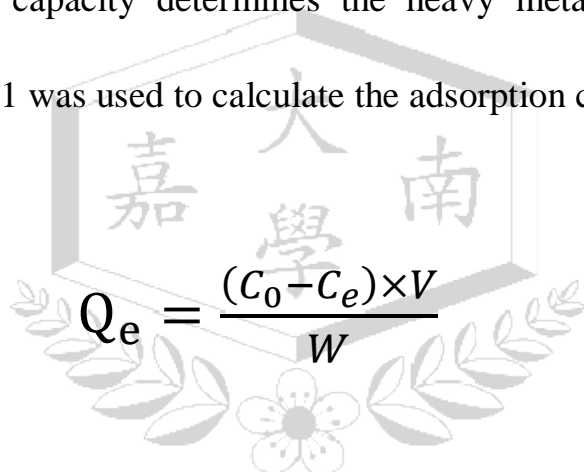
2.3.2 Adsorption Mechanism

Chitosan contain hydroxyl groups (-OH), and amino groups (-NH₂), that have the ability to bind the heavy metal ions. On the other hand, activated carbon has the -OH_x to bind the ions. Clay has anions and cations to do the ion

exchange. The anions are used by chitosan to coat the clay which gives chitosan more active sites. This will increase the number of amino and hydroxyl groups for adsorption. Using clay to immobilize the chitosan will also lower the cost of the adsorbent.

2.3.3 Batch Adsorption Studies - Adsorption Capacity

The adsorption capacity determines the heavy metal ion uptake of the adsorbent. Equation 1 was used to calculate the adsorption capacity.



$$Q_e = \frac{(C_0 - C_e) \times V}{W} \quad (\text{eq1.})$$

where Q_e is the adsorption capacity at equilibrium ($\mu\text{g/g}$), C_0 is the initial concentration of solution ($\mu\text{g/L}$), C_e is the equilibrium concentration ($\mu\text{g/L}$), V is the volume of the metal solution in milliliters, and the W is the weight of adsorbent in grams (Futalan, et al., 2010).

2.3.4 Adsorption Kinetic Study

The kinetic study determines the rate-determining step of the adsorption process, which usually follows the slowest reaction. This will tell if the physical or chemical reaction is the slowest step by finding the kinetic model that has the best fit. Kinetic study usually applies the following models: pseudo-first order, pseudo-second order, and intraparticle diffusion. The rate determining step in the pseudo-first model is physisorption, chemisorption is for the pseudo-second order and mass transfer for the intraparticle diffusion. It uses different contact times to calculate for the rate determining step of the adsorption process.

2.3.4.1 Pseudo-First Order

Pseudo-first order will indicate that the slowest step is the physical adsorption. Equation 2 was used for the pseudo-first order (Futalan, et al., 2010).

$$\log(Q_e - Q_t) = \log Q_e - \frac{k_1 t}{2.303} \quad (\text{eq2.})$$

where Q_t is the adsorption capacity of the adsorbent at a given contact time($\mu\text{g/g}$), k_1 is pseudo-first order kinetic constant(hour^{-1}), and t is the

time(hours) (Futalan, et al., 2010).

2.3.4.2 Pseudo-Second Order

For the pseudo-second order, it will indicate that the rate-determining step is the chemisorption. For the pseudo-second order, equation 3 was applied.

$$\frac{t}{Q_t} = \frac{1}{k_2 Q_e^2} + \frac{t}{Q_e} \quad (\text{eq3.})$$

where k_2 is pseudo-second order kinetic constant(hour^{-1}) (Futalan, et al., 2010).

2.3.4.3 Intraparticle Diffusion

In intraparticle diffusion, the rate of ions going inside the adsorbent is the slowest step. This diffusion model utilizes equation 4;

$$Q_t = k_i t^{0.5} + C_i \quad (\text{eq4.})$$

where k_i is the rate of intraparticle diffusion controlled sorption($\mu\text{g g}^{-1}\text{hour}^{-1.5}$) while C_i is the thickness of the boundary layer (Futalan, et al., 2010). Boundary layer refers to the layer of fluid adjacent to a physical boundary in which the

fluid motion is significantly affected by the boundary and has a mean velocity less than the free stream value.

2.3.5 Adsorption Isotherm Study

This study applied three of isotherm models: Langmuir, Freundlich, and Dubinin-Radushkevich. Isotherm uses either different concentration or the different mass of the adsorbent.

2.3.5.1 Langmuir isotherm Model

Langmuir assumes that only one functional group is used to bundle the heavy metal ions (Futalan, et al., 2010). Langmuir model utilizes the following equation,

$$\frac{1}{Q_e} = \frac{1}{q_{mL}} + \frac{1}{bq_{mL}C_e} \quad (\text{eq5.})$$

where the q_{mL} is the maximum sorption capacity ($\mu\text{g/g}$) while b corresponds to the affinity of the heavy metals to the binding sites on the adsorbent.

$$R_L = \frac{1}{1+bC_0} \quad (\text{eq6.})$$

where the R_L is the dimensionless separation factor.

2.3.5.2 Freundlich Isotherm Model

The Freundlich uses two or more functional group to catch the heavy metal ions. Equation 7 describes the Freundlich model. (Futalan, et al., 2010)

$$\log Q_e = \log K_F + \frac{1}{n} \log C_e \quad (\text{eq7.})$$

where K_F is the maximum adsorption capacity of the heavy metal , and $1/n$ is the intensity of metal ions on the adsorbent .

2.3.5.3 Dubinin-Radushkevich Model

Dubinin-Radushkevich model will determine if the adsorption is chemical or physical in the nature. The D-R model is illustrated by equation 8 (Futalan, et al., 2010).

$$\ln Q_e = \ln q_m - \beta \varepsilon^2 \quad (\text{eq8.})$$

where q_m is the maximum adsorption capacity ($\mu\text{g/g}$), β is the D-R constant (mol^2/kJ^2), and the ε is the Polanyi potential. The Polanyi potential formula is shown in equation 9.

$$\varepsilon = RT \ln \left[1 + \frac{1}{C_e} \right] \quad (\text{eq9.})$$

where R is the universal gas constant (kJ/mol-K), and T is the absolute temperature (K) (Futalan, et al., 2010).

The mean energy can be calculated by equation 10, the E value mean physical adsorption ($E < 8 \text{ kJ/mol}$), ion-exchange mechanism ($8 \text{ kJ/mol} < E < 16 \text{ kJ/mol}$) or chemisorption ($E > 16 \text{ kJ/mol}$) (Futalan, et al., 2010).

$$E = (-2\beta)^{-\frac{1}{2}} \quad (\text{eq10.})$$

2.3.6 Adsorption Thermodynamic Study

Thermodynamic study uses different temperatures to compute for the Gibbs

free energy, enthalpy, and entropy of the adsorption process. The following equations were used for the calculation of the data (Futalan, et al., 2010).

$$K_C = \frac{C_{ads}}{C_e} \quad (\text{eq11.})$$

$$\Delta G^\circ = -RT \ln K_F \quad (\text{eq12.})$$

$$\ln K_F = \frac{\Delta S^\circ}{R} - \frac{\Delta H^\circ}{RT} \quad (\text{eq13.})$$

where K_C is the equilibrium constant, C_{ads} is the amount of metal adsorbed at a time, and T is the absolute temperature of the solution (K).

2.4 Practical Adsorbents for Heavy Metal Removal from Aqueous Solution

2.4.1 Chitin and Chitosan

In recent years, chitin and chitosan are getting more popular in research as adsorbents. This is because both are effective in removing heavy metal ions and they have a large number of anion groups to initiate an exchange of ions and chelation.

Chitin is a natural biopolymer, which is the second most abundant in the

world after cellulose. It is a polysaccharide (β -(1-4)-N-acetyl-D- glucosamine) and can be found in crab or shrimp shells and fungal mycelia. Table 1 shows the percentage of chitin found in some species, specifically crustaceans and insects.

Chitosan is the deacetylated form of chitin. High concentrations of acid and high temperature are used in the deacetylation of chitin to form chitosan. Figure 4 shows the chemical structures of cellulose, chitin, and chitosan. (Majeti, and Kumar, 2000; Rinaudo, 2006)

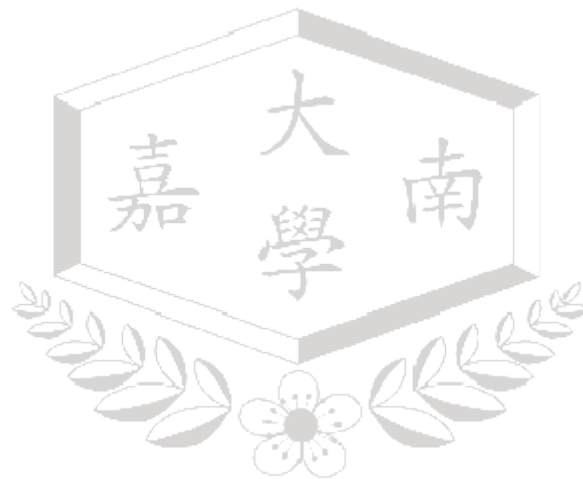
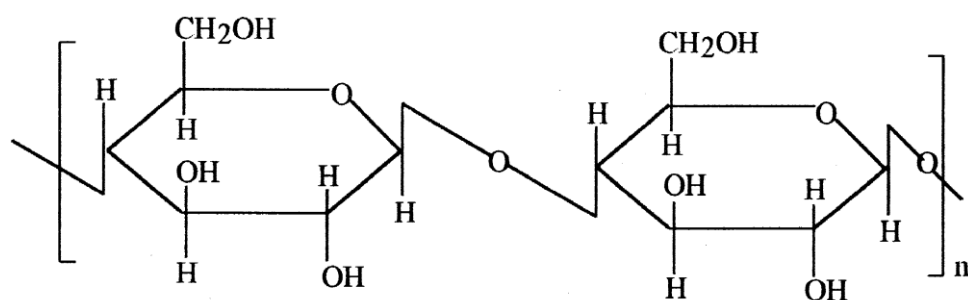


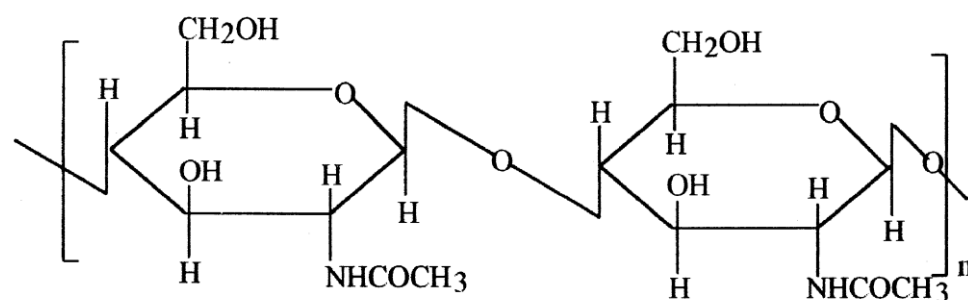
Table 1.Percentage of Chitin Present in the Bodies of the Crustacean and Insect Species

Species	% chitin	Species	% chitin
Crab	72.1 ^(c)	Tulfur fly	64 ^(c)
King Crab	35 ^(b)	Silkworm	44.2 ^(c)
Blue Crab	14 ^(a)	Wax worm	33.7 ^(c)
Red Crab	1.3-1.8 ^(b)	Krill	40-52
Shrimp	5.8 ^(b)	Squid	41
Alaskan shrimp	28 ^(d)	Oyster	3.6
Lobster	69.8 ^(c)	Clam	6.1
Lepas	58.3 ^(c)	<i>Aspergillus niger</i>	42.0 ^(e)
Cockroach	35 ^(c) 10 ^(b)	<i>Penicillium notatum</i>	18.5 ^(e)
Beetle	5-15 ^(b) 27-35 ^(c)	<i>Penicillium chrysoge</i>	20.1 ^(e)
May beetle	31.3 ^(c)	<i>Saccharomy cerevisiae</i>	2.9 ^(e)
True fly	54.8 ^(c)	<i>Lactarius vellereus</i> (mushrooms)	19.0 ^(e)

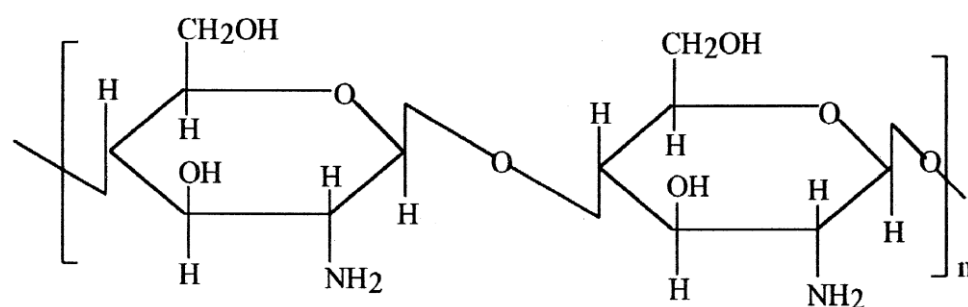
(a)wet body weight (b)dry body weight (c)organ weight of cuticle (d)total dry weight of cuticle (e)dry weight of the cell wall



Cellulose



Chitin



Chitosan

Figure 4. Structures of Cellulose, Chitin And Chitosan (Majeti N.V. Ravi Kumar, 2000)

2.4.2 Modification of chitosan

The organic material has the following advantages: hardness, high strength, and high rigidity. Chitosan has toughness, which makes it easier to modify to

make a chitosan composite. The new adsorbents can retain all the advantageous properties of chitosan and the organic material.

Chitosan can be dissolved in dilute acid such as HNO_3 , HCl , and H_3PO_4 . Figure 5 shows the derivation of chitin to chitosan. (Wan, et al., 2010; Kumar, 2000) Using pure chitosan as the adsorbent is expensive, hence; different types of material are investigated to support chitosan. The adsorbent will become low-cost but, the removal will have no significant change (Wan, Petrisor, Lai, Kim, Yen, 2004).

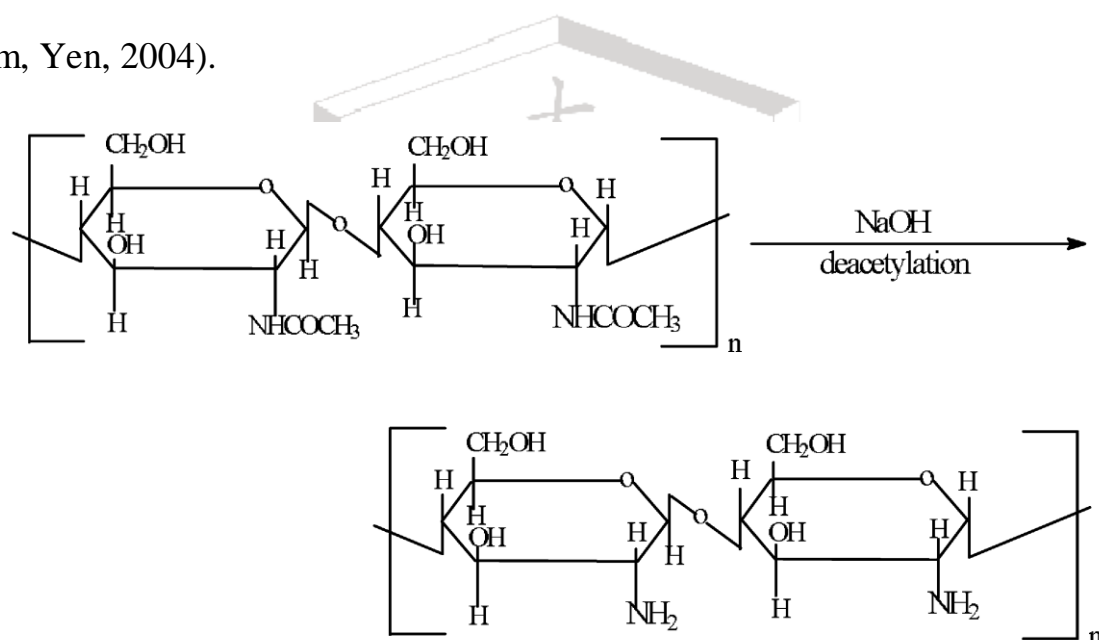


Figure 5. Chitosan Derived From Chitin (Kumar, 2000)

2.4.3 Interaction of pristine chitosan with metal ions

In removing heavy metal ions, chitosan has a relevant class of deacetylation, physical state, specific solution pH, adsorption contact time, and temperature.

The type of metal to be removed is also important. Chitosan have the following functional groups: hydroxyl group (-OH) and amino group (-NH₂). They have the ability to adsorb heavy metal ions such as copper, lead, gold, chromium, and cadmium (Futalan, et al., 2010; Wan, et al., 2004).

2.5 Adsorbent

Clay has a great heavy metal removal percentage due to their high thermal stability, high surface area, and intrinsic catalytic activity that can perform ion exchange or adsorption. These properties give more active sites for adsorption. Clay has many anions and cations on the surface such as SO₄²⁻, Cl⁻, PO₄³⁻, NO₃⁻, and Ca²⁺, Mg²⁺, H⁺, K⁺, NH₄⁺, Na⁺. These ions can be exchange with heavy metal ions or dyes (Bhattacharyya, Gupta, 2008).

2.5.1 Kaolinite

2.5.1.1 Physical nature and chemical structure of kaolinite

Clay, have two categories: one crystal structure has the 1:1 ratio of Al³⁺ octahedral sheet to Si⁴⁺ sheets, and the other is 2:1 (Hizal, Apak, 2005). Kaolinite is a 1:1 aluminosilicate which consists of SiO₂, Al₂O₃, and H₂O.

Figure 6 shows the chemical structure of kaolinite. (Goswami, et al., 2009; Bhattacharyya, et al., 2008) It is the most abundant among the phyllo minerals and it can be obtained from highly weathered soils. (Alkan, et al., 2007) Several studies have been made that kaolinite can adsorb the heavy metal ions from solution. (Lalithambika, 1998) X-Ray absorption spectroscopy confirmed the presence of cobalt ions on the surface of kaolinite (O'Day, 1994).

2.5.1.2 Chitosan- Kaolinite composite

Chitosan coated on kaolinite is one of the low cost adsorbents which have good adsorption capacity. Kaolinite has some anions on its surface, which makes it easier for positively-charged chitosan to coat. This makes it easier to immobilize chitosan. (Zhu et al., 2010)

Several studies used chitosan immobilized on the kaolinite in removing heavy metal ions and dyes, such as methyl orange, from aqueous solutions. (Ngah, et al., 2010) Since the composite beads have many pores and pleats on the surface, it can provide many active sites for the dye adsorption.

2.5.2 Bentonite

2.5.2.1 Physical nature and chemical structure of bentonite

Bentonite is a 2:1 type of aluminosilicate, shown as figure 7. It consists of one Al^{3+} octahedral sheet between two Si^{4+} sheets, which is composed of SiO_2 , Al_2O_3 , CaO , MgO , Fe_2O_3 , Na_2O , and K_2O . (Nghah, et al., 2010)

The cations Al^{3+} and Si^{4+} can be easily exchanged with Mg^{2+} , Fe^{2+} and Al^{3+} , respectively. This will get more negative charge which can get more ions to exchange in the adsorbent.

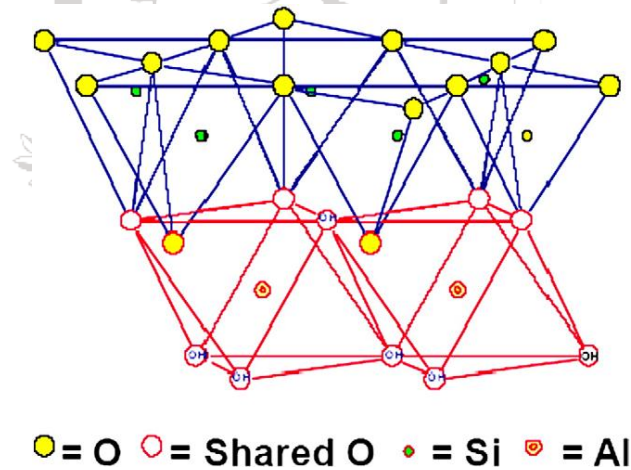


Figure 6. Structure of Kaolinite

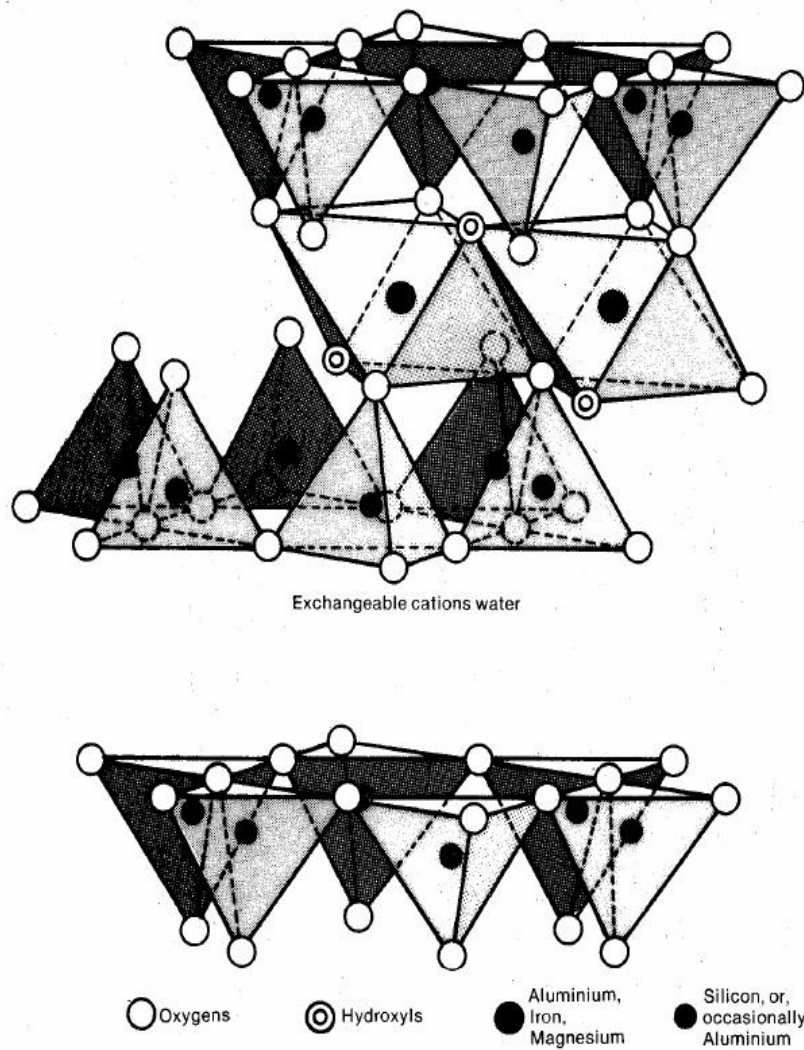


Figure 7. Chemical Structure of Bentonite

(<http://www.scribd.com/doc/55716739/2/Structure-and-Properties-of-Bentonite>, 2012)

2.5.2.2 Chitosan- Bentonite composite

Studies have been done to provide a proper and inexpensive material to support chitosan. Chitosan immobilized on bentonite is one of the cheaper adsorbents that have high adsorption capacity of heavy metal ions. (Grisdanurak et al., 2011)

Chitosan-bentonite composite is a favorable adsorbent in removing heavy

metal ions, such as mercury (Yan, Chen, 2007), copper, lead, and nickel (Futalan, et al., 2010). It can also remove the dyes such as tartrazine (Nghah, et al., 2010). Tartrazine molecules have negative charges while clay usually has positive charges. This would result to the attraction between the dye and the adsorbent.

2.5.3 Sand

2.5.3.1 Physical nature and chemical structure of sand

There are two kinds of sand that are usually used, one is the silica sand and other is local beach sand (Pan, Chen, Anderson, 2011). Sand comes from sandstone and quartzite and has a particle size range of up to 2 mm. Sand has some advantages such as hardness, chemical and heat resistant as well as low price (Sundararajan, et al., 2009). The three dimensional structure of sand makes it easier for chitosan to coat its surface (Nghah, et al., 2010). Figure 8 shows the physical surface of the sand. It can be seen that it has more holes and folds on its surface, which can provide more active sites to catch the heavy metal ions or dyes.

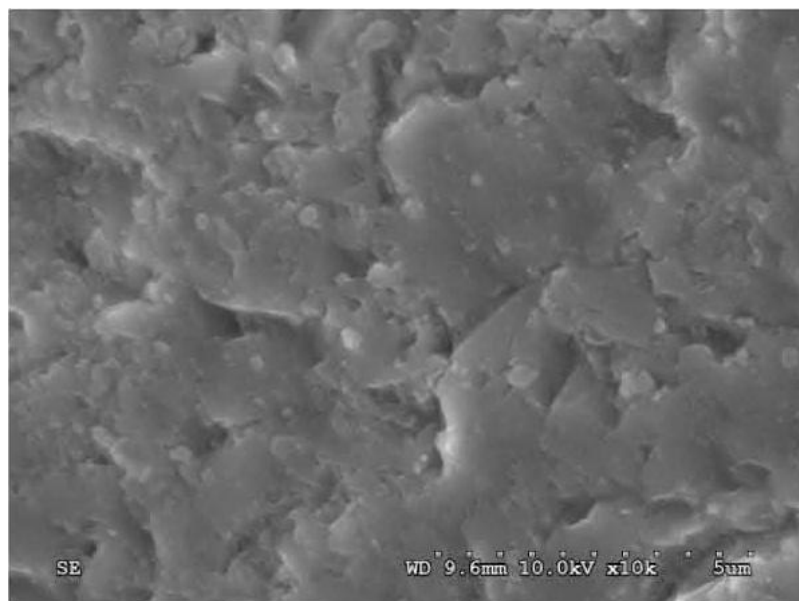


Figure 8. Scanning Electron Microscopy image of Sand

2.5.3.2 Chitosan- Sand composite

The sand can support structure of the chitosan; however, the adsorption capacity will be decreased (Nghah, et al., 2010). This is caused by the neutral charge of sand which makes it difficult for the positively-charged chitosan to coat. Consequently, very few chitosan will coat on the sand, thus, reducing the functional groups, which also decreases the adsorption capacity.

From literature, removal of heavy metal ions by chitosan coated on sand was already investigated such as copper (Wan et al., 2003) and lead (Wan et al., 2010). Sand is coarser than clay, hence; it does not easily disperse in the acidic solution.

2.5.4 Activated carbon

2.5.4.1 Physical nature and chemical structure of activated carbon

Activated carbon has a high surface area. It is usually used to treat air and water. (Liou, 2009) Activated carbon is low cost and can also remove pollutants: organic, such as surfactant and phenol from drinking water (Hong et al., 2008); and inorganic, modification of AC to treat the heavy metal is an example. The structure of activated carbon was illustrated and shown in figure 9. (Harris, Liu, Suenaga, 2008)

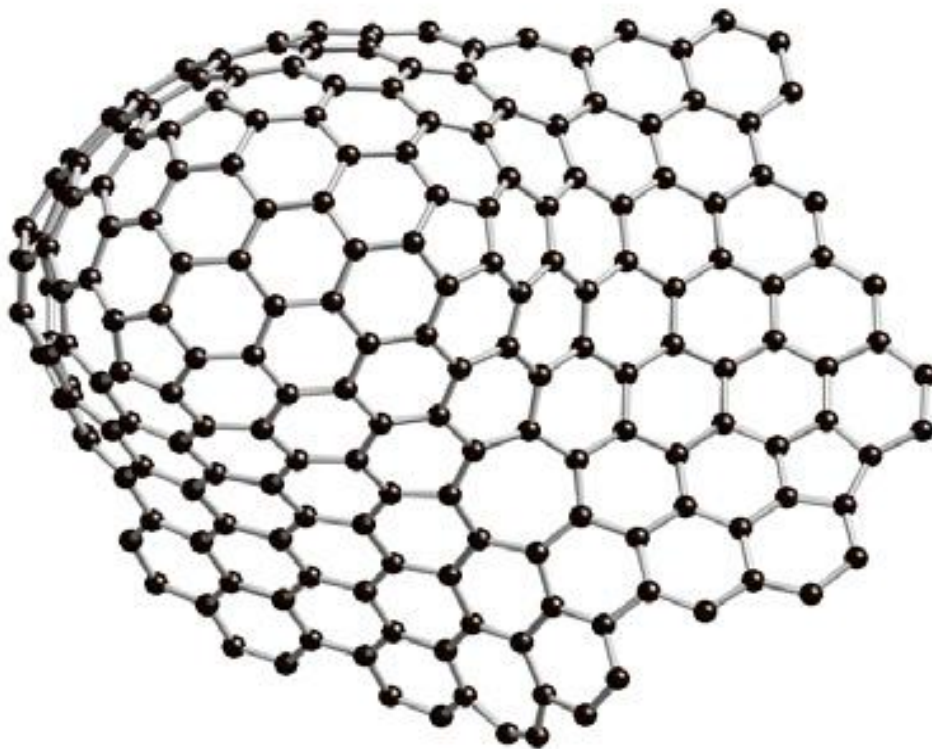


Figure 9. Illustration of Curved Carbon Fragments, Containing Pentagonal and Heptagonal Rings (Harris, Liu, Suenaga, 2008)

2.6 Brunauer, Emmett, and Teller Analysis

The Brunauer, Emmett, and Teller (BET) analysis can measure the surface area and pore size of the materials. This is important in the adsorption process, because the specific surface area of the adsorbent affects its adsorption capacity. The principle behind BET analysis is to use the same temperature to determine the adsorption quantity at relative pressure of gas and apply the BET equation to calculate the specific surface area.

2.7 Thermogravimetric Analysis

The thermogravimetric analysis has three kinds of analyses, such as isothermal thermogravimetry, quasi-isothermal thermogravimetry and dynamic thermogravimetry. These types of curves are shown in Fig 10.

TGA can give the following results: thermal stability, material life, inferior solution kinetics, oxidation stability, moisture, and percentage of volatile matter.

The thermogravimetric analysis (TGA) is used to determine the percentage of chitosan that was immobilized on the material which will lead to understanding the adsorption capacity of the adsorbent. It will also tell up to what degree the adsorbent can be safe. The principle of this method is to use

different temperature to determine the weight change of the material.

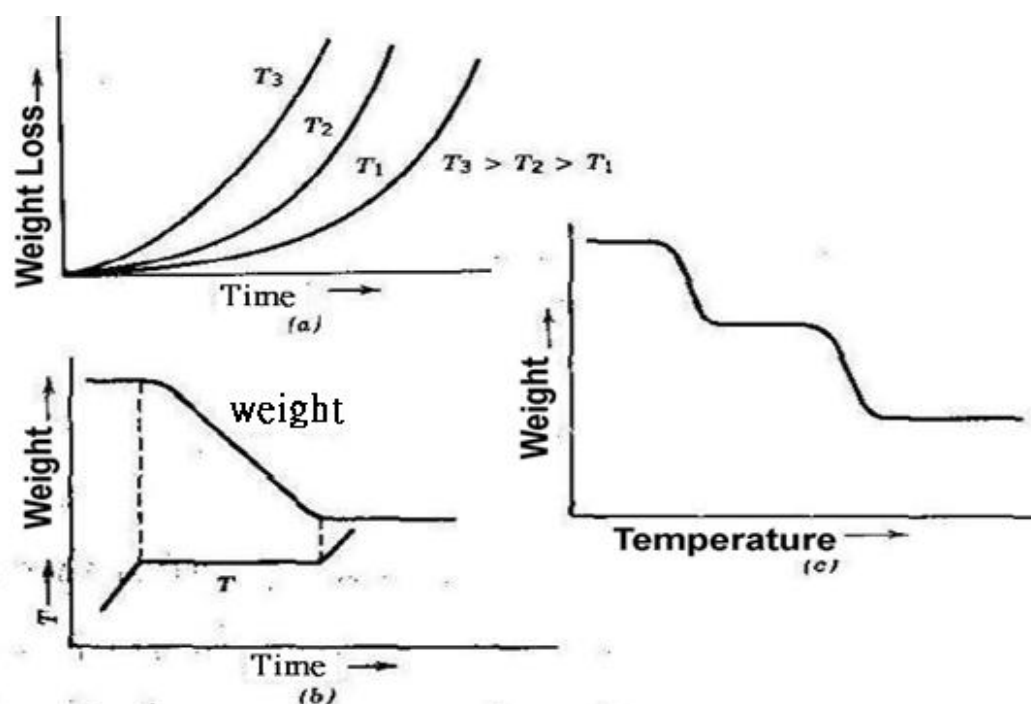


Figure 10. Curve of (a) Isothermal Thermogravimetry (b) Quasi-Isothermal Thermogravimetry (c) Dynamic Thermogravimetry

2.8 Fourier Transform Infrared Analysis

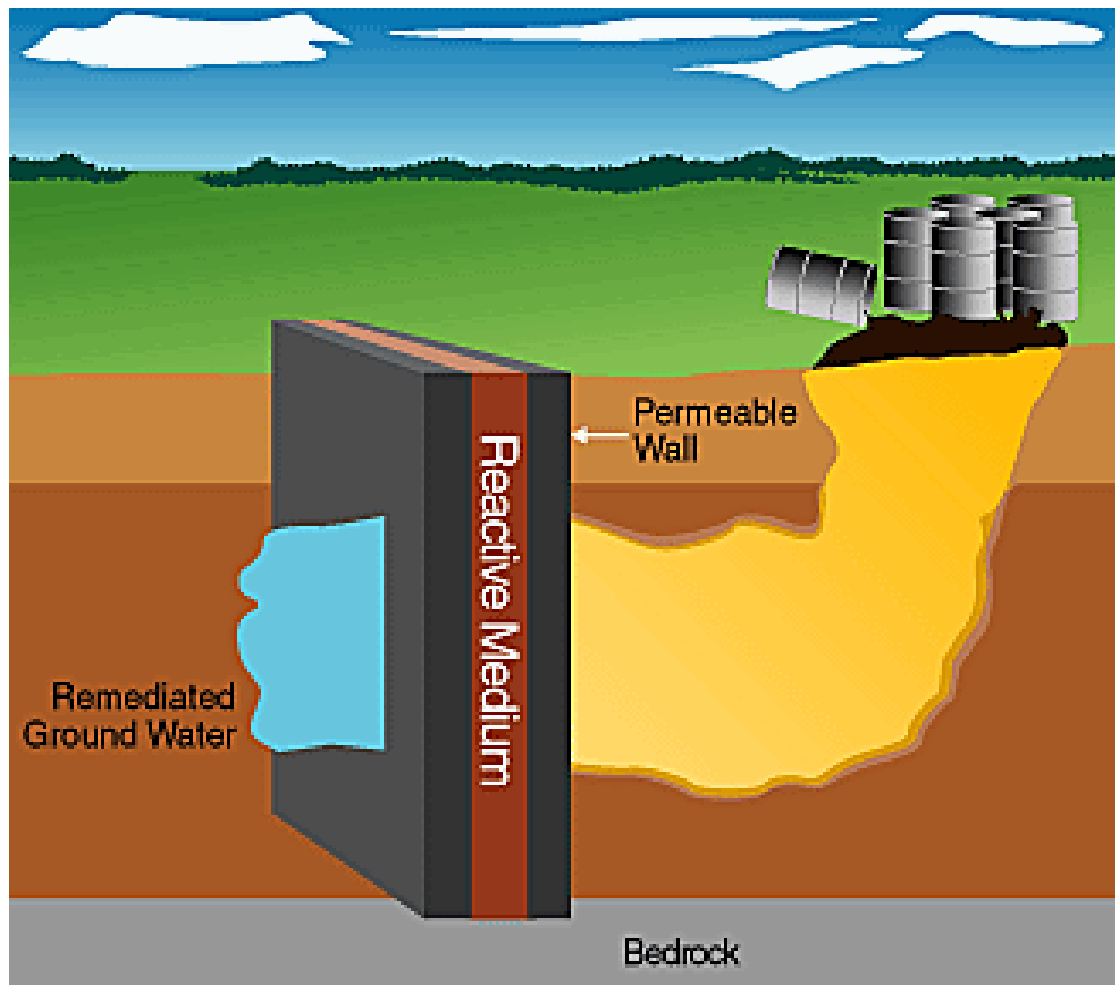
Infrared (IR) is just like a human's fingerprint; every material has a different spectrum. Fourier Transform Infrared (FT/IR) can provide the following information: it can identify the unknown material, determine the quality or consistency of the material, and amount of components in a mixture.

Fourier Transform Infrared Rays Spectrometer (FT/IR) can analyze gas, solutions and soil. In this research, FT/IR can verify what functional groups on the adsorbents attract the arsenate ions whether the -NH_2 groups or -OH groups. The principle behind FT/IR is to expose the flattened material to various infrared radiations and get the IR spectrum to identify the peaks.

2.9 Permeable Reactive Barrier System

Permeable reactive barrier (PRB) is one of the most promising technologies due to its many advantages which includes low operation costs, low maintenance, and low on-going energy requirements. Figure 11 shows how the treatment is done.

In Korea, PRB is used to treat the groundwater from ammonium and heavy metals. The process made use of adsorbents that was put at the subsurface path of a plume of contaminated groundwater. The adsorbent used was zeolite, because zeolite has many ions such as NH_4^+ , Pb^{2+} , Cd^{2+} , Zn^{2+} , and Cu^{2+} . Clay also has several ions, for instance, SO_4^{2-} , Cl^- , PO_4^{3-} , NO_3^- , and Ca^{2+} , Mg^{2+} , H^+ , K^+ , NH_4^+ , Na^+ . Zeolite can be replaced by clay composites as the adsorbent for the PRB.



Permeable reactive barriers have the potential to lower the cost and increase the effectiveness of groundwater cleanup.

Figure 11. Groundwater Treated by a Permeable Reactive Barrier

Chapter 3 Materials and Methods

3.1 Experimental Procedure

This study examines the removal of arsenic (V) ions from aqueous solution using chitosan, activated carbon (AC), chitosan-coated bentonite (CCB), chitosan-coated kaolinite (CCK), and chitosan-coated sand (CCS) beads. The different beads were characterized using BET surface area analysis, TGA and FTIR analysis.

Effect of different contact times (0.5, 1, 2, 4, 6, 12, 24 hours), initial As(V) concentrations (50, 100, 500, 1000 ppb) and different temperatures (25, 35, 45, 55°C) were evaluated. Kinetic studies (pseudo-first order, pseudo-second order, and intraparticle diffusion models), equilibrium studies (Langmuir, Freundlich, and Dubinin-Radushkevich isotherm), and thermodynamic studies were executed and confirmed the research results. The experimental procedures are shown as figure 12.

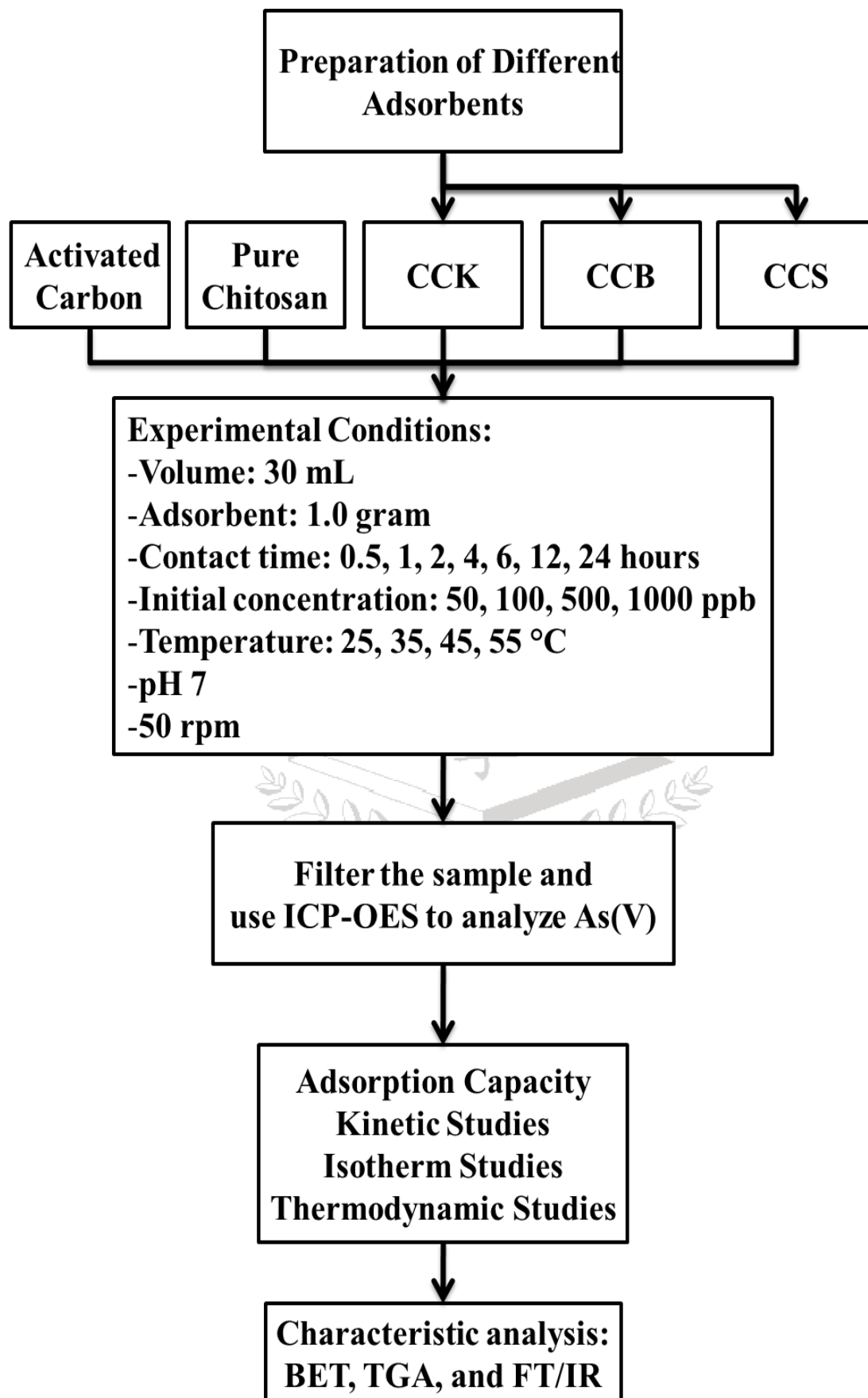


Figure 12.Experiment Procedure

3.2 Chemicals and Reagents

The low molecular weight chitosan with 75%-85% deacetylation, bentonite, and kaolinite are purchased from Sigma-Aldrich, the sand was acquired from Aquatek, and the activated carbon was procured from Taiwan Active Carbon Ind. The chemicals used were hydrochloric acid (37% fuming) from Merck Germany, and NaOH pellets from Formosoda-F. For the aqueous solution, the chemical used was *di*-sodium hydrogen arsenate 7-hydrate ($\text{Na}_2\text{HAsO}_4 \cdot 7\text{H}_2\text{O}$) from Panreac. The KI and Vitamin C which were used for the analysis were purchased from Merck Germany and Fisher Chemical respectively.

3.3 Instrumentation

Model no. 6011 pH meter and Model no. 6041 ORP meter were used to measure the pH and ORP of the aqueous solution. The adsorbents were dried in the Channel Oven (DV452), while the reciprocal shaker bath (YIH-DER BT-350) was used for the batch studies. For the analysis of arsenic, the ICP-OES Perkin Elmer Optima 2000DV was used. The BET analysis used ASAP 2010. The FTIR spectra of adsorbents were acquired using JASCO FT/IR-410 analysis.

3.4 Preparation of the CCK, CCB and CCS

In this experiment, 5 grams of chitosan and 100 grams of material were used for the adsorbent with a particle size of 0.5mm to 0.71mm. In the previous study (Kan et al., 2008), it used 100:2, 100:4, and 100:6 of sand is to chitosan ratio in removing the heavy metal ions. The adsorption capacity at 4 grams of chitosan is 6.66 mg/g which is about 88.82% removal of copper ions while 6 grams can remove 99.24% with a capacity of 7.44 mg/g. The adsorption capacities are shown in table 2, it can be concluded that using 5g chitosan and 100g of immobilization material is enough to remove the heavy metal ions. The particle size used was 0.5mm to 0.71mm since the size used for sand to support chitosan during the adsorption process has the best adsorption capacity (Wan, Kan, Rogel, Dalida, 2010).

Table 2. Adsorption Capacity of Different Chitosan to Support Material Ratio (adsorbent use 2g, concentration 500 mg/L, temperature 25 °C)

Adsorbents (chitosan:material)	Adsorption capacity (mg/g)
2:100	5.60
4:100	6.66
6:100	7.44

In this study, 5 grams of chitosan was dissolved in 300 ml of 5%(v/v) of hydrochloric acid for 2 hours at 300 rpm in room temperature. 100 grams of the

carrier (sand, bentonite, or kaolinite) was added and mixed for 3 hours. After mixing, 1N NaOH was added until the solution pH neutralized. NaOH will react with HCl producing H₂O (excess water). The excess water was filtered out after neutralization. The adsorbent was then oven dried at 105°C for 24 hours. After drying, it was ground and sieved to achieve the particle size range of 0.50mm to 0.71mm for the batch studies. Figure 13, 14, and 15 shows the flowchart of the procedure on the preparation of the adsorbents.

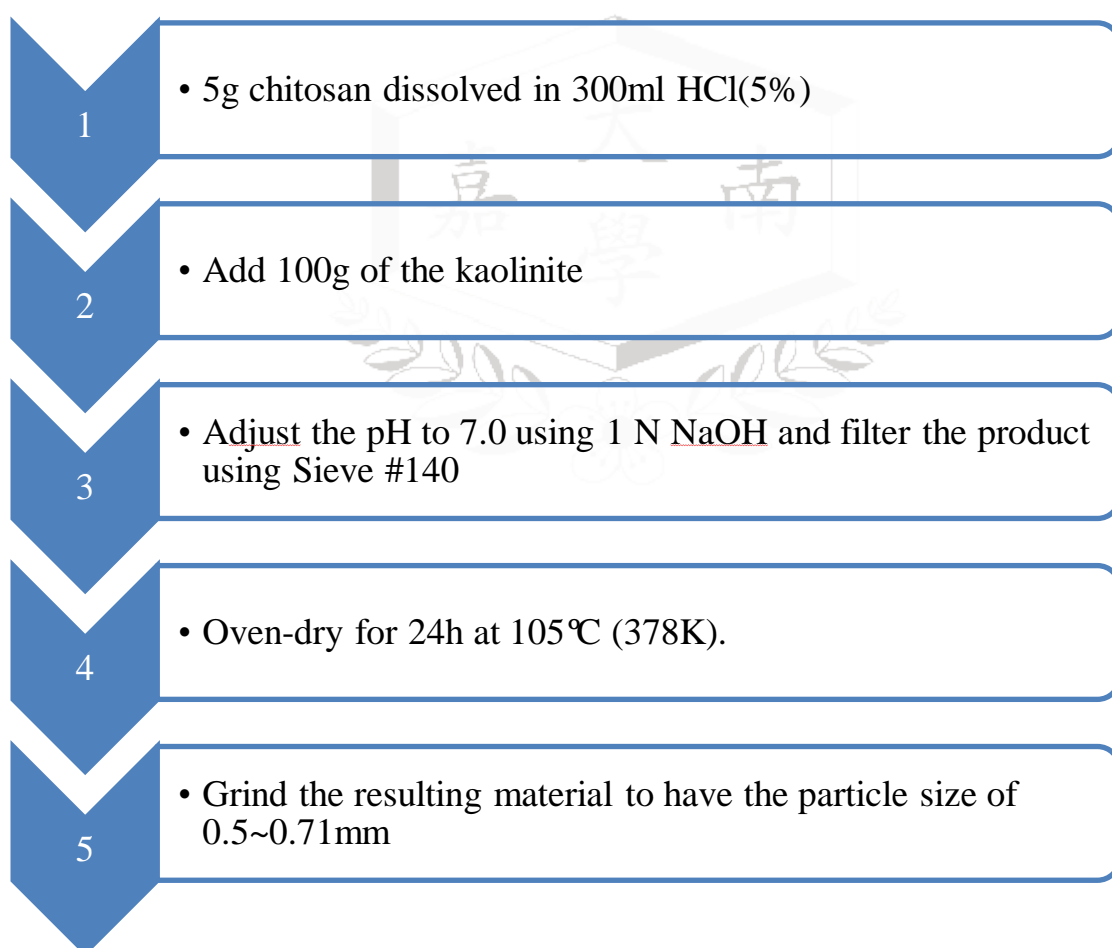


Figure 13. Preparation of Chitosan Coated on Kaolinite

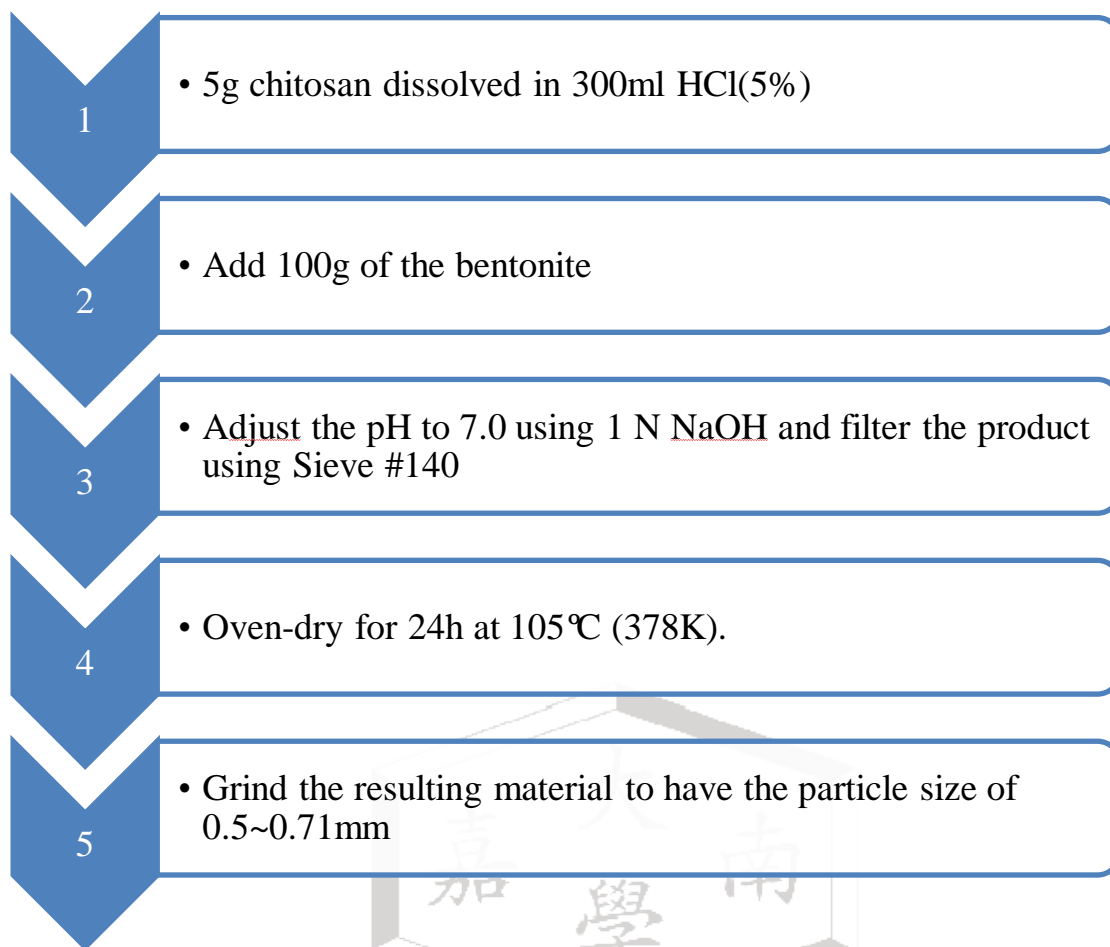


Figure 14. Preparation of Chitosan Coated on Bentonite

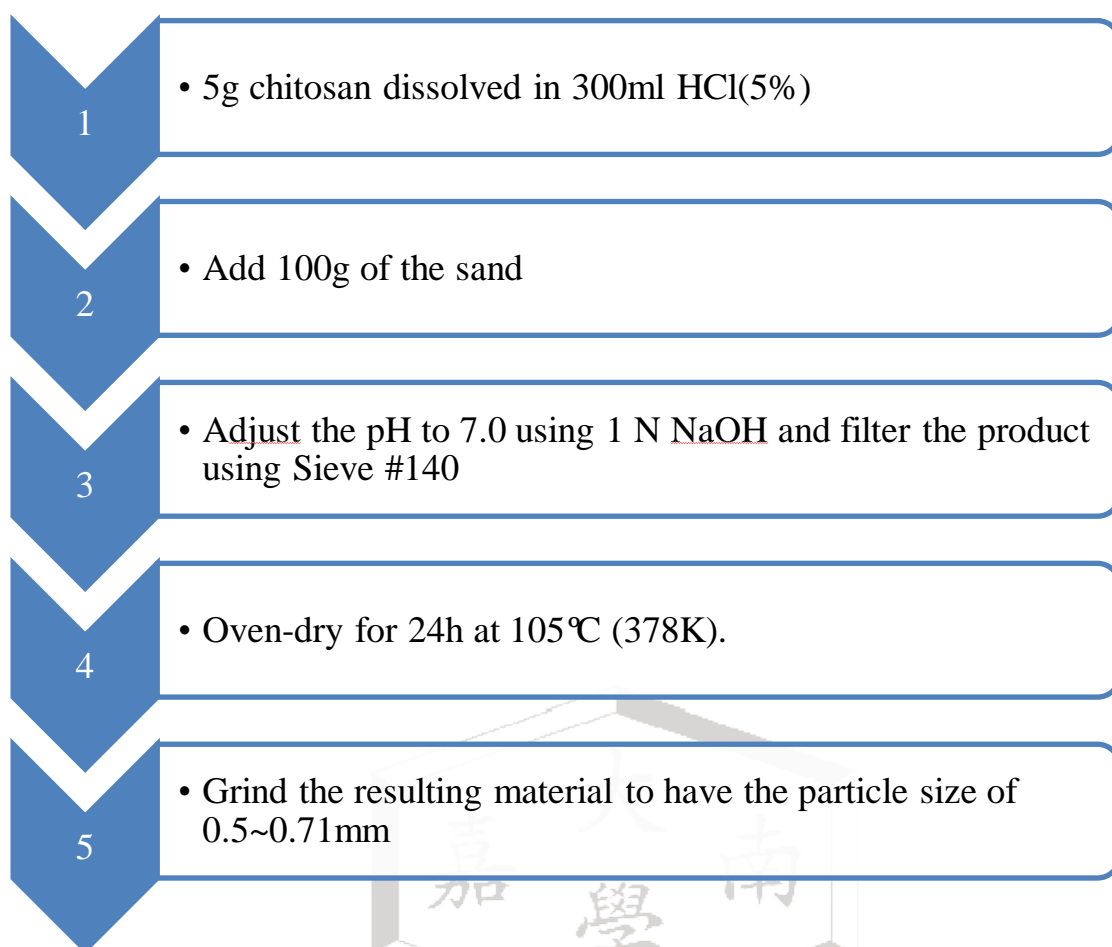


Figure 15. Preparation of Chitosan Coated on Sand

3.5 Preparation of Stock Solutions and Reagents

3.5.1 Arsenic (V) Aqueous Solution (Stock Solution)

Dissolve 0.4163 g Of $\text{Na}_2\text{HAsO}_4 \cdot 7\text{H}_2\text{O}$ in 100 ml deionized (DI) water for the 1000mg/L concentration. Dilute the solution in volumetric flasks with DI water using equation 13 to achieve the following concentrations: 50 ppb, 100 ppb, 500 ppb, 750 ppb, and 1000 ppb. The solutions prepared were 50 to 1000

ppb since the standard for drinking water in Taiwan is 10 ppb while for the wastewater is 0.5 ppm.

$$C_1 V_1 = C_2 V_2 \quad (\text{eq13.})$$

Where C_1 and V_1 is the concentration ($\mu\text{g/L}$) and volume (mL) of stock solution, C_2 is the desired concentration ($\mu\text{g/L}$), and V_2 is final volume of solution.

3.5.2 Standard Solutions and Reagents for ICP-OES Analysis

The initial concentration of the standard is 1000mg/l. Equation 13 was used to calculate for the following concentrations: 1000, 100, 50, 25, 10, and 5 $\mu\text{g/l}$. These are used as analytical standards for the ICP-OES. For the preparation of KI, 5 g of KI was dissolved in DI using a 100-ml volumetric flask. For vitamin C, 5 g was dissolved in DI using a 100-ml volumetric flask.

Perkin Elmer 2000DV Inductively Coupled Plasma-Optical Emission Spectrometer (ICP-OES) was used for quantitative determination of metal ion concentration. Standard solutions for the instrument's calibration curve were prepared as indicated: For the ICP-OES reduction solution, 200 ml of DI water

was poured in a 1000-ml volumetric flask. 0.5 gram of NaOH was then added to the flask. The flask was swirled slowly to dissolve the NaOH. 5 grams of NaBH₄ was added into the flask. The flask was filled with DI to the mark. For acid wash, 10 ml each of HCl and HNO₃ were mixed in DI using a 1000-ml volumetric flask.

3.6 Batch Adsorption Studies

1.0 g of adsorbent (Chitosan, AC, CCS, CCB, or CCK) was placed in a 125-ml Erlenmeyer flask. 30 ml of aqueous solution, with 50, 100, 500, or 1000 ppb as an initial concentration, was added in the flask. The flasks were then put in the shaker at different contact times ranging from 30 minutes to 24 hours. The shaker bath was run at 50 rpm and a temperature of 25°C. The final solution was then filtered using Whatman#40 filter paper and 0.45µm filter for ICP-OES analysis. After analysis, the kinetic, isotherm and thermodynamics were studied. 1 g was chosen to be adsorbent weight, because in the preliminary experiment, different mass of the adsorbent were compared: 2.5, 1.0, 0.5, and 0.1 g. Table 3 shows that the mass of the adsorbents with the highest equilibrium concentration is 2.5 grams. However, the equilibrium concentration of 1 gram is relatively near

the value of 2.5 grams, hence; it is more practical to use 1 gram as the mass of the adsorbent compared to 2.5 grams to reduce the amount of the adsorbent that will be used. Figure 16 and 17 shows the flowchart of the procedure for the batch adsorption studies.

Table 3. Preliminary Experiment: Effect of Different Adsorbents weight on the Equilibrium Concentration

Adsorbents weight (g)	Adsorbents				
	AC (µg/L)	Pure chitosan (µg/L)	CCS (µg/L)	CCB (µg/L)	CCK (µg/L)
2.5	470.9	1357	984	1073	303.3
1	250.7	865	914	1002	194.8
0.5	125.6	543	300	926	189
0.1	97	375	84	430.2	65

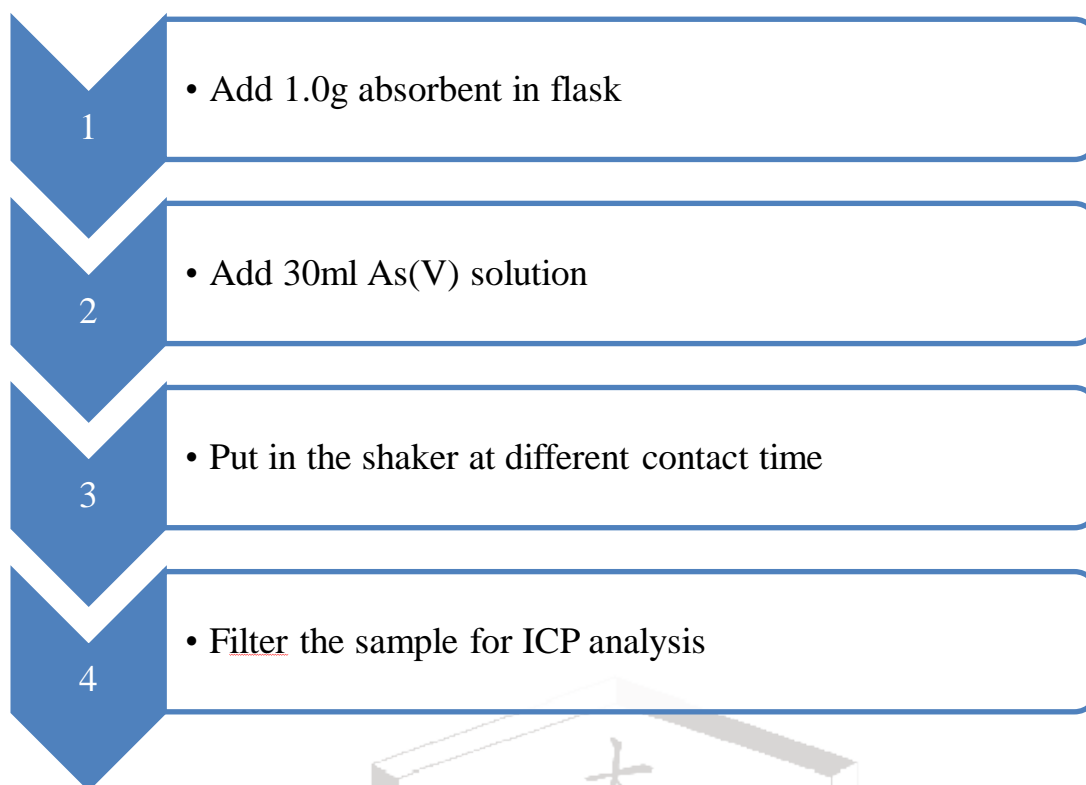
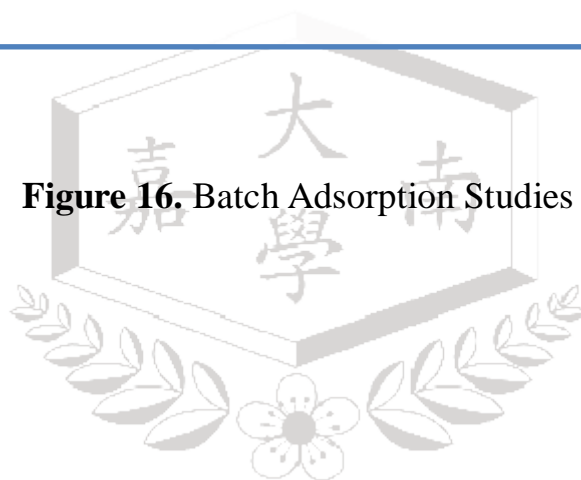


Figure 16. Batch Adsorption Studies



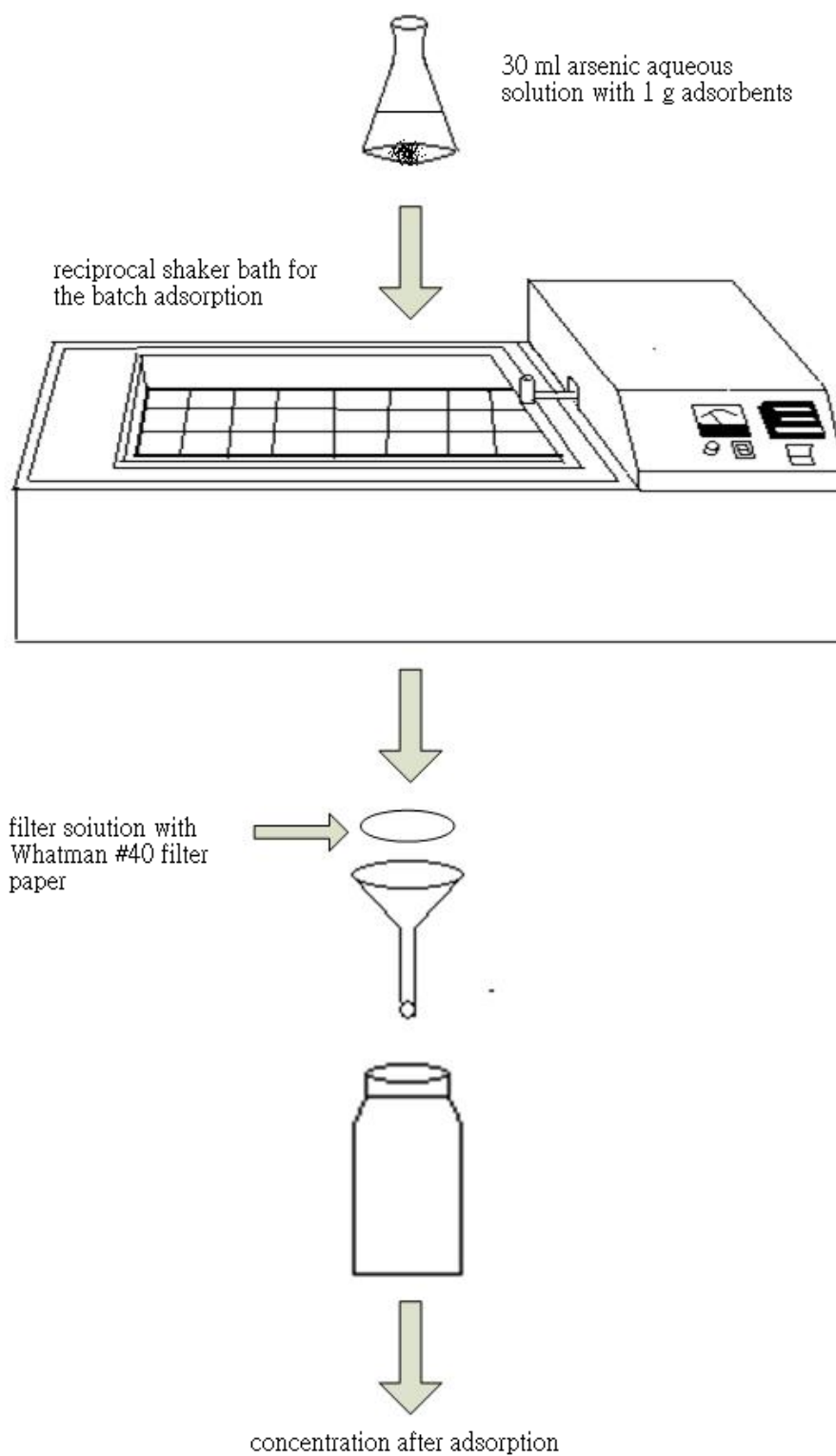


Figure 17. Batch Adsorption Experiment

3.7 Adsorption kinetic studies

Different contact times were used for the kinetic studies: 0.5, 1, 2, 4, 6, 12, and 24 hours. 1.0 gram of adsorbent was put in a 125-ml Erlenmeyer flask. 30 ml of the initial concentrations of 50 ppb, 100 ppb, 500 ppb, and 1000 ppb were added in their respective flasks. They were then placed in the shaker bath. The samples were filtered using Whatman#40 after the applied contact times and were prepared for analysis using ICP-OES. The kinetic models used were pseudo-first, pseudo-second, and Intraparticle diffusion.

3.8 Adsorption isotherm studies

Isotherm uses different concentration or different mass of the adsorbent. This study used different concentrations: 50, 100, 500, 750 and 1000 ppb. The mass of the adsorbent was kept constant at 1.0 gram per sample. The adsorbent was put in the Erlenmeyer flask followed by 30-ml aqueous solutions of arsenic (V). The flasks were put in the shaker bath for 24 hours. The resulting solutions were filtered using Whatman#40 and were prepared for analysis. The models applied were Langmuir, Freundlich and Dubinin–Radushkevitch (D–R).

3.9 Adsorption thermodynamics study

Thermodynamics study makes use of different temperatures. In this experiment 25°, 35°, 45°, and 55° Celsius were applied. 1.0 gram of adsorbent and 30 ml of the aqueous solution with the following concentrations were prepared in flasks: 50 ppb, 100 ppb, 500 ppb, and 1000 ppb. The flasks were put in the shaker bath for 24 hours. The solutions were then filtered using Whatman#40 and were then prepared for ICP-OES analysis.



Chapter 4 Results and Discussion

4.1 Characteristic analysis of the Adsorbents

4.1.1 BET Analysis

The pore size can be classified into three types: macroporous ($d > 50$ nm), mesoporous ($2 < d < 50$ nm), and microporous ($d < 2$ nm). The BET study shows the pore size and specific surface area of AC, pure chitosan, CCB, CCK and CCS as shown in table 4. The AC is microporous; chitosan, sand, and CCK are mesoporous; bentonite, CCB, CCS, and kaolinite are macroporous. The values of the micropore area of the adsorbents followed the sequence: $AC > CCK > CCS > CCB > \text{pure chitosan}$.

The specific surface area followed the sequence: $AC > CCB > CCK > \text{pure chitosan} > CCS$. When the chitosan coated on support material, their surface area becomes lower compared to their original specific surface of the support material. This is because the chitosan molecules block the pores of carrier (bentonite, kaolinite, and sand). The surface area of the composites (CCS, CCK, and CCB) decreased by 11.32%, 15.21%, and 67.27% respectively. If the decrease of percentage value of the BET surface area is larger, this means that

when the chitosan coated on the carrier, the sorbents will coagulate before coating. Moreover, the hydroxylated edges of clay act as the bridging mechanisms to bind chitosan on their surface. These edges also interact with each other which also decrease their respective specific surface area. (Wan et al., 2010)

Table 4. BET Analysis of Different Adsorbents

Adsorbent	BET surface area (m²/g)	Micropore area (m²/g)	Average pore diameter (nm)	Total pore volume (cm³/g)
AC	732.5143	530.7534	1.0211	0.3999
Chitosan	2.1200	0.3800	11.6100	0.0320
Bentonite	28.1680	7.2487	57.6401	0.0878
CCB	9.2216	0.5600	80.5387	0.0479
Sand	0.5261	1.0673	45.1346	0.0005
CCS	0.4712	0.7055	683.8042	0.0042
Kaolinite	6.5096	0.2417	95.4353	0.0356
CCK	5.5208	1.5556	28.97705	0.030868

4.1.2 TGA Analysis

The TGA Analysis in this study analyzed the CCB, CCK, and CCS. The results are shown in figures 25, 26 and 27. The chitosan has two decomposition sites: the first one is at 240°C and the second at 320°C. It was then completely burnt out at 600°C. The carriers which include bentonite, kaolinite and sand were also analyzed. Bentonite has two sites which it will lose weight; 90°C and 600°C; kaolinite has two main decomposition stages with one starting at 350°C and the other 490°C; for sand, almost have little weight lost, which can be found at 800°C.

Based on figures 18, 19 and 20 the thermogram of CCB, CCK and CCS which show similar decomposition stages of chitosan with a relatively less weight loss indicates that about 5.9% of chitosan is successfully coated on bentonite, 6.0% of chitosan is successfully coated on kaolinite, and 2.1% of chitosan is successfully coated on sand. The TGA analysis confirmed that the chitosan has successfully coated with supported materials, such as bentonite, kaolinite, and sand.

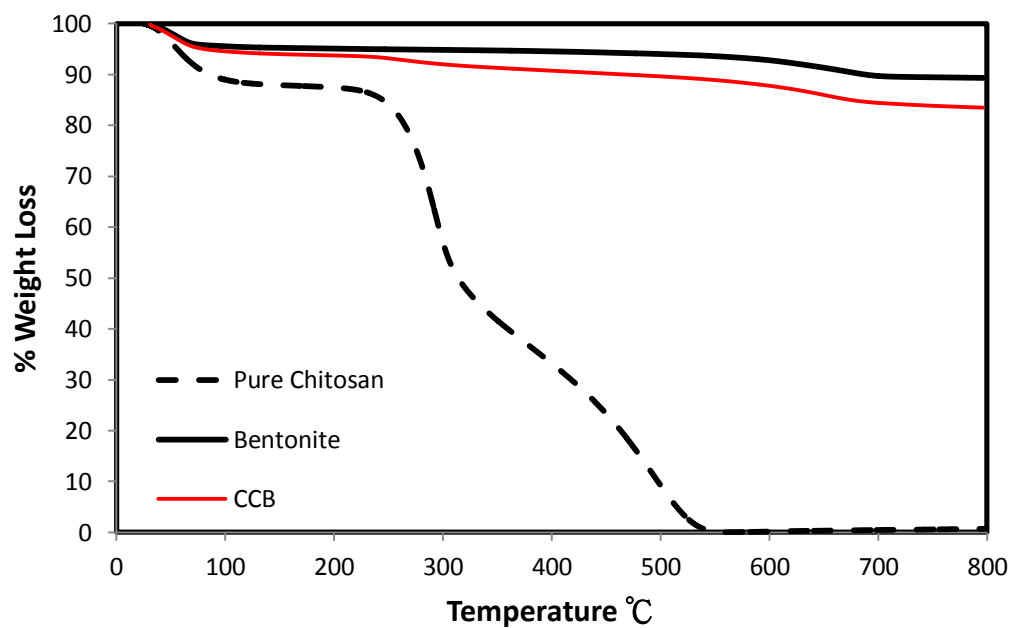


Figure 18. TG Analysis of Chitosan Coated on Bentonite

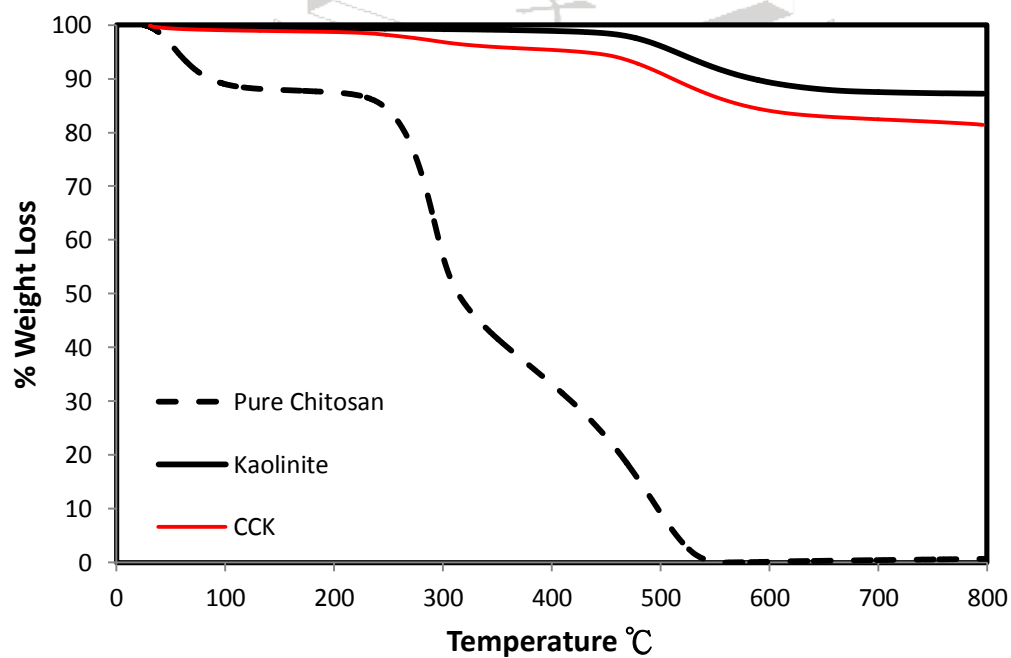


Figure 19. TG Analysis of Chitosan Coated on Kaolinite

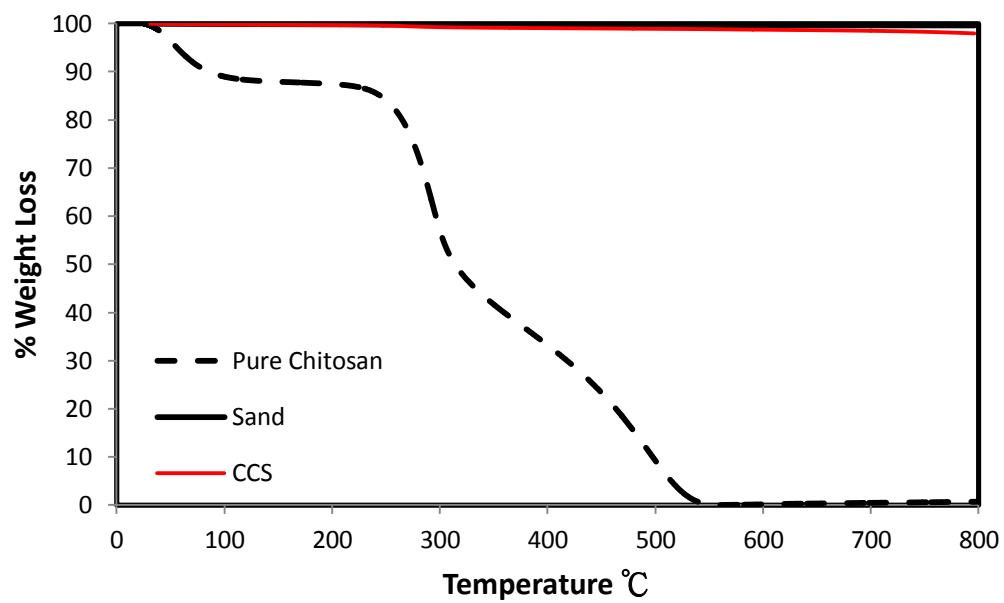
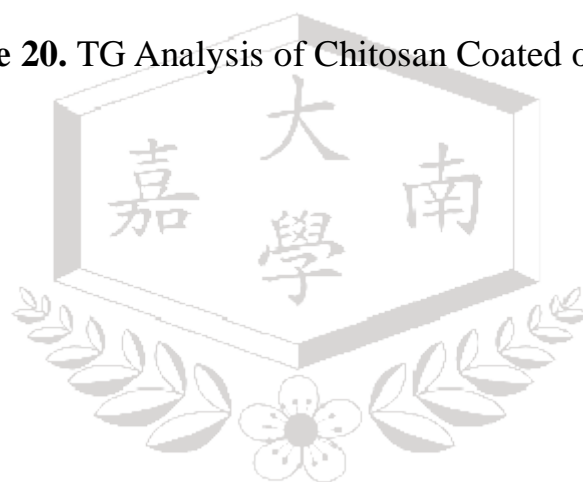


Figure 20. TG Analysis of Chitosan Coated on Sand



4.2 Effect of contact time on adsorption capacity using different adsorbents and concentration

This experiment determines the adsorption capacity at different contact times and initial concentrations. As shown in Figures 21, 22, 23, 24, and 25, it is remarkable that an increase in the initial concentration (C_0) for As (V) ions led to an increase in the adsorption capacity of five different adsorbents at various contact times. This can be attributed to the mass transfer effects and the driving force of the concentration gradient being directly proportional to the initial concentrations. An exposure time of 24 hours was used during batch studies. It demonstrated that chitosan and chitosan derived adsorbents can potentially reach the equilibrium after 12 hours regardless of the initial concentrations (C_0). AC also reached the equilibrium time at 12 hours since there is no significant change in the concentration after 12 hours.

At the beginning, the adsorption of As (V) ions is very fast, because the adsorbents still contain many available functional groups, such as ($-NH_2$) and ($-OH$), which swiftly adsorb the heavy metal ions. The increase of adsorption capacity finally reached equilibrium owing to the saturation of the binding sites.

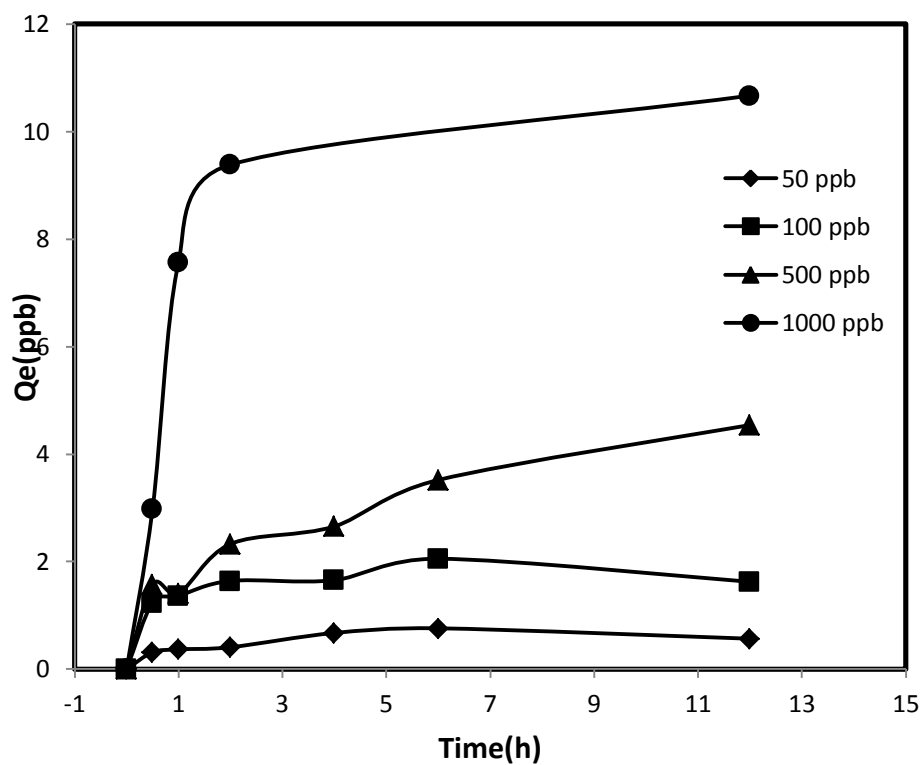


Figure 21. Adsorption Capacity of Activated Carbon

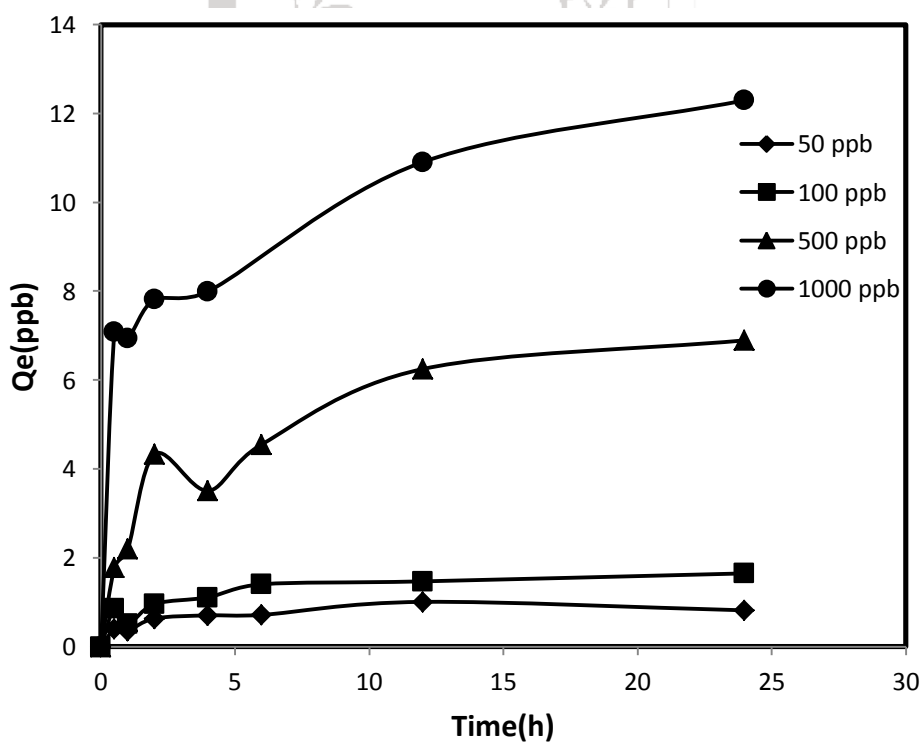


Figure 22. Adsorption Capacity of Pure Chitosan

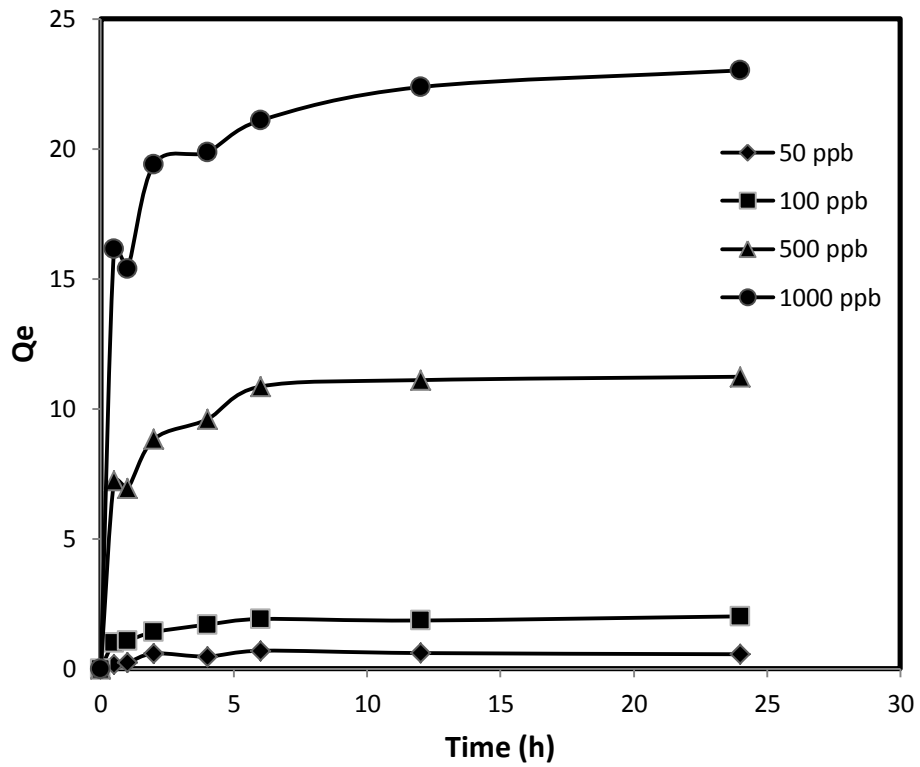


Figure 23. Adsorption Capacity of Chitosan-Coated Bentonite

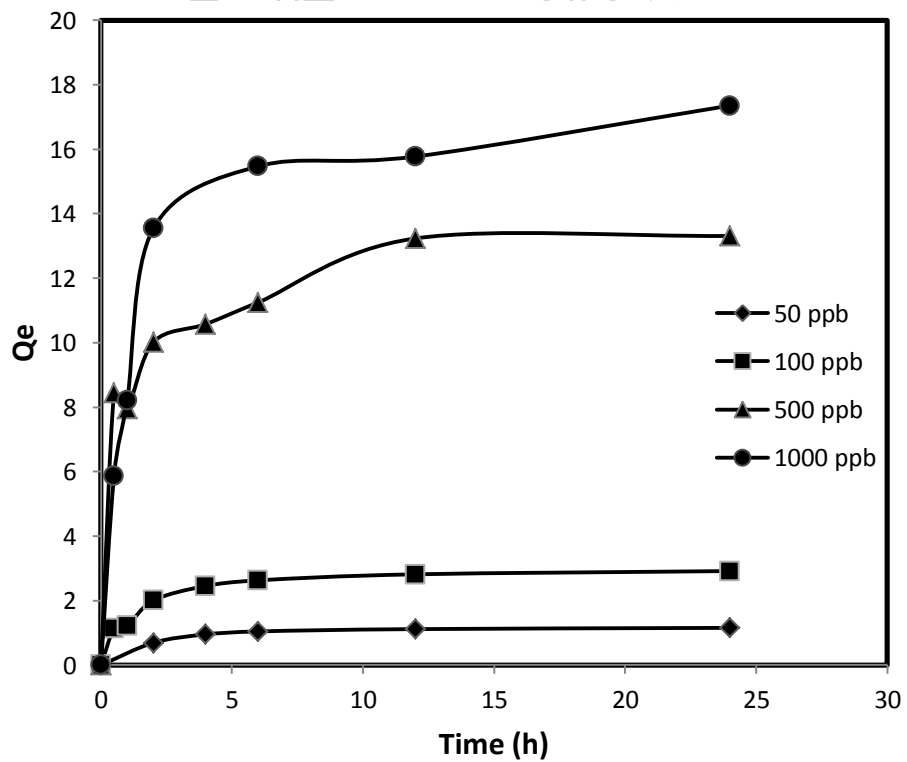


Figure 24. Adsorption Capacity of Chitosan-Coated Kaolinite

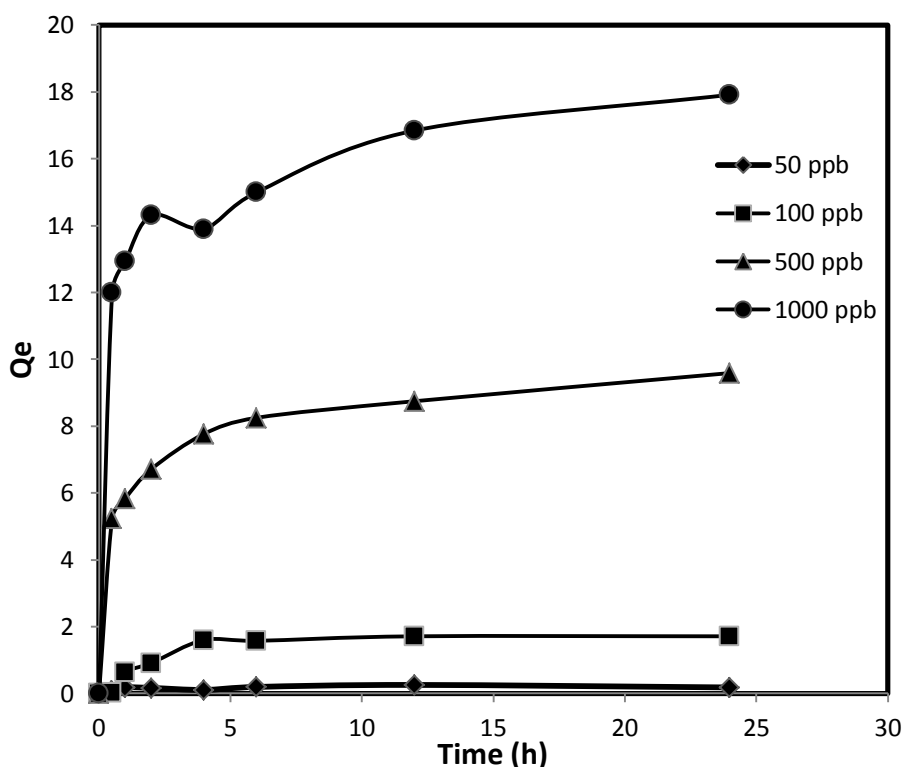


Figure 25. Adsorption Capacity of Chitosan-Coated Sand

Based on Table 13, the activated carbon resulted in less efficiency of As(V) adsorption. According to previous studies, the adsorption mechanism of AC is based on physical adsorption, which is mainly used the high surface area in uptaking the heavy metals. In this study, the adsorption capacity of AC is less compared to the other adsorbents, which confirmed that the pure chitosan and its complex beads containing many available functional groups (amino group) perform better As(V) adsorption than surface adsorption of AC.

As shown in Table 5, the adsorption of As(V) ions using pure chitosan, CCB, CCK, and CCS occurred rapidly. As(V) adsorption increased with contact time and attained equilibrium at 12 hours for all four adsorbent beads. The adsorption

capacity of pure chitosan, CCB, CCK, and CCS was observed to increase with initial concentration. A high initial concentration means an increase in the driving force caused by the concentration gradient and mass transfer effects, resulting to an increase in its capacity. The order of the adsorption capacity using these four adsorbents was as follows: CCK ~ CCB > CCS > pure chitosan.

Table 5. Equilibrium Adsorption Capacity of Different Initial Concentration using Different Adsorbents

Adsorbent	Equilibrium Time (hours)	Equilibrium Adsorption Capacity ($\mu\text{g/g}$)			
		50 ppb	100 ppb	500 ppb	1000 ppb
AC	12	0.565	1.624	4.541	10.670
pure chitosan	12	0.817	1.649	6.894	12.295
CCB	12	0.555	2.013	11.234	23.021
CCK	12	1.155	2.917	13.308	17.351
CCS	12	0.180	1.710	9.588	17.916

4.3 Adsorption Kinetics studies

Adsorption kinetic studies determine the adsorption mechanism occurring on different adsorbents. In this research, three kinds of kinetic models, namely pseudo-first order, pseudo-second order, and intraparticle diffusion model, were executed. Different contact times that were 0.5, 1, 2, 4, 6, 12, and 24 hours were used to confirm the models. Equations 3, 4, and 5 were applied in model calculations.

4.3.1 Pseudo- first order model

The pseudo-first order rate expression has been widely used for sorption of metals (Sağ & Aktay, 2002), which was widely used for reversible reactions with an equilibrium being established between liquid and solid phases. In many cases, the pseudo-first order do not fit well to the whole range of contact time and is generally applicable over the initial stage of adsorption process (Ho & McKay, 1998). Figure 26, 27, 28, 29, and 30 show the pseudo-first order models of the five adsorbents used in this study. Table 6 illustrates the kinetic parameters of the pseudo-first order model of the adsorbents. The k_1 constant is the rate of the particles to adsorb on the adsorbent.

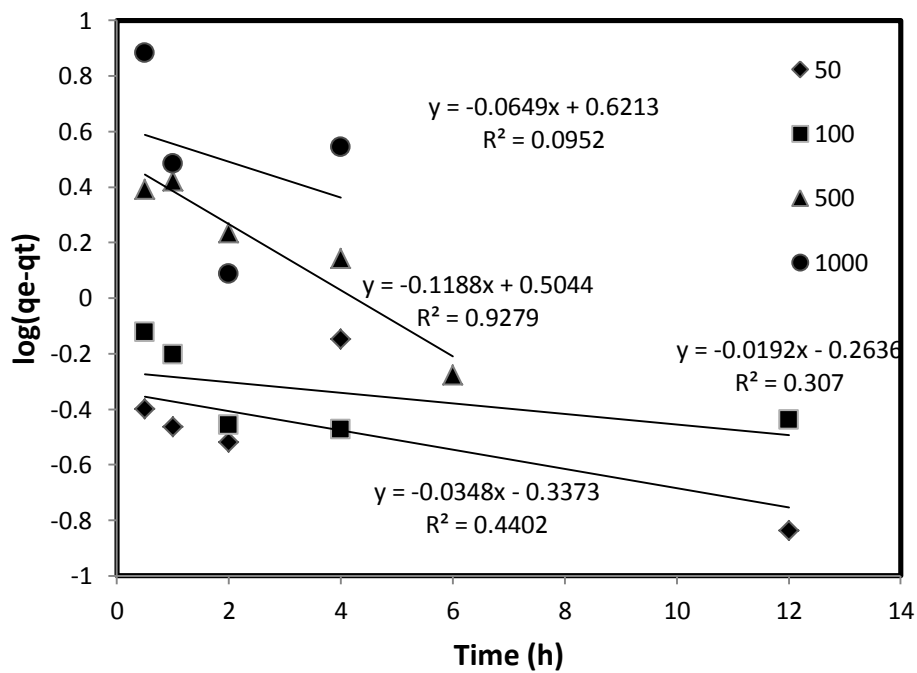


Figure 26. Pseudo-First Order Model of Activated Carbon

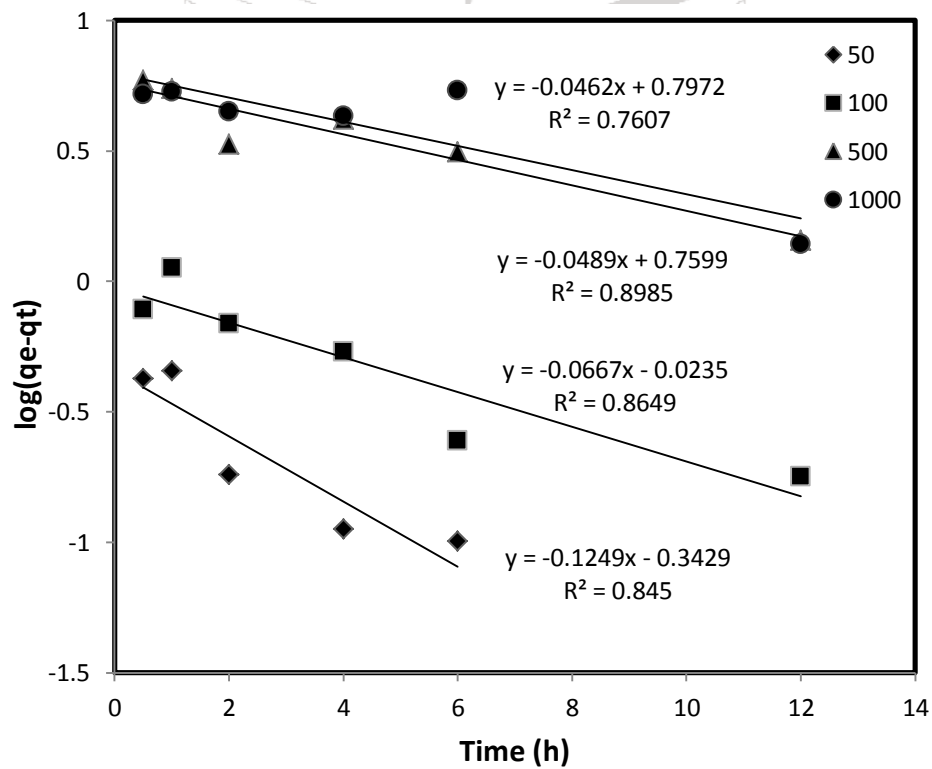


Figure 27. Pseudo-first Order Model of Pure Chitosan

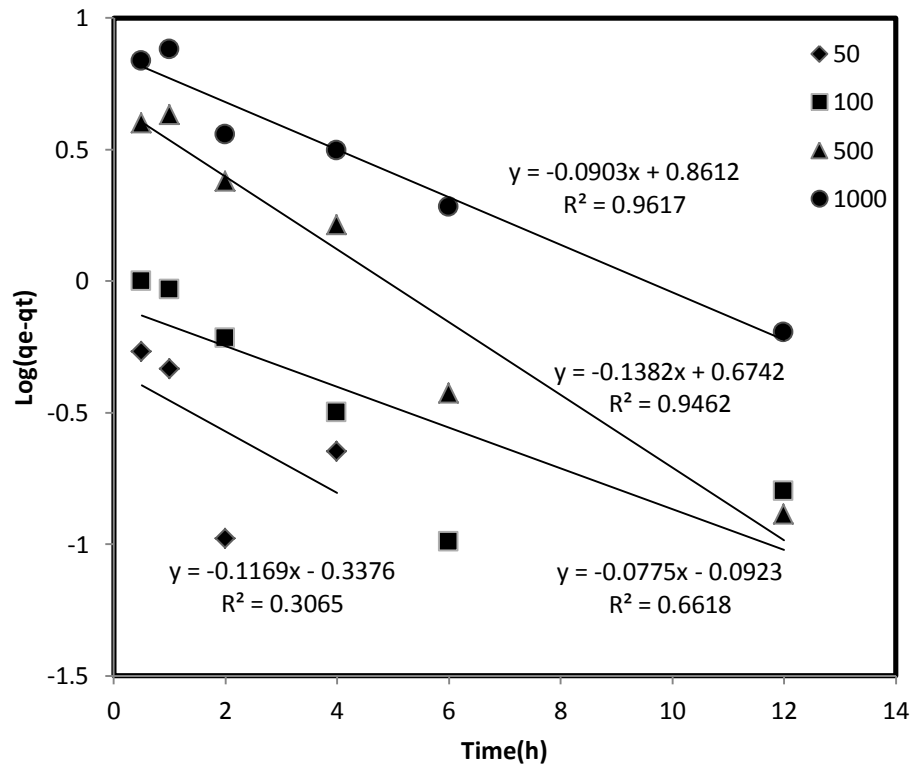


Figure 28. Pseudo-first Order Model of CCB

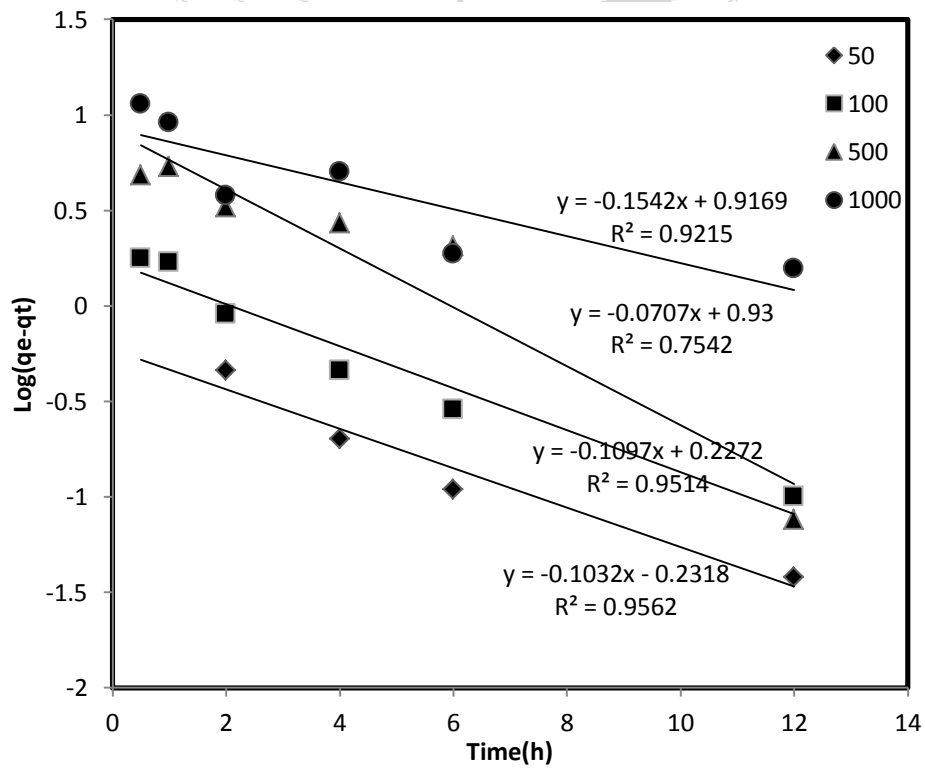


Figure 29. Pseudo-first Order Model of CCK

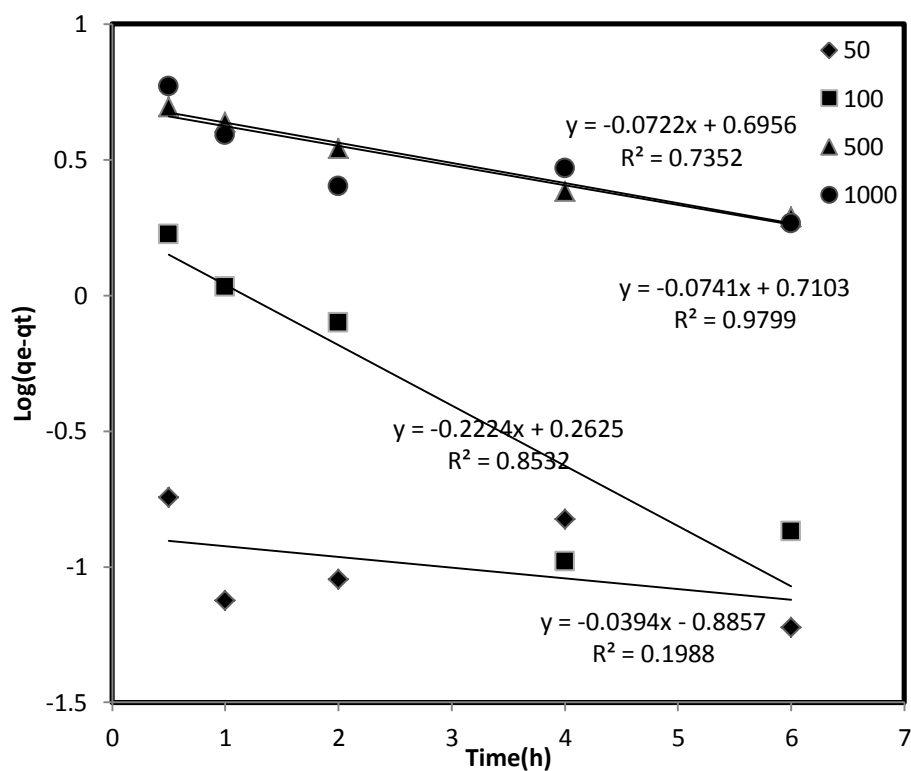


Figure 30. Pseudo-first Order of CCS

Table 6. Kinetic Parameters for the Pseudo-first Order Model of Different Adsorbents at Different initial Concentrations

Adsorbent	50 ppb		100 ppb		500 ppb		1000 ppb	
	R ²	k ₁	R ²	k ₁	R ²	k ₁	R ²	k ₁
AC	0.4402	0.8014	0.307	0.0442	0.0272	0.2736	0.0952	0.1495
pure chitosan	0.845	0.2876	0.8649	0.1536	0.8985	0.1126	0.7607	0.1064
CCB	0.3065	0.2692	0.6618	0.1785	0.9617	0.3183	0.9617	0.2080
CCK	0.9562	0.2377	0.9514	0.2546	0.9215	0.2526	0.9215	0.3551
CCS	0.1988	0.0907	0.8532	0.5122	0.9799	0.1707	0.7352	0.1663

4.3.2 Pseudo-second order model

Ho (2006) illustrated that the pseudo second-order reaction was used to distinguish the kinetic equation based on the concentration of a solution from the adsorption capacity of a solid. In this study, the rate constant k_2 was determined experimentally by plotting the slopes and intercepts of t/qt against t . Figures 31, 32, 33, 34, and 35 illustrates the pseudo-second order models of the five adsorbents used in this study. Table 7 illustrates the kinetic parameters of the pseudo-second order model of the adsorbents. The k_2 is the rate of the particles to chemically bond onto the adsorbent. k_2 have higher values at lower concentrations. A low concentration means less competition between metal ions in binding to the functional groups, thus heavy metals are adsorbed quickly (Futalan et al., 2011).

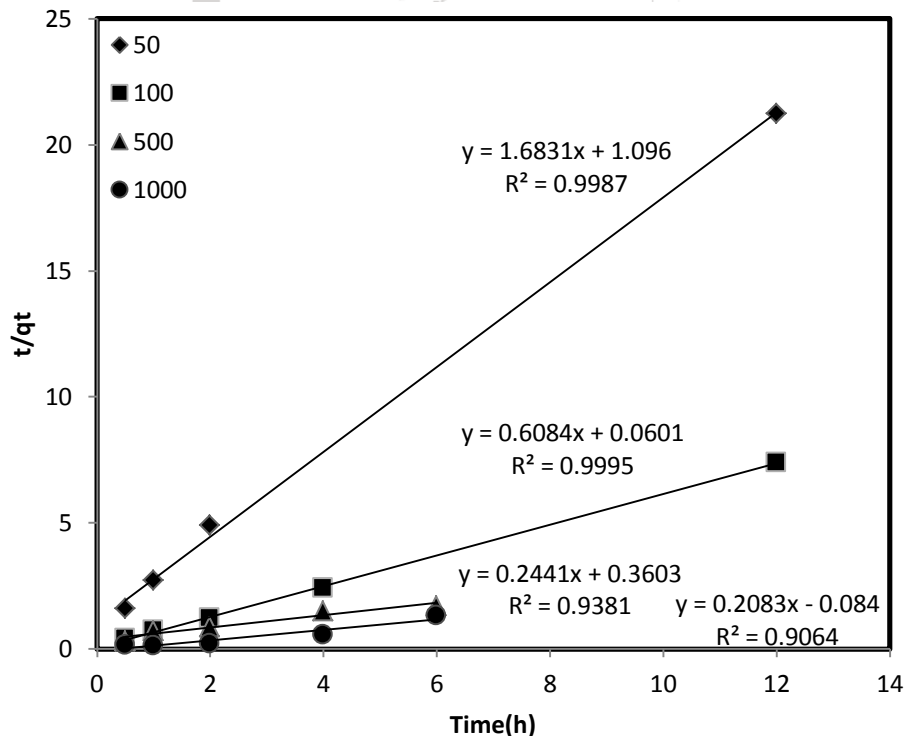


Figure 31. Pseudo-second Order Model of Activated Carbon

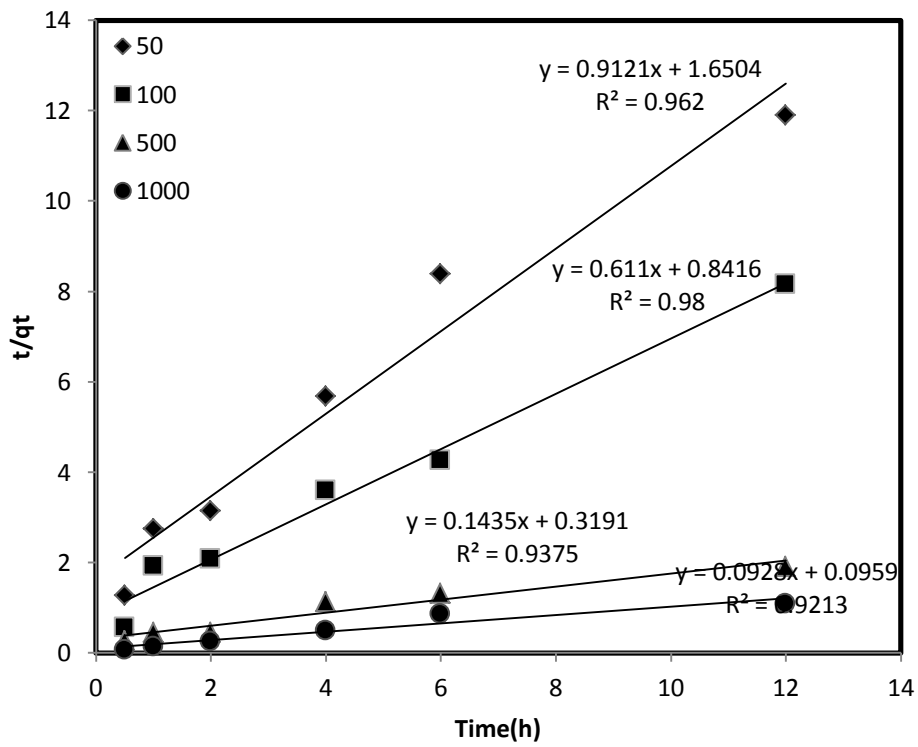


Figure 32. Pseudo-second Order Model of Pure Chitosan

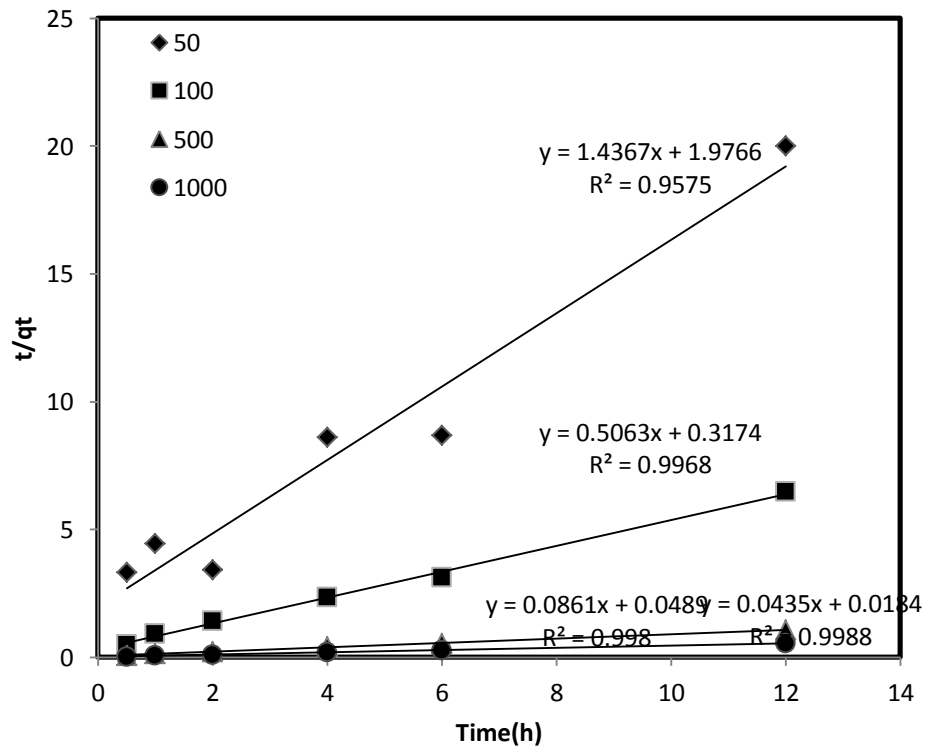


Figure 33. Pseudo-second Order Model of CCB

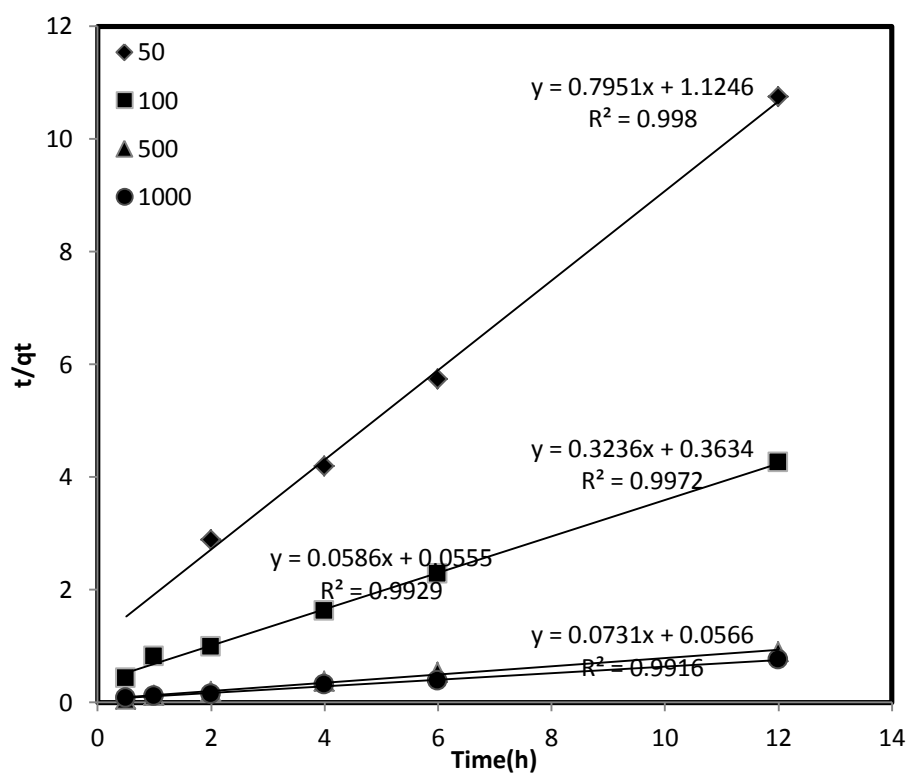


Figure 34. Pseudo-second Order Model of CCK

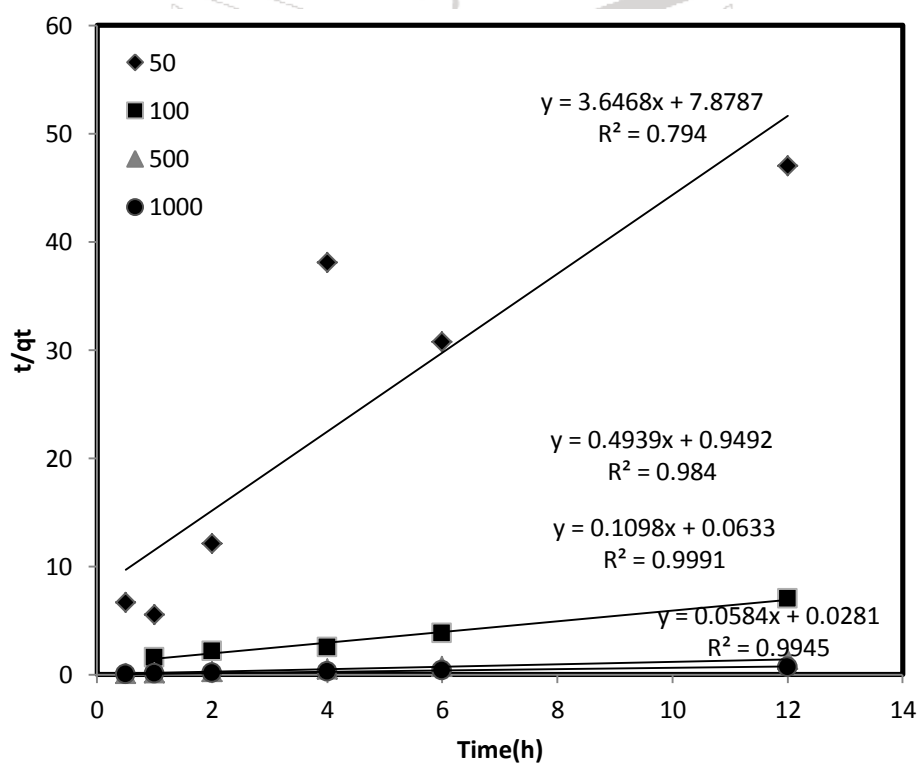
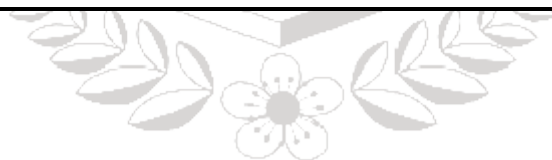


Figure 35. Pseudo-second Order Model of CCS

Table 7. Kinetic Parameters for the Pseudo-second Order Model of Different Adsorbents at Different Initial Concentrations

Adsorbent	50 ppb		100 ppb		500 ppb		1000 ppb	
	R^2	k_2	R^2	k_2	R^2	k_2	R^2	k_2
AC	0.999	1.805	0.999	4.202	0.938	0.169	0.906	-0.105
Pure chitosan	0.962	0.909	0.980	0.437	0.938	0.066	0.922	0.690
CCB	0.958	1.643	0.997	0.777	0.998	0.162	0.999	0.103
CCK	0.998	0.667	0.997	0.323	0.992	0.100	0.993	0.0599
CCS	0.794	3.917	0.984	0.360	0.999	0.152	0.995	0.111



4.3.3 Intraparticle Diffusion Model

The intraparticle diffusion model (IPD) proposed by Weber and Morris has been widely applied for the analysis of adsorption kinetics. In this work, the characteristic curves based on this model were plotted with various initial adsorption factors, shown as Figures 36, 37, 38, 39, and 40.

Table 8 illustrates the kinetic parameters of the intraparticle diffusion model of the adsorbents. The k_i is the rate of the mass transfer of the particles into the adsorbent. k_i can be related to the pore diameter of the adsorbents. CCS has the biggest pore diameter followed by CCB, CCK, pure chitosan and AC. CCK has the highest k_i which means that the pore diameter of CCK has the best fit for As(V) adsorption.

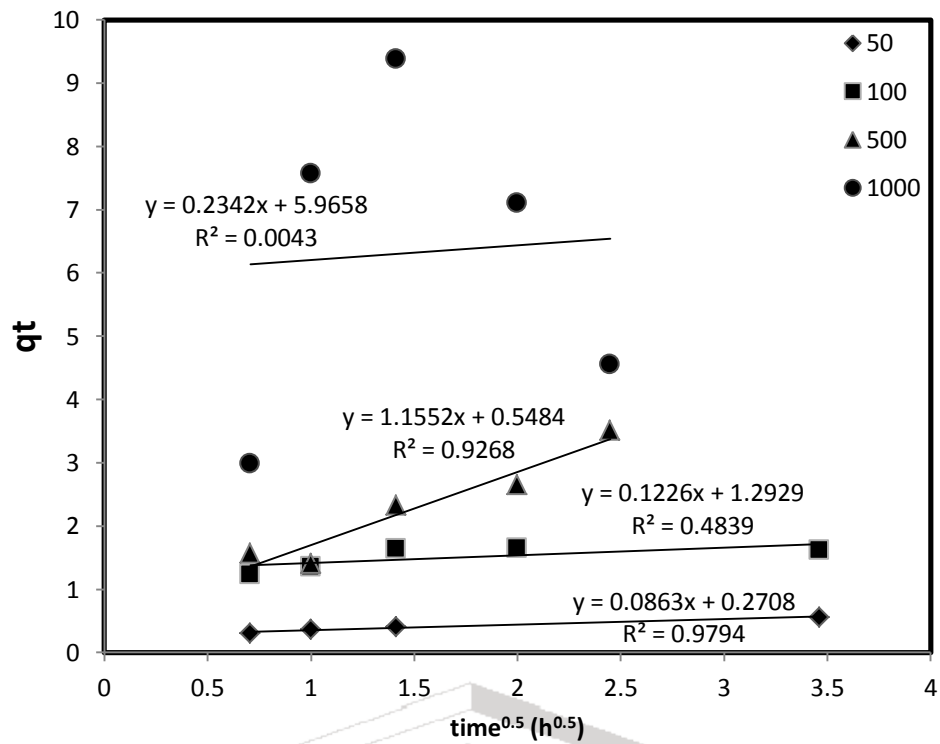


Figure 36. Intraparticle Diffusion Model of Activated Carbon

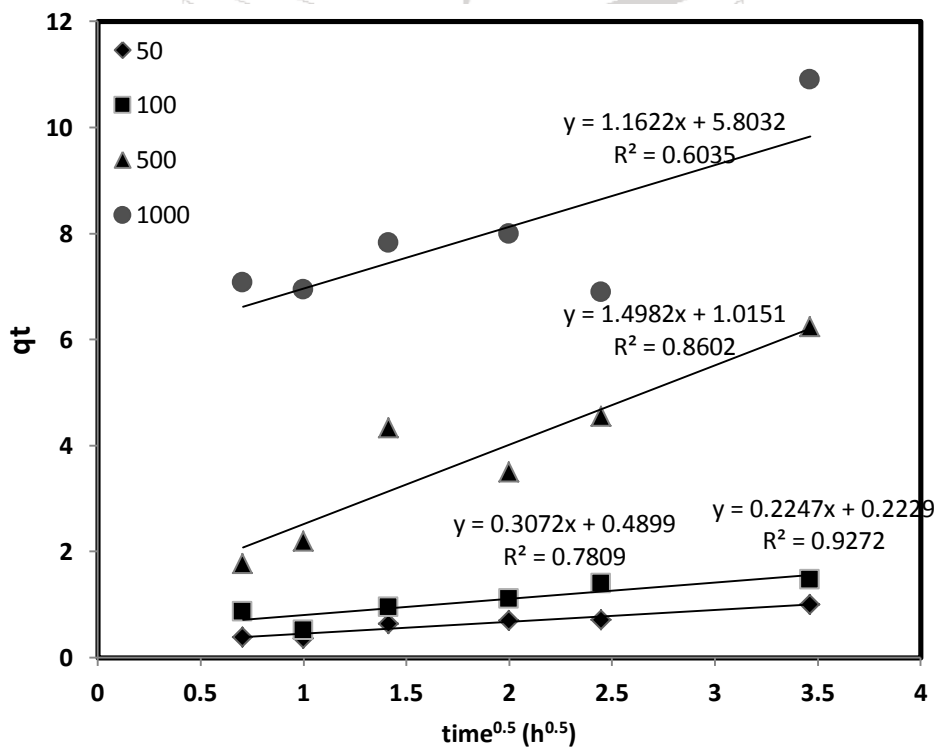


Figure 37. Intraparticle Diffusion Model of Pure Chitosan

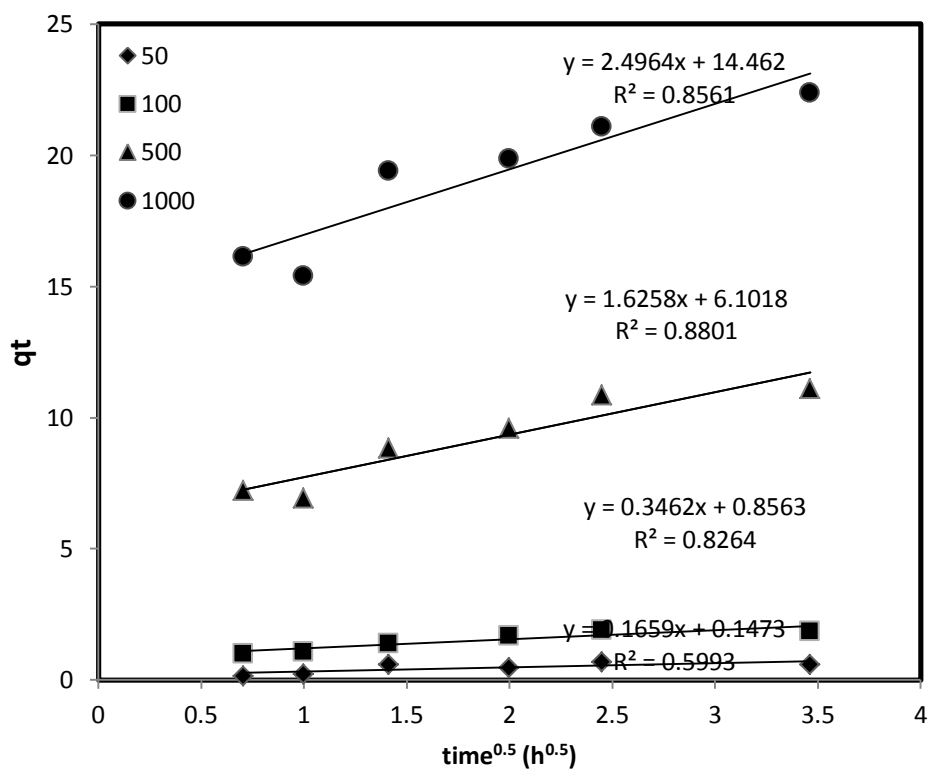


Figure 38. Intraparticle Diffusion Model of CCB

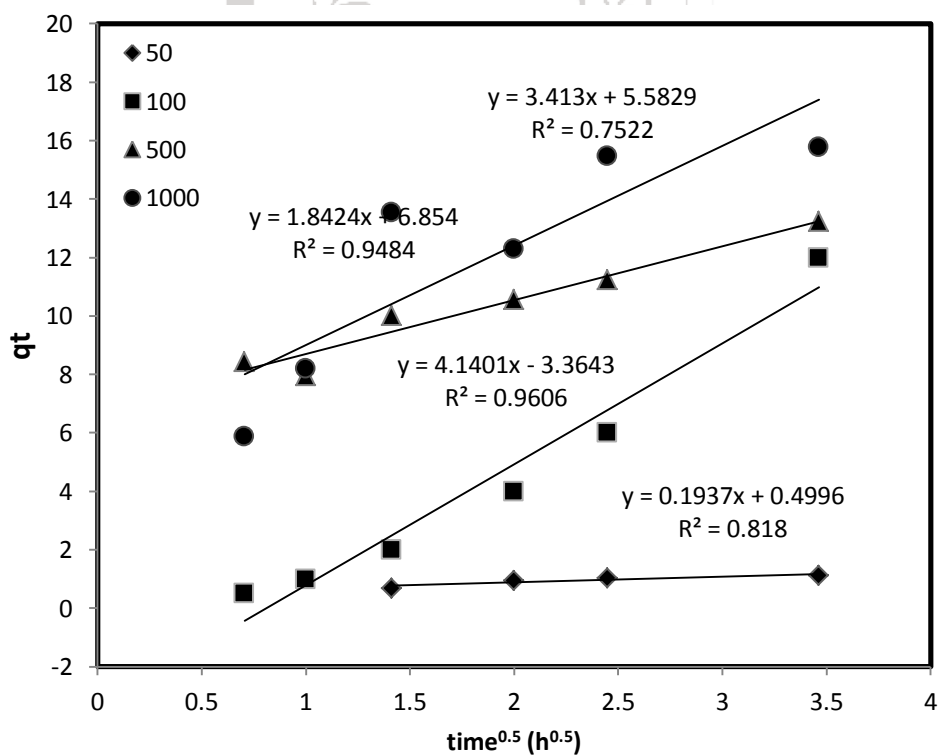


Figure 39. Intraparticle Diffusion Model of CCK

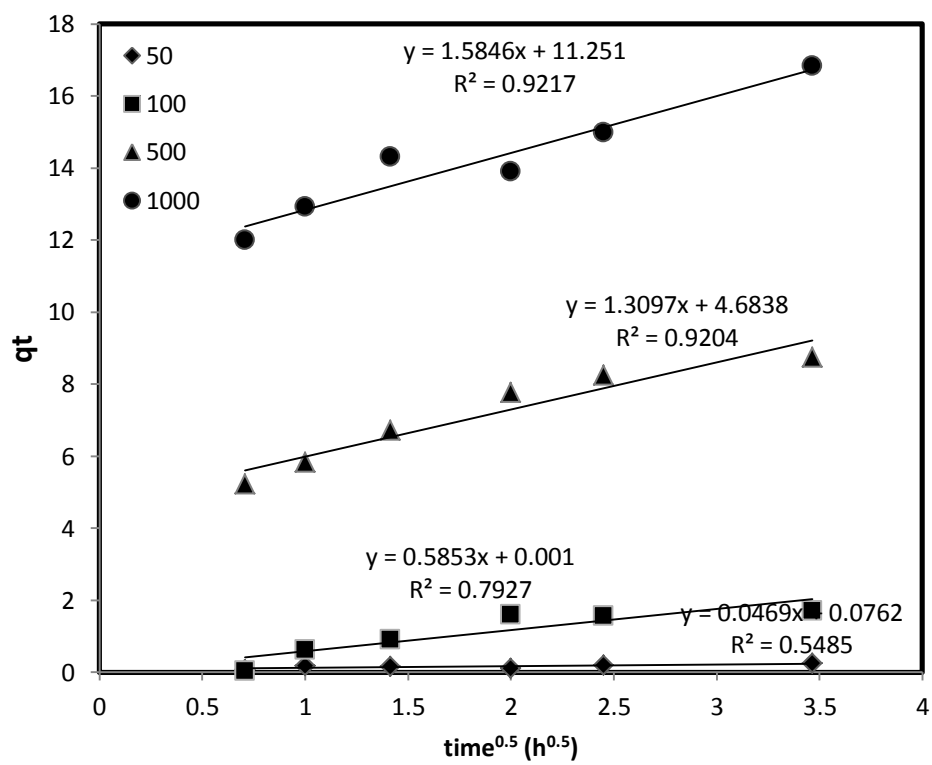


Figure 40. Intraparticle Diffusion Model of CCS

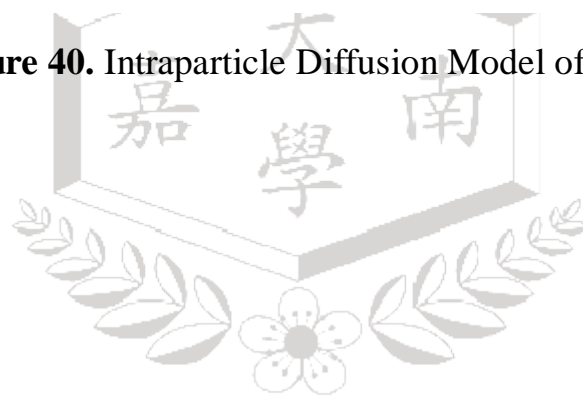


Table 8. Kinetic Constants for the Intraparticle Diffusion Model of Different Adsorbents at Different Initial Concentrations

Adsorbent	50 ppb		100 ppb		500 ppb		1000 ppb	
	R ²	ki	R ²	ki	R ²	ki	R ²	ki
AC	0.532	0.1	0.4839	0.1266	0.9268	1.1552	0.0043	0.2342
pure chitosan	0.927	0.2247	0.7809	0.3072	0.8602	1.4982	0.6035	1.1622
CCB	0.599	0.1659	0.8264	0.3462	0.8801	1.6258	0.8561	2.4964
CCK	0.8181	0.9316	0.9606	4.1401	0.9484	1.8424	0.7522	3.413
CCS	0.5485	0.0469	0.7927	0.5853	0.9204	1.3097	0.9217	1.5846

4.3.4 Analysis Summary of Three Kinetic Models

The ranges of R² values for the pseudo-first model at different initial concentrations follows the trend of AC (0.0272<R²<0.9279), pure chitosan (0.7607<R²<0.8985), CCB (0.3065<R²<0.9617), CCK (0.7542<R²< 0.9562), and CCS (0.1988<R²<0.9799). The R² values of five different adsorbents are not good fit with the pseudo-first order kinetic Model.

The ranges of R² for the pseudo-second order model at different initial

concentrations follows the trend of $0.9064 < R^2 < 0.9987$ for AC, $0.9213 < R^2 < 0.98$ for pure chitosan, $0.9575 < R^2 < 0.9988$ for CCB, $0.9916 < R^2 < 0.998$ for CCK, and $0.794 < R^2 < 0.9991$ for CCS. The R^2 of CCS at 50 ppb is not good, but compared to the other kinetic models, the R^2 values of five different adsorbents fit well with the pseudo-second order kinetic Model.

The ranges of R^2 for the intraparticle diffusion model at different initial concentrations follows the trend of $0.0043 < R^2 < 0.9794$ for AC, $0.6035 < R^2 < 0.9272$ for pure chitosan, $0.5993 < R^2 < 0.8801$ for CCB, $0.7522 < R^2 < 0.9606$ for CCK and $0.5485 < R^2 < 0.9217$ for CCS. The R^2 values of five different adsorbents are not good fit with the intraparticle model.

Based on the analysis results, all the adsorbents follow the pseudo-second order model, which means that the overall adsorption rate for both ions appeared to be controlled by the chemical process. The conclusion is based on the assumption that chemisorption involved valence forces, via sharing or exchange of electrons as covalent forces between the transition metal cations and adsorbent and ion exchange.

4.4 Adsorption isotherm studies

Adsorption isotherm models describe the relationship between adsorbates

and adsorbents at equilibrium. The three well-known isotherm models are the Langmuir, Freundlich, and Dubinin-Radushkevich (D-R) isotherm models. In this study, equilibrium isotherms were used to determine the adsorption mechanism of five different adsorbents for As (V) ions. 1 g of adsorbents were combined with fixed volumes (30 mL) of metal ion solutions varying the initial concentrations 50, 100, 500, and 1000 ppb) at 24 hours contact time. The relation between the amount of adsorbed metal and the remaining concentration of metal ions in solution is described by the isotherm studies.

4.4.1 Freundlich model

The Freundlich model is based on an empirical equation. It is usually applied to adsorption of solute on active sites with heterogenous energy levels on rough surfaces. The experimental data are plotted against the linear plots generated by the Freundlich equation (eq. 7), shown as Figures 41, 42, 43, 44, and 45. The parameters calculated by Freundlich models are arranged in Table 14.

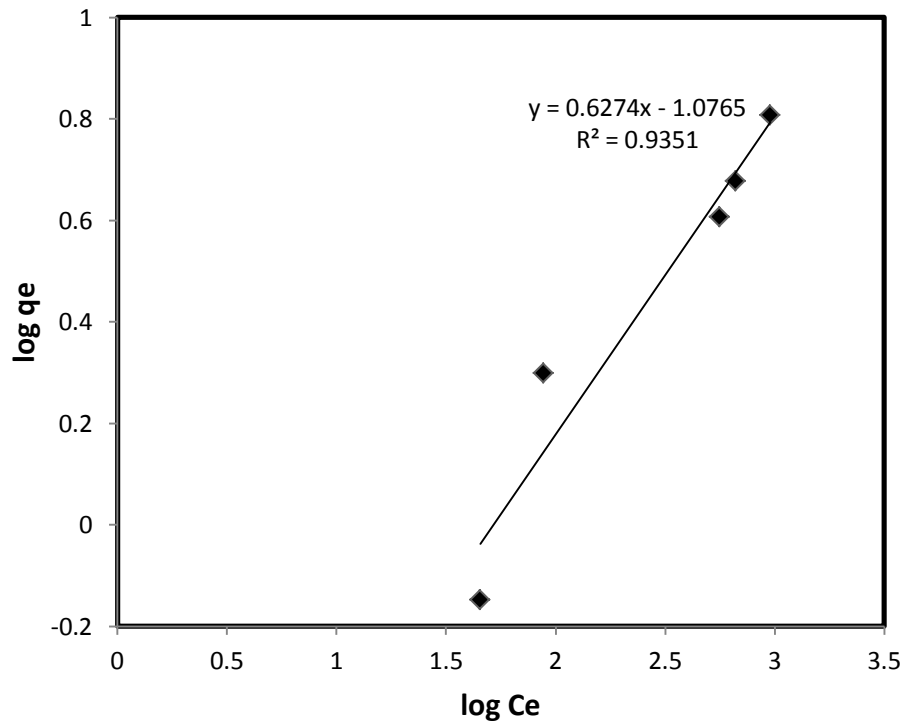


Figure 41. Freundlich Isotherm of Activated Carbon

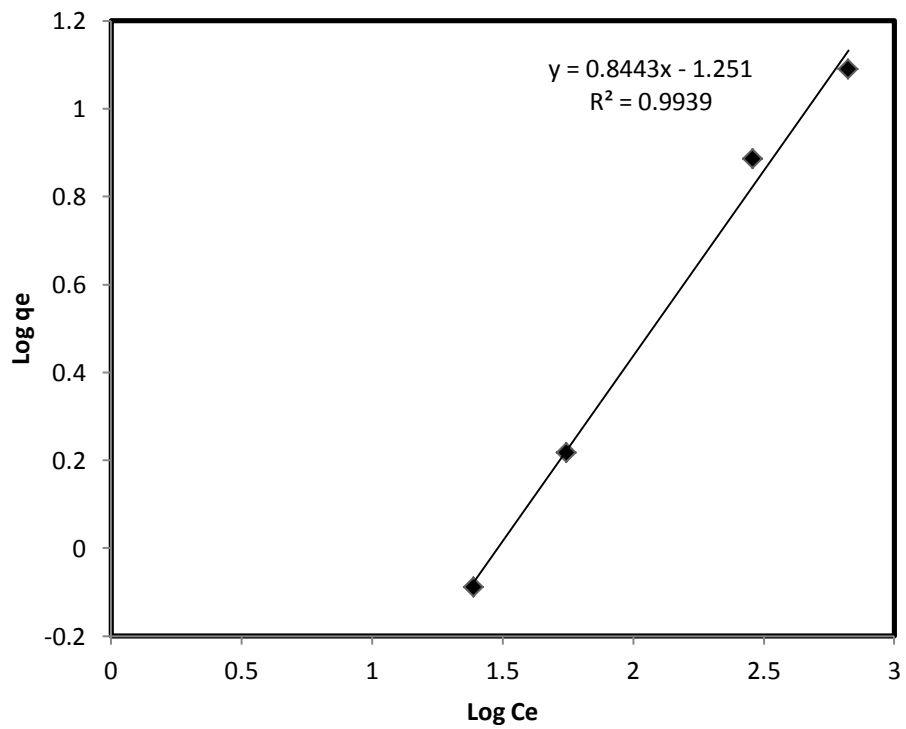


Figure 42. Freundlich Isotherm of Pure Chitosan

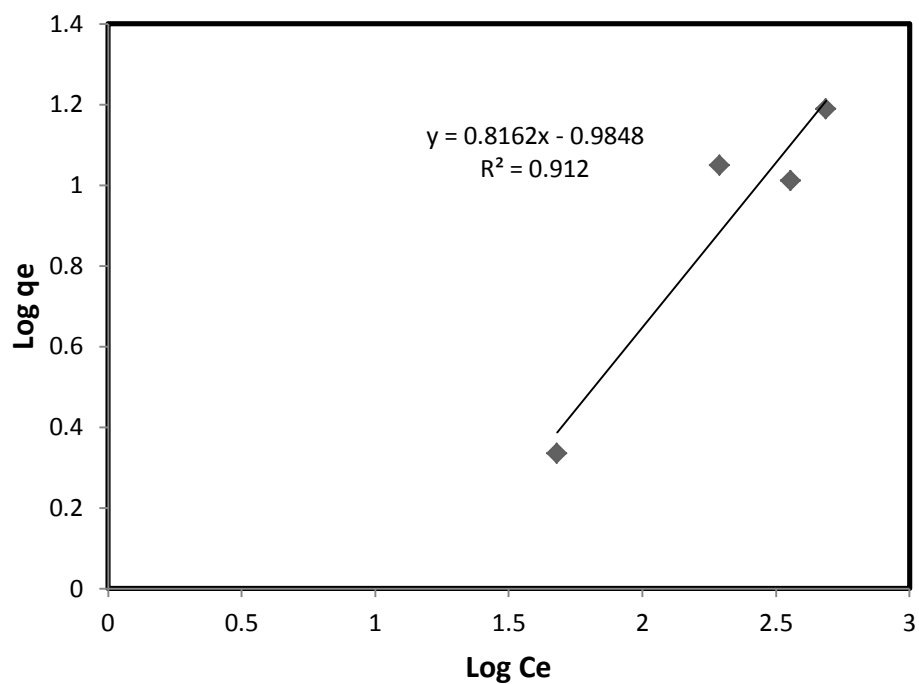


Figure 43. Freundlich Isotherm of Chitosan-Coated Bentonite

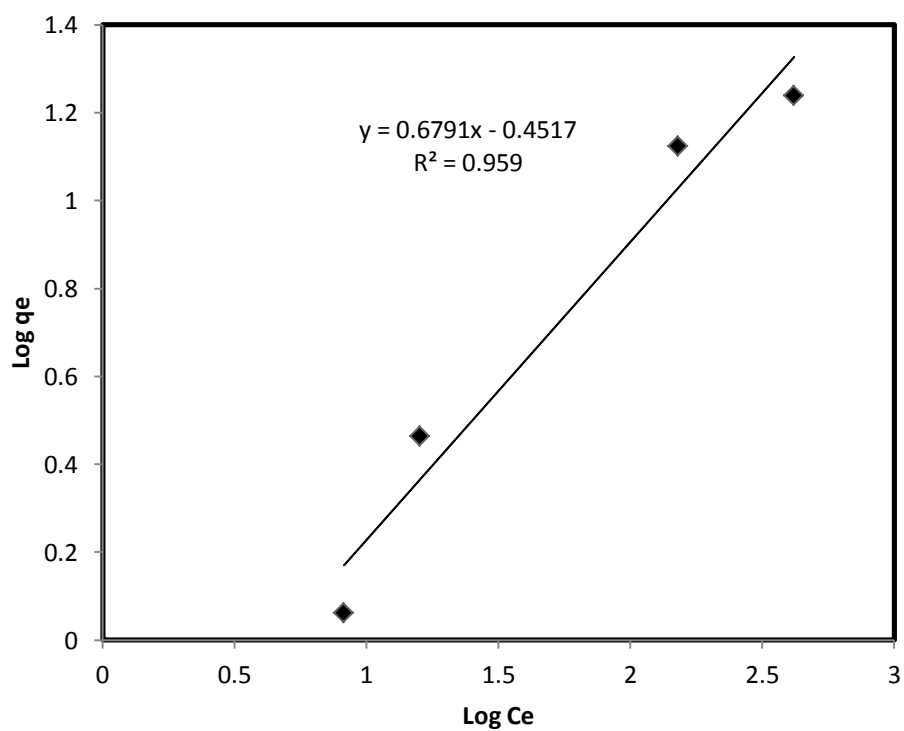


Figure 44. Freundlich Isotherm of Chitosan-Coated Kaolinite

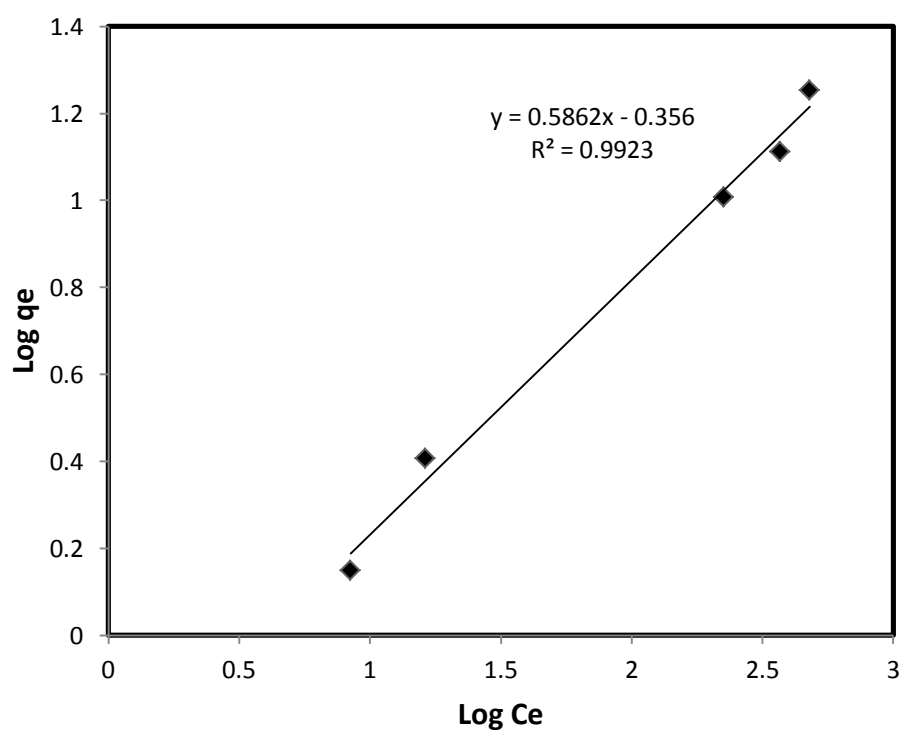


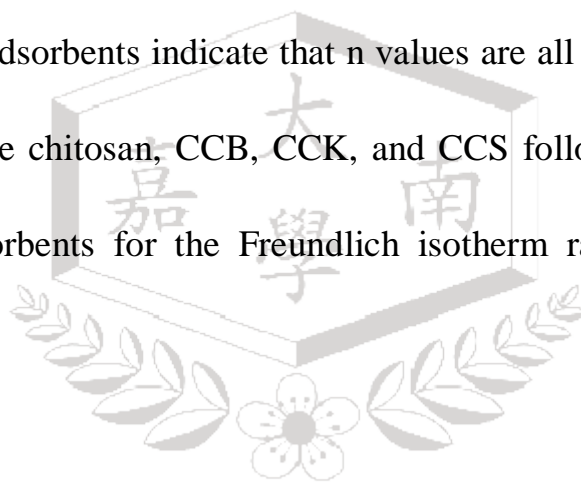
Figure 45. Freundlich Isotherm of Chitosan-Coated Sand

Table 9. Freundlich Constants under Different Adsorbents

Adsorbent	R^2	K_F	$1/n$	n
AC	0.9351	0.0838	0.6274	1.5939
pure chitosan	0.9939	0.0561	0.8443	1.1844
CCB	0.912	0.1036	0.8162	1.2252
CCK	0.959	0.3530	0.6791	1.4725
CCS	0.9923	0.4406	0.5862	1.7059

Table 9 indicates the values of $1/n$ which is the intensity of the attraction of the arsenic ions to the adsorbent. Freundlich isotherm revealed that all adsorbents have n value greater than 1 (if $1/n$ is less than 1, this means that the n value is greater than 1). Moreover, the n value was also essential in the sorption mechanism. When n value is greater than 1, physical sorption is the sorption mechanism. If n value is equal to 1, it is considered to be linear. Chemisorption is the sorption mechanism, if n value is less than 1.

All of the five adsorbents indicate that n values are all greater than 1, which proves that AC, pure chitosan, CCB, CCK, and CCS follow physical sorption. The R^2 of the adsorbents for the Freundlich isotherm ranges from 0.912 to 0.9939.



4.4.2 Langmuir model

The Langmuir model assumes that the solute is adsorbed on a finite number of binding sites with the same energy levels found on a homogenous surface. Langmuir isotherm is described as adsorption occurring on a monolayer surface coverage where there is no net interaction between adsorbed molecules.

Langmuir isotherm model is the most suitable for monolayer adsorption

based on the assumption described that there are finite numbers of adsorption sites. All sites are equivalent and there is no interaction between adsorbed ions. The result indicates the applicability of monolayer coverage on the surface of adsorbents in spite of the surface modification.

The experimental data are plotted against the linear plots generated by the Langmuir equation (eq.5, eq.6), shown as Figures 46, 47, 48, 49, and 50. The parameters calculated by Langmuir models are arranged in Table 10.

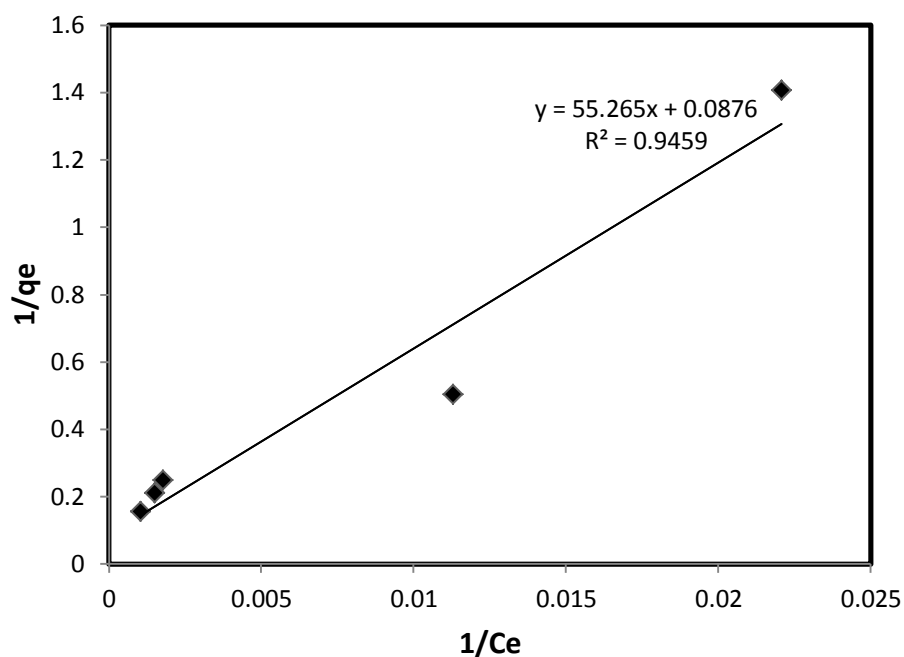


Figure 46. Langmuir Isotherm of Activated Carbon

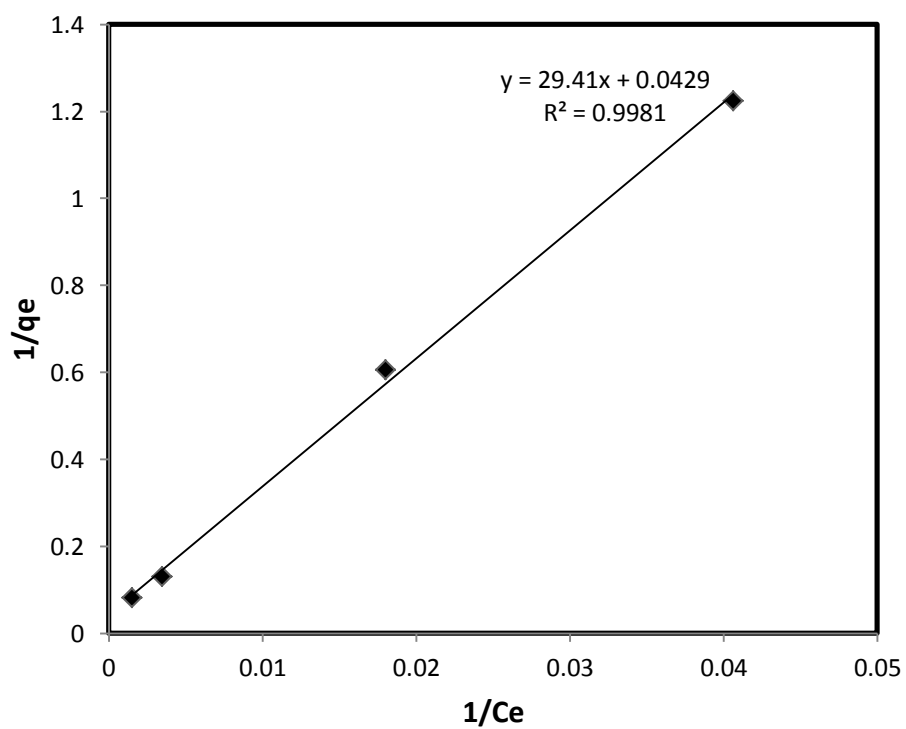


Figure 47. Langmuir Isotherm of Pure Chitosan

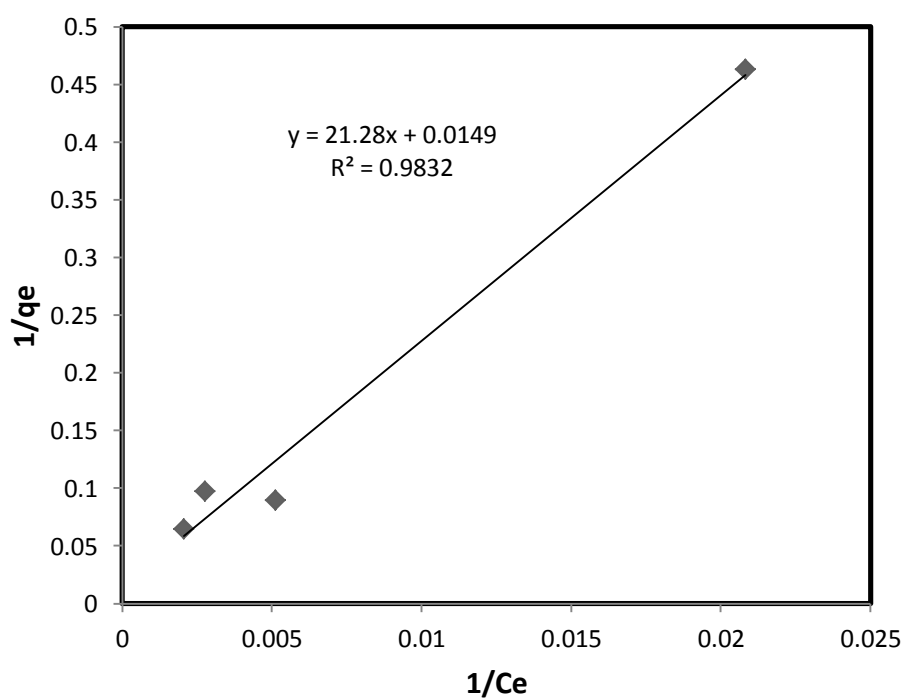


Figure 48. Langmuir Isotherm of Chitosan -Coated Bentonite

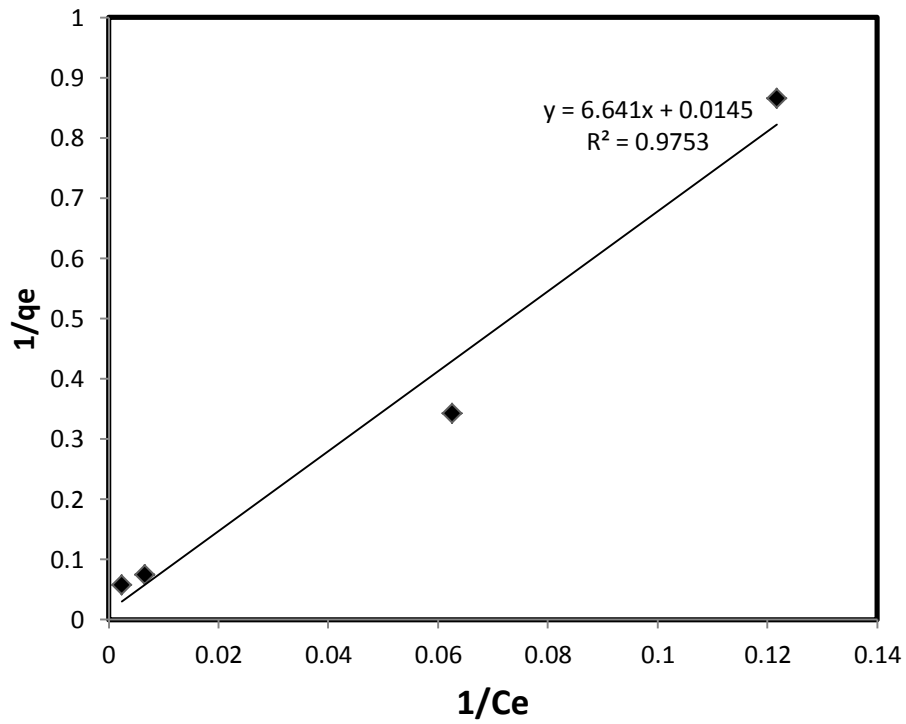


Figure 49. Langmuir Isotherm of Chitosan-Coated Kaolinite

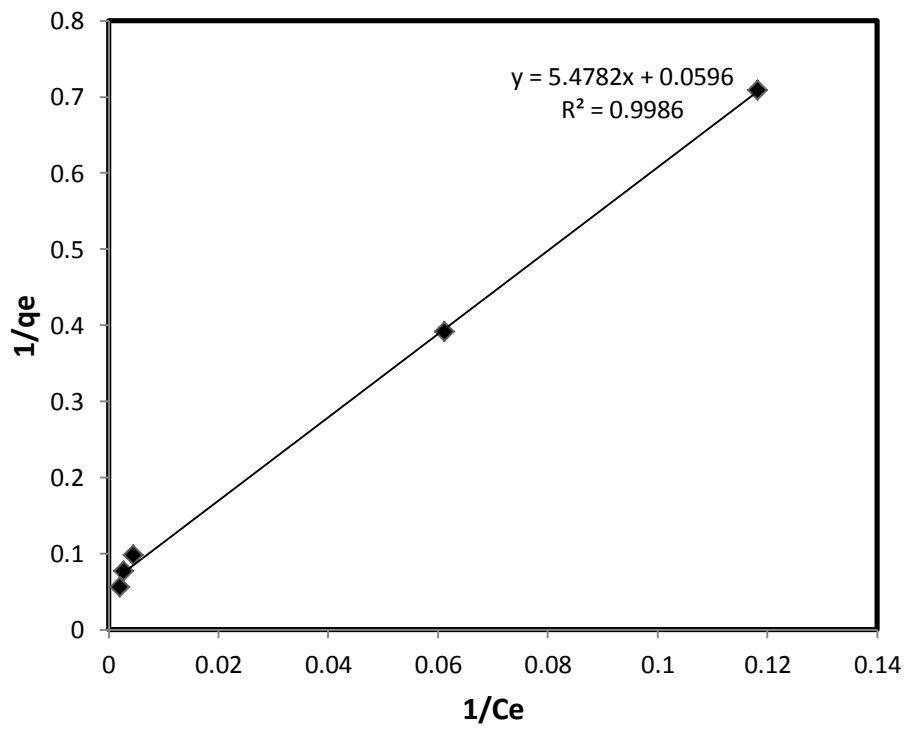


Figure 50. Langmuir Isotherm of Chitosan-Coated Sand

Table 10. Langmuir Constants under Different Adsorbents

Adsorbent	R^2	b	q_{mL}
AC	0.9459	0.0016	11.4155
pure chitosan	0.9981	0.0015	23.3100
CCB	0.9832	0.0007	67.1141
CCK	0.9753	0.0022	68.9655
CCS	0.9986	0.0109	16.7785

Compared to Table 9 and Table 10, AC, Chitosan, CCB, CCK and CCS best fits the Langmuir isotherm with high correlation coefficient values ($R^2 > 0.99$). This implies that As(V) ions form a monolayer coverage on the homogenous surface of the adsorbent. On the other hand, Figure 53-56 illustrate a good fit to the linear plots based on the Langmuir isotherm. This result agrees with the obtained correlation coefficient values (R^2) listed in Table 15.

The maximum adsorption capacity of AC, pure chitosan, CCB, CCK, and CCS are 11.41553, 23.31002, 67.11409, 68.96552, and 16.77852 respectively. This result indicates that the adsorption capacity of the adsorbents follows the trend of CCK > CCB > pure chitosan > CCS > AC. AC removes As(V) using –OH, which is the functional group. The electron of –OH is harder to share than

the -NH_2 , so it has the least adsorption capacity. For the composites, the sequence, $\text{CCK} > \text{CCB} > \text{CCS}$, is due to the negative surface charges of the carrier which follows the sequence: kaolinite > bentonite > sand.

Langmuir model could also determine that the adsorbents are belong to favorable adsorption or not. Table 11 shows the R_L of adsorbents under Langmuir isotherm. R_L value is the indication to prove the adsorbent is a favorable adsorption or unfavorable adsorption. If the R_L value < 1 , it is the favorable adsorption. If the $R_L > 1$, it depicts an unfavorable adsorption. In this study, all adsorbents under different concentrations illustrate R_L values are all less than 1, which indicates that AC, pure chitosan, CCB, CCK, and CCS are belong to favorable adsorption.

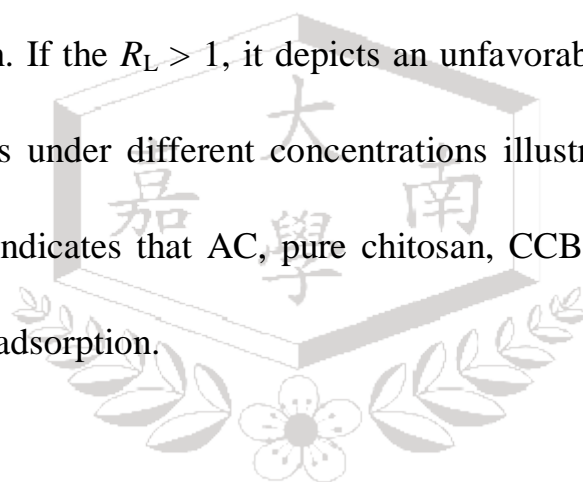


Table 11. R_L of Adsorbents from Langmuir Isotherm

Adsorbent	R_L			
	50(ppb)	100(ppb)	500(ppb)	1000(ppb)
AC	0.9266	0.8632	0.5579	0.3869
pure chitosan	0.9320	0.8727	0.5782	0.4067
CCB	0.9662	0.9346	0.7407	0.5882
CCK	0.9016	0.8208	0.4781	0.3142
CCS	0.6477	0.4790	0.1553	0.0842

4.4.3 Dubinin-Radushkevich model

The Dubinin-Radushkevich (D-R) isotherm model was chosen to estimate the characteristic porosity of the adsorbents and the apparent energy of adsorption. It could indicate that the adsorption mechanism is chemical, physical, or nature adsorption.

The experimental data are plotted against the linear plots generated by the Dubinin-Radushkevich (D-R) (eq.8, eq.9), shown as Figures 51, 52, 53, 54, and 55. The parameters calculated by Dubinin-Radushkevich models are arranged in Table 12.

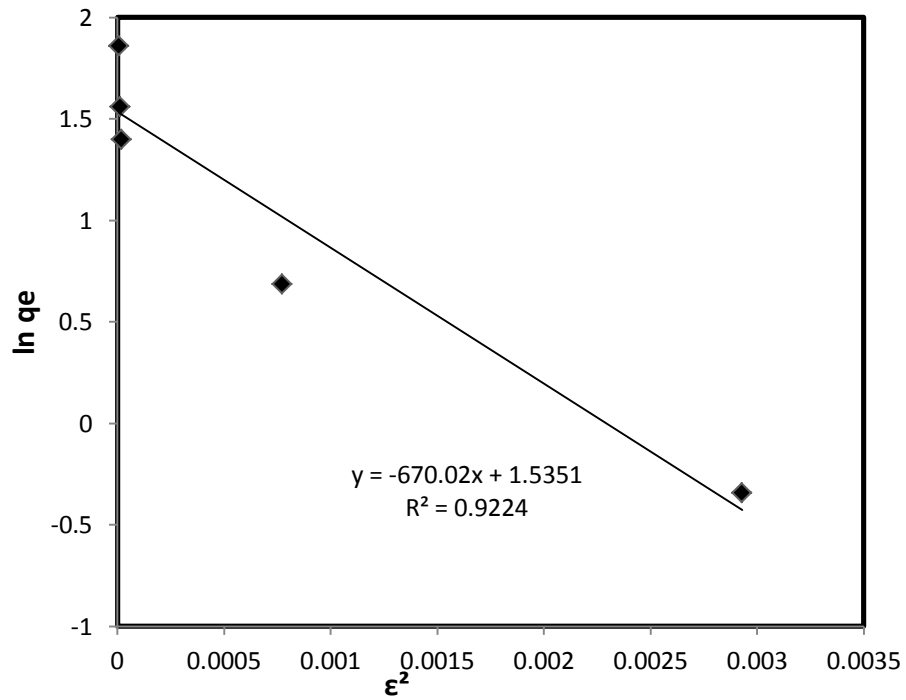


Figure 51. Dubinin-Radushkevich Isotherm of Activated Carbon

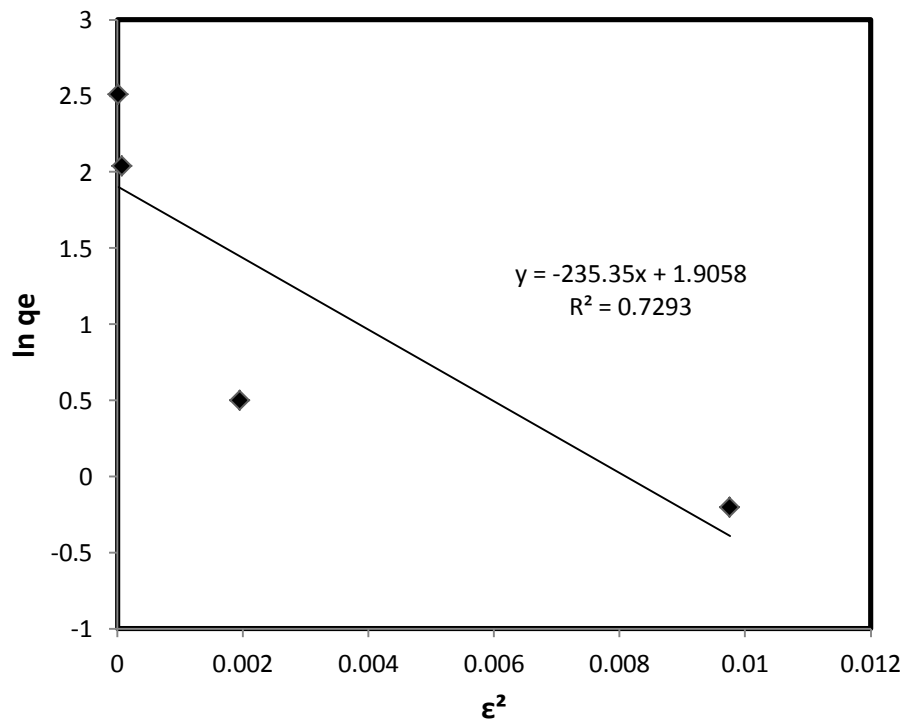


Figure 52. Dubinin-Radushkevich Isotherm of Pure Chitosan

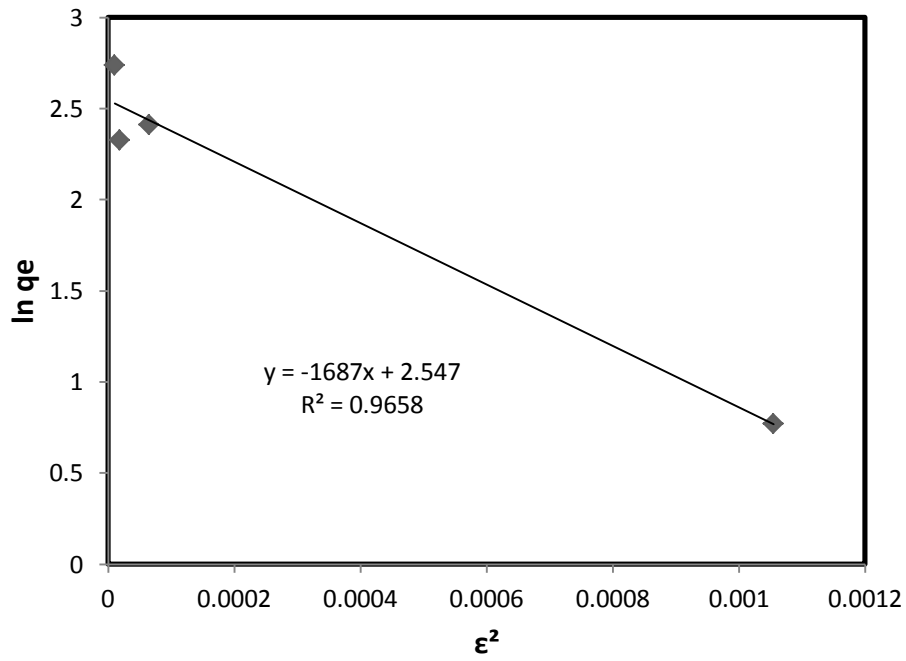


Figure 53. Dubinin-Radushkevich Isotherm of Chitosan-Coated Bentonite

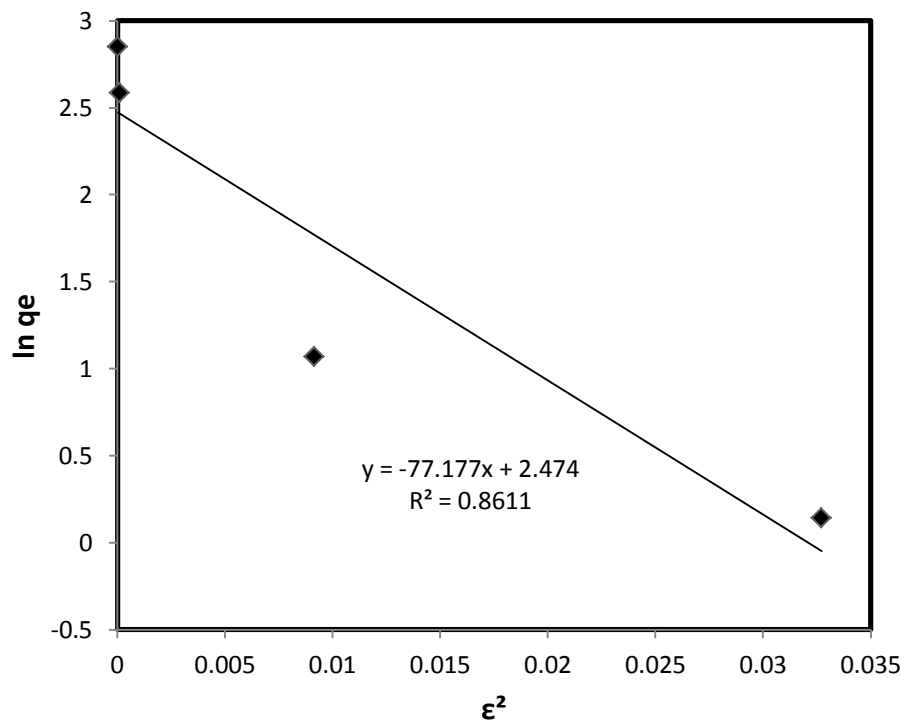


Figure 54. Dubinin-Radushkevich Isotherm of Chitosan-Coated Kaolinite

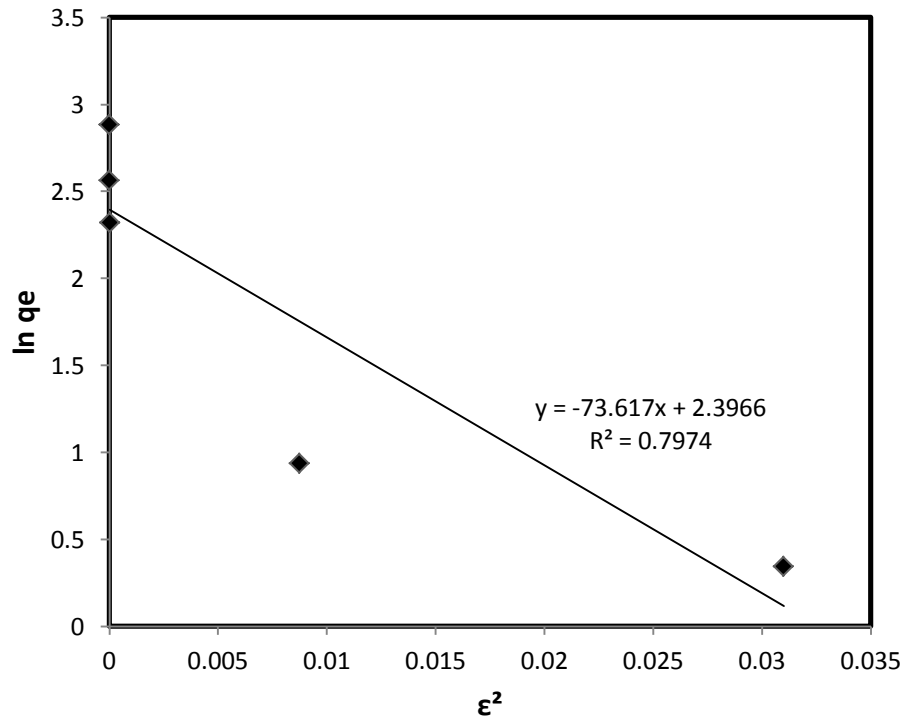


Figure 55. Dubinin-Radushkevich Isotherm of Chitosan-Coated Sand

Table 12. Contacts of D-R Model Using Different Adsorbents

Adsorbent	R^2	β	q_m	$E(kJ)$
AC	0.9224	-670.02	4.6418	0.0273
pure chitosan	0.7293	-235.35	6.7248	0.0461
CCB	0.9658	-1687.00	12.7687	0.01722
CCK	0.8611	-77.18	11.8698	0.0805
CCS	0.7974	-73.63	10.9858	0.0824

R^2 values of the D-R model of AC, pure chitosan, CCB, CCK, and CCS are 0.9224, 0.7293, 0.9658, 0.8611, and 0.7974 respectively. These values are lower compared to the R^2 of Langmuir isotherm, which indicates that these five adsorbents still fit well with Langmuir isotherm.

The most important application of the D-R isotherm is computing for the energy of adsorption (E). The value of E would determine the dominant mechanism of the adsorption experiments, whether it is physical adsorption ($E < 8$ kJ), ion-exchange mechanism ($8 \text{ kJ} < E < 16$ kJ) or chemisorption ($E > 16$ kJ). Table 12 shows that the five adsorbents follow physical adsorption, which means that desorption can be applied to these adsorbents in order to recover the heavy metal ions. Physical adsorption depends on the specific surface area.

4.5 Fourier Transformation-Infrared Analysis

The Fourier transformation-infrared (FT/IR) spectroscopy can determine the functional groups of the adsorbents using the recorded spectra, which can be found in the appendix. Based on the previous researches, there are two functional groups of chitosan that were used for the adsorption, including -OH and C=C . Their respective wavelength ranges are shown on the table 5.

Table 13. FT/IR of AC (before and after adsorption)

IR peak	Peak value(cm^{-1})			Functional group
	Before adsorption	After adsorption	Difference	
1	3423	3425	2	-OH
2	2362	2362	0	-C=C

Table 13 shows the peak values of active carbon (AC) before and after adsorption. If the peak value changes, this means that the functional groups of the adsorbent has bonded with arsenate. Two function groups are found for AC, including -C=C and -OH, at 2362 and 3423 cm^{-1} , respectively. After adsorption, the values became 2362 and 3425. -OH stretching was observed at 3425, which shows that -OH functional group of AC are used to catch the arsenate.

Table 14 shows the peak values of pure chitosan before and after adsorption. Chitosan has two function groups, such us -OH and -NH₂, which are interpreted by the peaks at 2922 and 3429 cm^{-1} , respectively. Based on the Table 14, the peak value of -NH₂ functional group changed from 3429 to 3449. It confirmed that -NH₂ group is the main function for chitosan adsorption. It is different from AC, which uses -OH to remove As(V), because the -NH₂ groups easily shares

electrons than –OH groups.

Table 14. FT/IR of Pure Chitosan (before and after adsorption)

IR peak	Peak value(cm^{-1})			Functional group
	Before adsorption	After adsorption	Difference	
1	2922	2922	0	-OH
2	3429	3449	20	-OH or –NH ₂

Table 15 shows the peak values of CCB before and after adsorption,. CCB has three function groups, such as –N-H, –NH₂ or –OH and –NH₂, which are interpreted by the peaks at 3613, 3450, and 1641 cm^{-1} , respectively. Based on the Table 7, the peak values of -OH and –NH₂ functional group changed from 3450 to 3448, and it of –NH₂ changed from 1641 to 1640, respectively. It confirmed that –NH₂ group is the main function for CCB adsorption.

Table 15. FT/IR of Chitosan Coated on Bentonite

(before and after adsorption)

IR peak range	Peak value			Functional group
	Before adsorption	After adsorption	Difference	
1	3612	3612	0	-N-H
2	3450	3448	-2	-OH or -NH ₂
3	1641	1640	-1	-NH ₂

Table 16 shows the peak values of CCK before and after adsorption,. CCK has three types of functional groups, such us -N-H, -NH₂ or -OH and -NH₂, which are interpreted by the peaks at 3619, 3695, 3431, and 1628 cm⁻¹, respectively. Based on the Table 8, the peak values of -OH and -NH₂ functional group changed from 3431 to 3430, and it of -NH₂ changed from 1628 to 1631, respectively. It confirmed that -NH₂ group is the main function for CCK adsorption.

Table 16. FT/IR of Chitosan Coated on Kaolinite

(before and after adsorption)

IR peak range	Peak value			Functional group
	Before adsorption	After adsorption	Difference	
1	3695	3695	0	-N-H
2	3619	3619	0	-N-H
3	3431	3430	-1	-OH or -NH ₂
4	1628	1631	3	-NH ₂

Table 17 shows the peak values of CCS before and after adsorption,. CCS has three types of functional groups, such as -N-H, -OH, -NH₂ or -OH and -NH₂, which are interpreted by the peaks at 3696, 3657, 3428 and 1628 cm⁻¹, respectively. Based on the Table 9, the peak values of -OH and -NH₂ functional group changed from 3428 to 3426, and it of -NH₂ changed from 1628 to 1595, respectively. It confirmed that -NH₂ group is the main function for CCS adsorption.

Table 17. FT/IR of Chitosan Coated on Sand (before and after adsorption)

IR peak range	Peak value			Functional group
	Before adsorption	After adsorption	Difference	
1	3696	3696	0	-N-H
2	3657	3657	0	-OH
3	3428	3426	-2	-OH or -NH ₂
4	1628	1595	33	-NH ₂

Notably, chitosan has the highest adsorption capacity among the biopolymers. Base on the above studies, the structure of chitosan and chitosan derived adsorbents contain chemically active functional groups such as hydroxyl (-OH) and amino (-NH₂) that serves as efficient sites to bind metal ions.

4.6 Adsorption Thermodynamic studies

In thermodynamic study, the temperatures used start at 25° to 55°C. The adsorption capacities at different temperatures were also computed. The thermodynamic parameters, Gibb's free energy (ΔG), enthalpy (ΔH), and

entropy (ΔS), are listed in Tables 18 and 19. The Gibb's free energy will tell if the adsorption process is spontaneous or non-spontaneous, when the ΔG is negative and positive respectively. The ΔH determines if the process is exothermic or endothermic, when the value is negative and positive respectively. If the ΔH is high, the adsorption capacity of all adsorbents will be low.

Table 18. Thermodynamic of Arsenic Using Different Adsorbents

Adsorbent	Pure chitosan	AC	CCK	CCB	CCS
Temp (K)	ΔG^0				
298	0.4369	3.1754	-2.6650	-1.6049	-0.0951
308	0.2452	2.5297	-3.0087	0.0070	1.5761
318	0.0484	2.0236	-3.6219	-0.0059	1.4151
328	0.2917	2.1991	-3.8548	-3.8548	2.5563

Table 18 shows the ΔG values of the different adsorbents from 25°C to 55°C. Pure chitosan got a positive value as well as activated carbon, which means that both are non-spontaneous. CCK got negative values for the temperatures 25°C to 55°C, which means that it is spontaneous. The arsenate ions find the functional group by itself. CCB also illustrates the same trend with

CCK, however, when the temperature reached 35 °C, it became non-spontaneous. Moreover, CCS is spontaneous when the temperature is 25 °C, but it becomes non-spontaneous at the other temperatures. When ΔG gets more negative, the adsorption capacity of the adsorbents increases because it will be more spontaneous. Thus, Table 19 lists the respective adsorption capacities of the adsorbents.

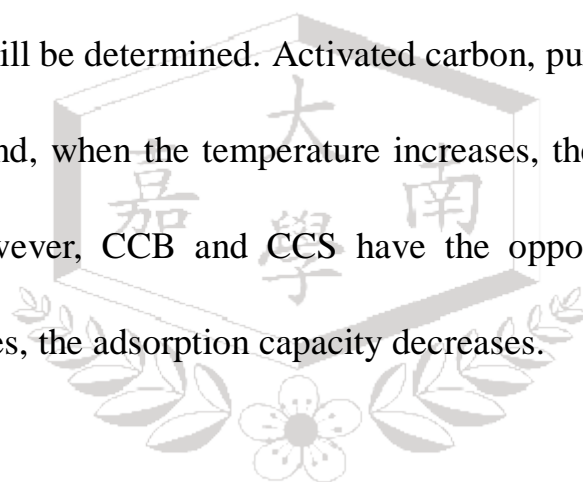
Table 19. Adsorption Capacity of Different Temperature

Adsorbent	AC	Pure chitosan	CCK	CCB	CCS
Temp(K)		Q _e			
298	7.447	4.541	13.308	11.181	8.745
308	8.420	4.799	13.512	8.8305	6.204
318	8.762	5.615	14.1015	8.9415	6.531
328	8.370	5.459	14.2245	10.4145	4.977

In this study, figures 56, 57, 58, 59, and 60 show the trend of the adsorption capacity of the five adsorbents. It indicated that the removal of arsenate by adsorbents illustrate big difference from one temperature to another. This is

because that the arsenate ion has a higher energy in the solution at higher temperatures where make the ions move faster. Under this temperature, arsenic ions have more chances in colliding with the adsorbents. Moreover, since all the adsorbents follow physical sorption, desorption can be applied. The thickness of the boundary layer decreases at high temperature, which makes it easier to desorb the ions.

Despite this, the trend of adsorption capacity respected to corresponding temperature could still be determined. Activated carbon, pure chitosan, and CCK follow the same trend, when the temperature increases, the adsorption capacity also increases. However, CCB and CCS have the opposite trend, when the temperature increases, the adsorption capacity decreases.



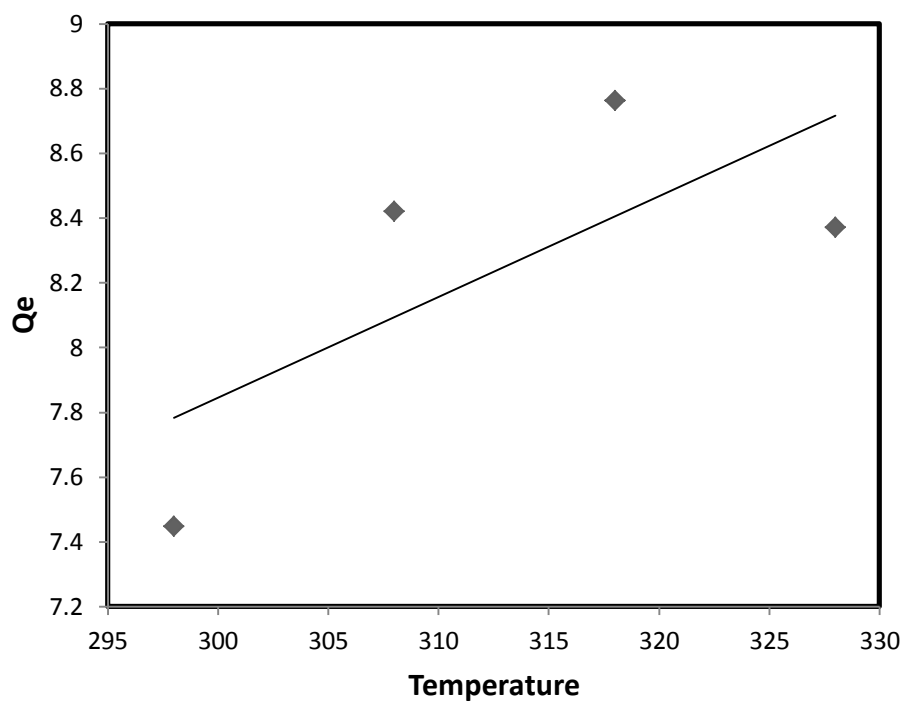


Figure 56. Adsorption Capacity of Activate Carbon

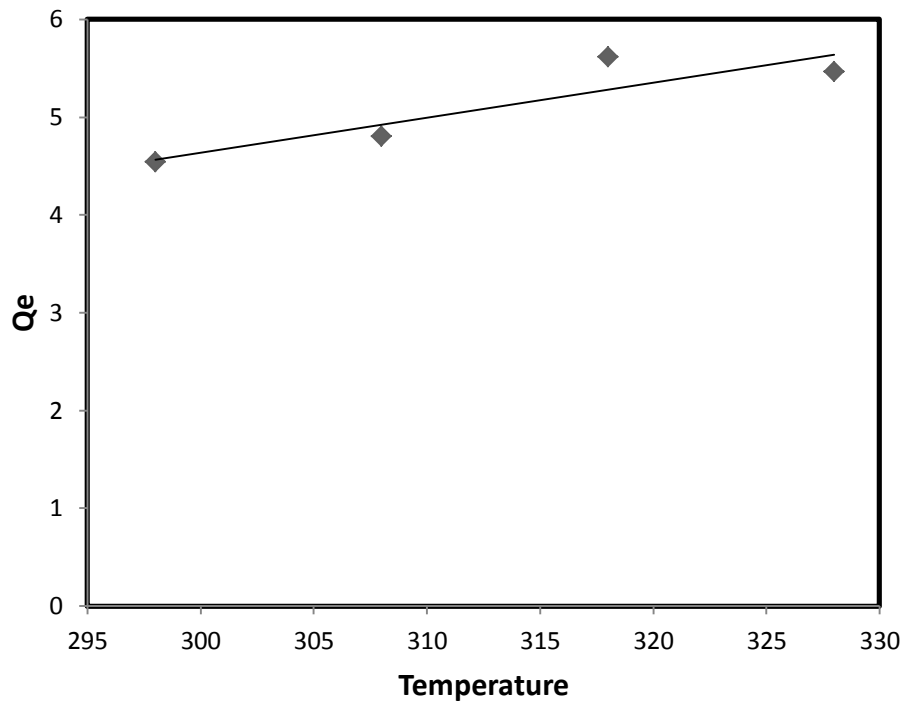


Figure 57. Adsorption Capacity of Pure Chitosan

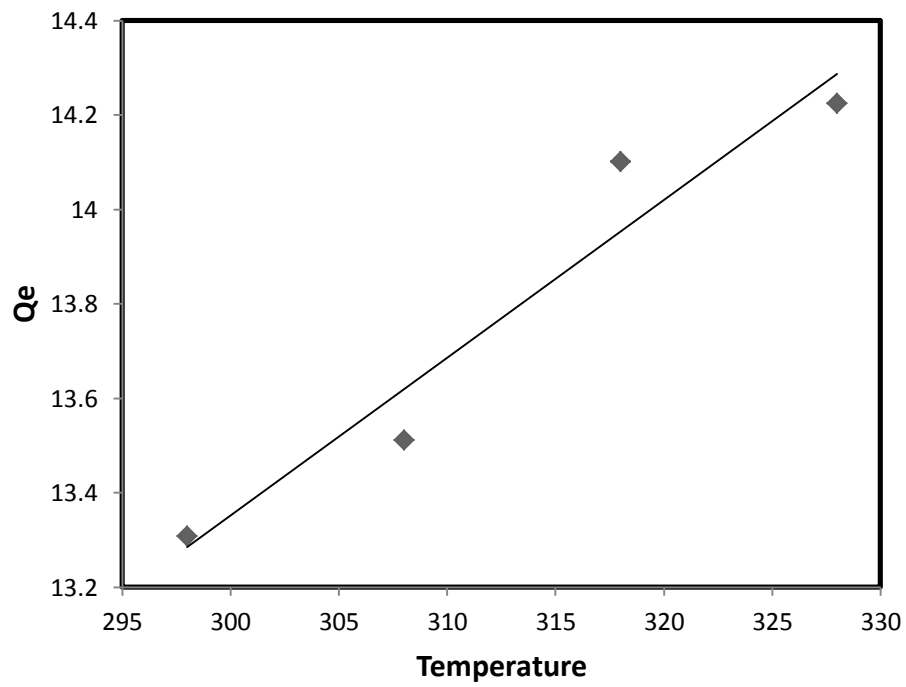


Figure 58. Adsorption Capacity of Using Chitosan-Coated Kaolinite

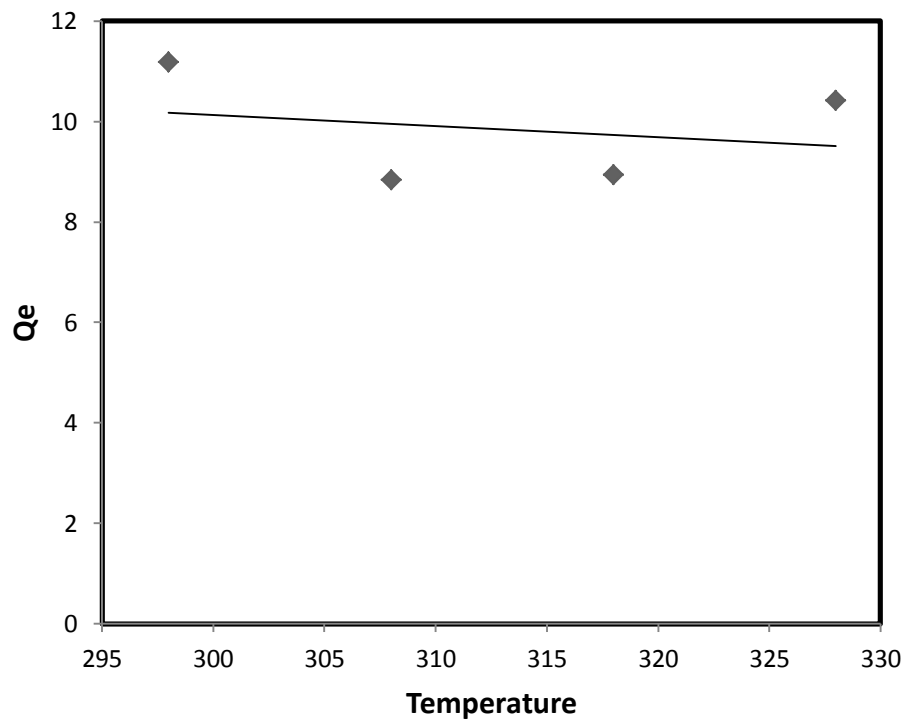


Figure 59. Adsorption Capacity of Chitosan -Coated Bentonite

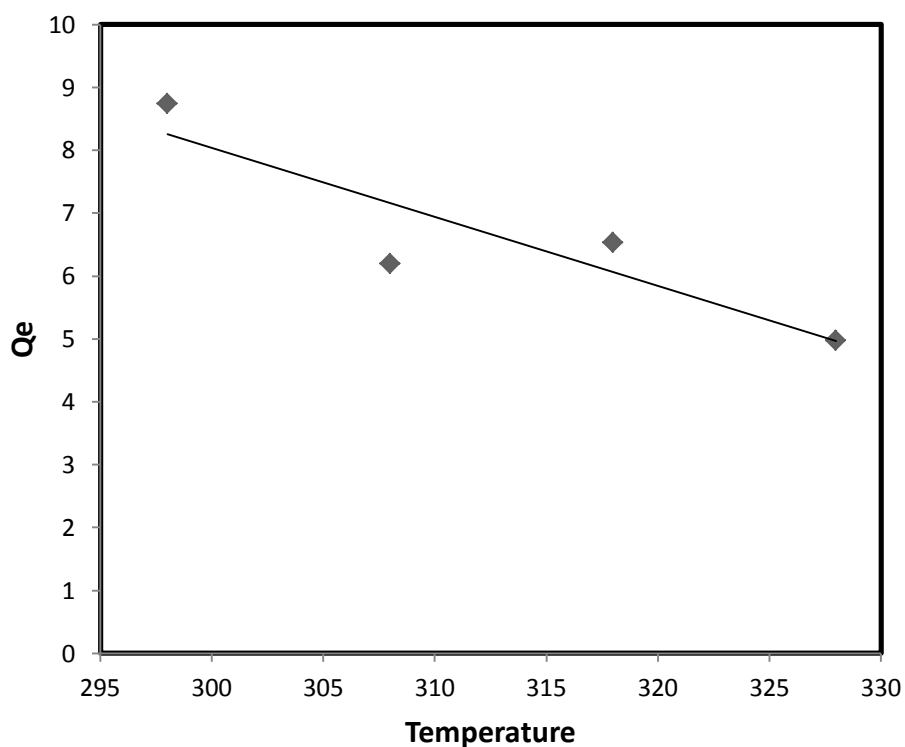


Figure 60. Adsorption Capacity of Chitsan-Coated Sand

Figure 61 and table 20 show the thermodynamic parameters, ΔH and ΔS , of the five adsorbents. Chitosan, AC, and CCK have positive values which mean that they are endothermic. When the temperature of the solution is high, the adsorption capacity will increase. However, CCB and CCS have negative values, which mean that they are exothermic. When the temperature is high, the adsorption capacity will decrease. Moreover, ΔS of all adsorbents is positive which depicts disorder on the solid/liquid interface of the adsorbent. CCS has the most disordered solid/liquid interface while pure chitosan has the least.

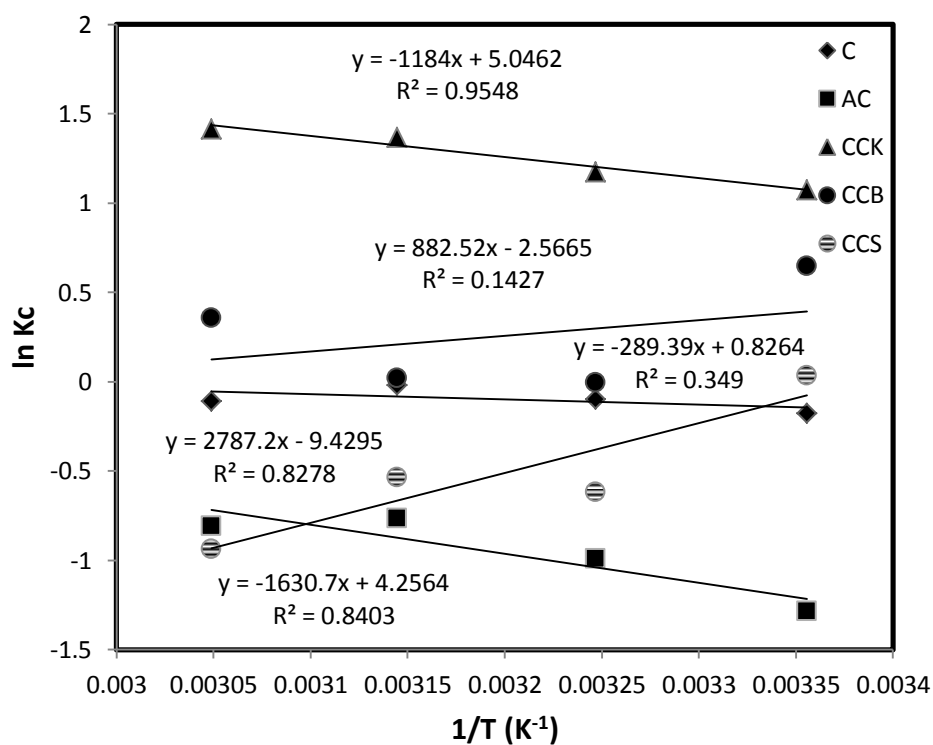


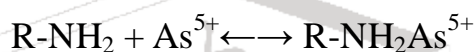
Figure 61. Thermodynamic Study of the Five Adsorbents

Table 20. Thermodynamic Parameters of the Different Adsorbents Using 500 ppb of As(V) Initial Concentration

Adsorbent	slope	y-intercept	ΔH^0 (kJ/mol·K)	ΔS^0 (kJ/mol·K)
chitosan	-289.39	0.8264	2.4061	0.0069
AC	-1630.70	4.2564	13.5585	0.0354
CCK	-1184..00	5.0462	9.8444	0.0420
CCB	882.52	-2.5665	-7.3377	0.0213
CCS	2787.20	-9.4295	-23.1742	0.0784

4.7 Adsorption mechanism of As(V) and chitosan

The binding sites of pure chitosan and chitosan composites are the hydroxyl (–OH) and amino (–NH₂) groups. The nitrogen of amino group and the oxygen of hydroxyl group have an attraction with heavy metal ions. The oxygen atom in the hydroxyl group has a stronger attraction to each oxygen atom, hence; the electron of the nitrogen atom in the amino group therefore the amino group is more likely to donate the lone pairs to the heavy metal ions.



According to the isotherm studies, As(V) follows the Langmuir isotherm, indicating that it binds to one type of functional group in pure chitosan and chitosan of composites, which is the amino group. On the other hand IR mentions how many –NH₂ group to binding of As(V) as shown on figure 62.

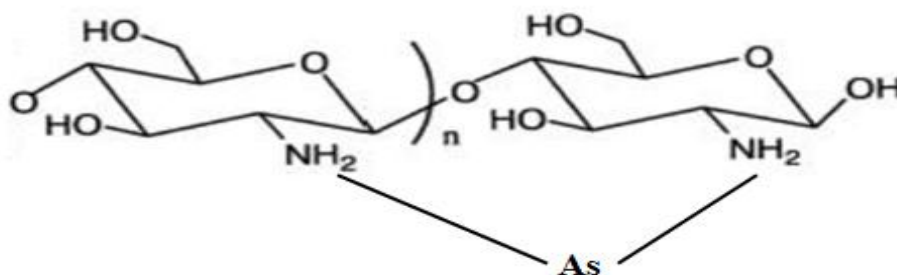


Figure 62. Adsorption mechanism of As(V) and chitosan

Chapter 5 Conclusion

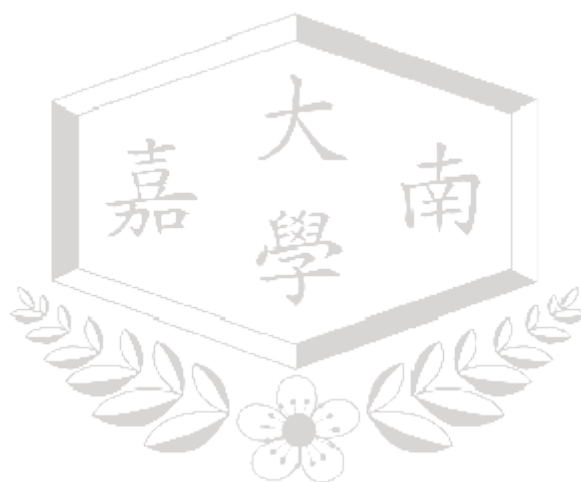
This study used five kinds of adsorbent, including activated carbon, pure chitosan, CCK, CCB, and CCS, to remove arsenate from aqueous solution. The BET, TGA and FT-IR analysis confirmed that the chitosan has successfully coated with supported materials, such as bentonite, kaolinite, and sand.

An increase in the adsorption capacity of the adsorbent beads was observed at higher initial concentration. The adsorption equilibrium could be reached after 12 hours. Under equilibrium conditions, the adsorption isotherm of five adsorbents could be well fitted using the Langmuir isotherm, which describes monolayer coverage on a homogeneous adsorbent surface. The adsorption capacity is $CCK > CCB > \text{Chitosan} > CCS > AC$. The maximum adsorption capacity of AC, chitosan, CCB, CCK, and CCS, are 11.41553, 23.31002, 67.11409, 68.96552, and 16.77852 ($\mu\text{g/g}$) respectively.

The overall kinetic data was best described by the pseudo-second-order equation, which suggests that chemisorption is the rate-determining step. Moreover, Thermodynamic study applied the temperatures 25° to 55°C. The Gibb's free energy of AC and chitosan are non-spontaneous, CCK is spontaneous, CCB is only non-spontaneous at 35°C, and CCS is only spontaneous at 25°C. The

more negative the value of ΔG , the adsorption capacity increases. The AC, chitosan, and CCK are exothermic, while CCB and CCS are endothermic.

This study has evidenced that the possible adsorption behavior of CCK, CCB, and CCS to remove arsenate from aqueous solution. In conclusion, these preliminary results indicate the possibility of using CCK, CCB, and CCS to establish inexpensive large-scale filters as a permeable reactive barrier for metal removal in nature groundwater resources or contaminated groundwater plumes.



References

- Ahalya, N., Ramachandra, T., & Kanamadi, R. (2003). Biosorption of Heavy Metals. *Research Journal Of Chemistry And Environment*, 71-79.
- Alkan, M., Kalay, B., Dogan, M., & Demirbas, O. (2008). Removal of copper ions from aqueous solutions by kaolinite and batch design. *Journal of Hazardous Materials*, 867–876.
- Altundogan, H., Altundogan, S., Tumen, F., & Bildik, M. (2002). Arsenic adsorption from aqueous solutions by activated red mud. *Waste Management*, 357–363.
- Anirudhan, T., & Rijith, S. (2012). Synthesis and characterization of carboxyl terminated poly(methacrylic acid) grafted chitosan/bentonite composite and its application for the recovery of uranium(VI) from aqueous media. *Journal of Environmental Radioactivity*, 8-19.
- Bauer, M., & Blodau, C. (2006). Mobilization of arsenic by dissolved organic matter from iron oxides, soils and sediments. *Science of the Total Environment*, 179– 190.
- Bhattacharyya, K. G., & Gupta, S. S. (2008). Adsorption of a few heavy metals on natural and modified kaolinite and montmorillonite: A review. *Advances in Colloid and Interface Science*, 114–131.
- Boddu, V. M., Abbur, K., Talbott, J. L., & Smith, E. D. (2003). Removal of Hexavalent Chromium from Wastewater Using a New Composite Chitosan Biosorbent. *Environ. Sci. Technol*, 4449-4456.

- Boddu, V. M., Abburi, K., & Talbott, J. L. (2008). Removal of arsenic (III) and arsenic (V) from aqueous medium using chitosan-coated biosorbent. *WATER RESEARCH*, 633 -642.
- Chang, Q., Lin, W., & Ying, W. c. (2010). Preparation of iron-impregnated granular activated carbon for arsenic removal from drinking water. *Journal of Hazardous Materials*, 515–522.
- Chen, C. Y., Chang, T. H., Kuo, J. T., Chen, Y. F., & Chung, Y. C. (2008). Characteristics of molybdate-impregnated chitosan beads (MICB) in terms of arsenic removal from water and the application of a MICB-packed column to remove arsenic from wastewater. *Bioresource Technology*, 7487–7494.
- Choong, T. S., Chuah, T., Robiah, Y., Koay, F. G., & Azni, I. (2007). Arsenic toxicity, health hazards and removal techniques from water: an overview. *Desalination*, 139–166.
- Chuang, C., Fan, M., Xu, M., Brown, R., Sung, S., Saha, B., et al. (2005). Adsorption of arsenic(V) by activated carbon prepared from oat hulls. *Chemosphere*, 478–483.
- Dalida, M. L., Mariano, A. F., Futralan, C. M., Kan, C.-C., Tsai, W.-C., & Wan, M.-W. (2010). Adsorptive removal of Cu(II) from aqueous solutions using non-crosslinked and crosslinked chitosan-coated bentonite beads. *Desalination xxx*, 1-6.
- Dou, X., Li, R., Zhao, B., & Liang, W. (2010). Arsenate removal from water by zero-valent iron/activated carbon galvanic couples. *Journal of Hazardous Materials*, 108–114.

- Gavrilescu, M. (2004). Removal of Heavy Metals from the Environment by Biosorption. *Eng. Life Sci.*, 219-232.
- Gérente, C., Andrès, Y., McKay, G., & Cloirec, P. L. (2010). Removal of arsenic(V) onto chitosan: From sorption mechanism explanation to dynamic water treatment process. *Chemical Engineering Journal*, 593–598.
- Goldberg, S. (2002). Competitive Adsorption of Arsenate and Arsenite on Oxides and Clay Minerals. *Soil Sci. Soc. Am. J.*, 413-421.
- Gomez-Serrano, V., Pastor-Villegas, J., Perez-Florindo, A., Duran-Valle, C., & Valenzuela-Calahorro, C. (1996). FT-IR study of rockrose and of char and activated carbon. *Journal of Analytical and Applied Pyrolysis*, 71-80.
- Grisdanurak, N., Akewaranugulsiri, S., Futralan, C. M., Tsai, W.-C., Kan, C.-C., Hsu, C.-W., et al. (2011). The Study of Copper Adsorption from Aqueous Solution Using Crosslinked Chitosan Immobilized on Bentonite. *Journal of Applied Polymer Science*, 132-142.
- Guibal, E. (2005). Heterogeneous catalysis on chitosan-based materials: a review. *Prog. Polym. Sci.*, 71–109.
- Gupta, A., Chauhan, V. S., & Sankararamakrishnan, N. (2009). Preparation and evaluation of iron–chitosan composites for removal of As(III) and As(V) from arsenic contaminated real life groundwater. *Water Research*, 3862-3870.
- Harris, P. J., Liu, Z., & Suenaga, K. (2008). Imaging the atomic structure of activated carbon. *J. Phys.: Condens. Matter*, 1-5.

- Ho, Y. S. (2006). Second-order kinetic model for the sorption of cadmium onto tree fern: A comparison of linear and non-linear methods. *Water Research*, 119 – 125.
- Ho, Y., & McKay, G. (1998). A comparison of chemisorption kinetic models applied to pollutant removal on various sorbents. *Institution of Chemical Engineers*, 332-340.
- Hong, H.-J., Kim, H., Baek, K., & Yang, J.-W. (2008). Removal of arsenate, chromate and ferricyanide by cationic surfactant modified powdered activated carbon. *Desalination*, 221–228.
- Ijagbemi, C. O., Baek, M.-H., & Kim, D.-S. (2009). Montmorillonite surface properties and sorption characteristics for heavy metal removal from aqueous solutions. *Journal of Hazardous Materials*, 538–546.
- Jeong, Y., Maohong, F., Leeuwen, J. V., & Belczyk, J. F. (2007). Effect of competing solutes on arsenic(V) adsorption using iron and aluminum oxides. *Journal of Environmental Sciences*, 910–919.
- Lorenzen, L., van Deventer, J., & Landi, W. (1994). Factors affecting the mechanism of the adsorption of arsenic species on activated carbon. *Pergamo*, 557-569.
- Maji, S. K., Pal, A., & Pal, T. (2008). Arsenic removal from real-life groundwater by adsorption on laterite soil. *Journal of Hazardous Materials*, 811–820.
- Mohana, D., & Pittman, C. U. (2007). Arsenic removal from water/wastewater using adsorbents—A critical review. *Journal of Hazardous Materials*, 1-53.

- Ng, J. C., Wang, J., & Shraim, A. (2003). A global health problem caused by arsenic from natural sources. *Chemosphere*, 1353–1359.
- Niu, C. H., Volesky, B., & Cleiman, D. (2007). Biosorption of arsenic (V) with acid-washed crab shells. *Water Research*, 2473 – 2478.
- O'Day, P. A., Parks, G. A., & Brown, G. E. (1994). Molecular structure and binding sites of cobalt(II) surface complexes on kaolinite from X-ray absorption spectroscopy. *Clays and Clay Minerals*, 337-355.
- Pan, G., Chen, J., & Anderson, D. M. (2011). Modified local sands for the mitigation of harmful algal blooms. *Harmful Algae*, 381–387.
- Pontoni, L., & Fabbricino, M. (2012). Use of chitosan and chitosan-derivatives to remove arsenic from aqueous solutions—a mini review. *Carbohydrate Research*.
- Popuri, S. R., Vijaya, Y., Boddu, V. M., & Abburi, K. (2009). Adsorptive removal of copper and nickel ions from water using chitosan coated PVC beads. *Bioresource Technology*, 194–199.
- Ravi Kumar, M. N. (2000). A review of chitin and chitosan applications. *Reactive & Functional Polymers*, 1–27.
- Rinaudo, M. (2006). Chitin and chitosan: Properties and applications. *Prog. Polym. Sci.*, 603–632.
- Sağ, Y., & Aktay, Y. (2002). Kinetic studies on sorption of Cr(VI) and Cu(II) ions by. *Biochemical Engineering Journal*, 143–153.
- Salameh, Y., Al-Lagtah, N., Ahmad, M., Allen, S., & Walker, G. (2010). Kinetic and thermodynamic investigations on arsenic adsorption onto dolomitic sorbents. *Chemical Engineering Journal*, 440–446.

- Schmidt, G. T., Vlasova, N., Zuzaan, D., Kersten, M., & Daus, B. (2008). Adsorption mechanism of arsenate by zirconyl-functionalized activated carbon. *Journal of Colloid and Interface Science*, 228-234.
- Sundararajan, M., Ramaswamy, S., & Raghavan, P. (2009). Evaluation for the Beneficiability of White Silica Sands from the Overburden of Lignite Mine situated in Rajpardi district of Gujarat, India. *Journal of Minerals & Materials Characterization & Engineering*, 701-714.
- Suraj, G., Iyer, C., & Lalithambika, M. (1998). Adsorption of cadmium and copper by modified kaolinites. *Applied Clay Science*, 293–306.
- Tian, Y., Wu, M., Lin, X., Huang, P., & Huang, Y. (2011). Synthesis of magnetic wheat straw for arsenic adsorption. *Journal of Hazardous Materials*, 10–16.
- Vasconcelos, I. F., Haack, E. A., Maurice, P. A., & Bunker, B. A. (2008). EXAFS analysis of cadmium(II) adsorption to kaolinite. *Chemical Geology*, 237–249.
- Vold, I. M., Vaørum, K. M., Guibal, E., & Smidsrød, O. (2003). Binding of ions to chitosan—selectivity studies. *Carbohydrate Polymer*, 471–477.
- Wan Ngah, W. S., Teong, L., & Hanafiah, M. (2011). Adsorption of dyes and heavy metal ions by chitosan compsites: A review. *Carbohydrate Polymers* 83, 1446-1456.
- Wan, M. W., Kan, C. C., Rogel, B. D., & Dalida, M. P. (2010). Adsorption of copper (II) and lead (II) ions from aqueous solution on chitosan-coated sand. *Carbohydrate Polymers*, 891–899.

- Wan, M. W., Petrisor, I. G., Lai, H. T., Kim, D., & Yen, T. F. (2004). Copper adsorption through chitosan immobilized on sand to demonstrate the feasibility for in situ soil decontamination. *Carbohydrate Polymers*, 249–254.
- Wan, M.-W., Kan, C.-C., Lin, C.-H., Rogel, B. D., & Wu, C.-H. (2007). Adsorption of Copper (II) by Chitosan Immobilized on Sand. *嘉南學報*, 96-106.
- Zhao, F., Yu, B., Yue, Z., Wang, T., Wen, X., Liu, Z., et al. (2007). Preparation of porous chitosan gel beads for copper(II) ion adsorption. *Journal of Hazardous Materials*, 67–73.
- Zhu, H.-Y., Jiang, R., & Xiao, L. (2010). Adsorption of an anionic azo dye by chitosan/kaolin/ γ -Fe₂O₃ composites. *Applied Clay Science*, 522–526.
- 甘其銓, 萬孟瑋, 張喬峻, 江尙育, & 程嫻儒. (2008). 幾丁聚醣固化於氫氧化鐵吸附水中二價銅之研究. *嘉南學報*, 257-269.

Appendix: FTIR spectra of Five Different Adsorbents

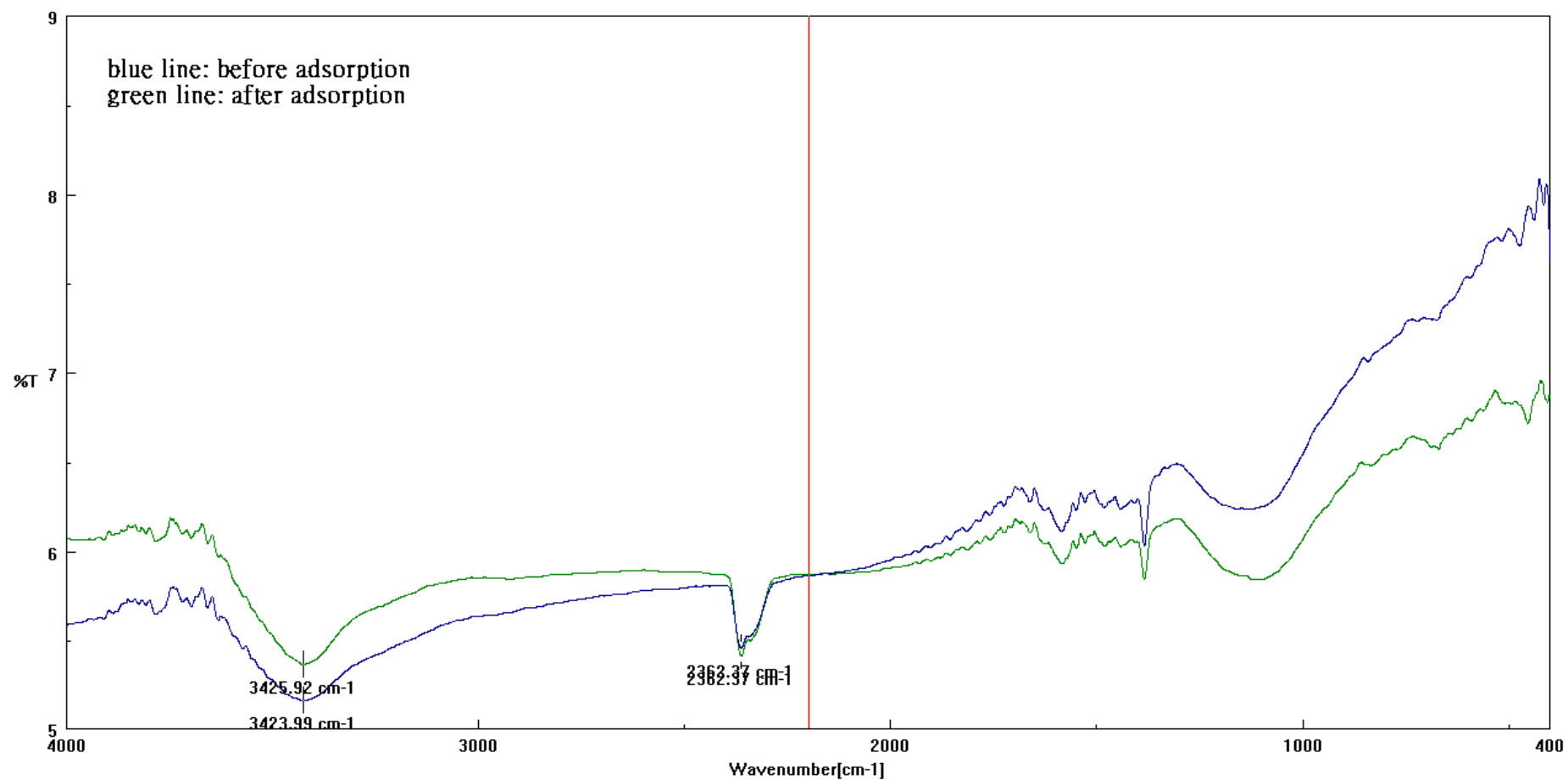


Figure 63. FTIR Spectra of AC Before And After Adsorption

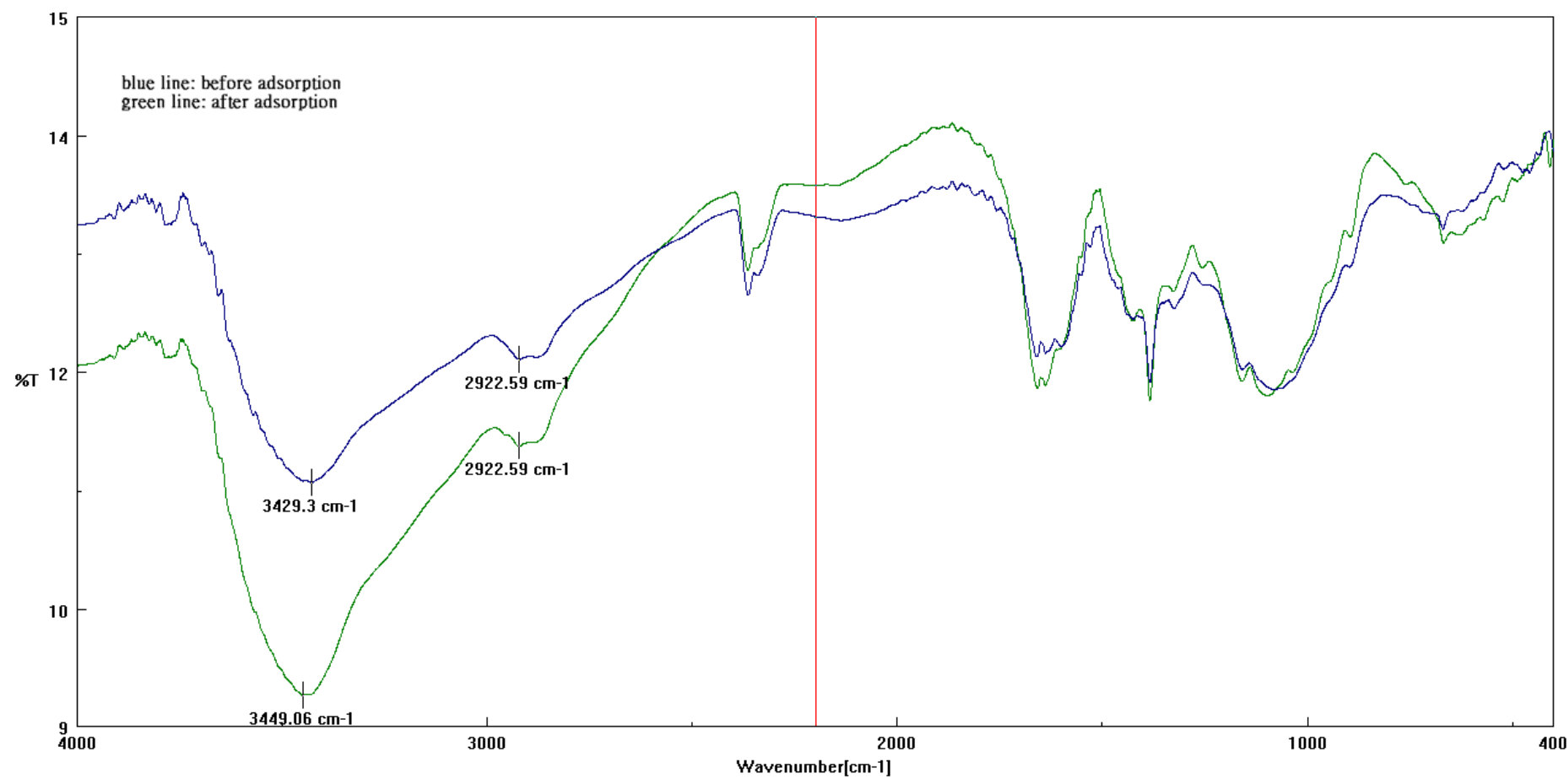


Figure 64. FTIR Spectra of Pure Chitosan Before And After Adsorption

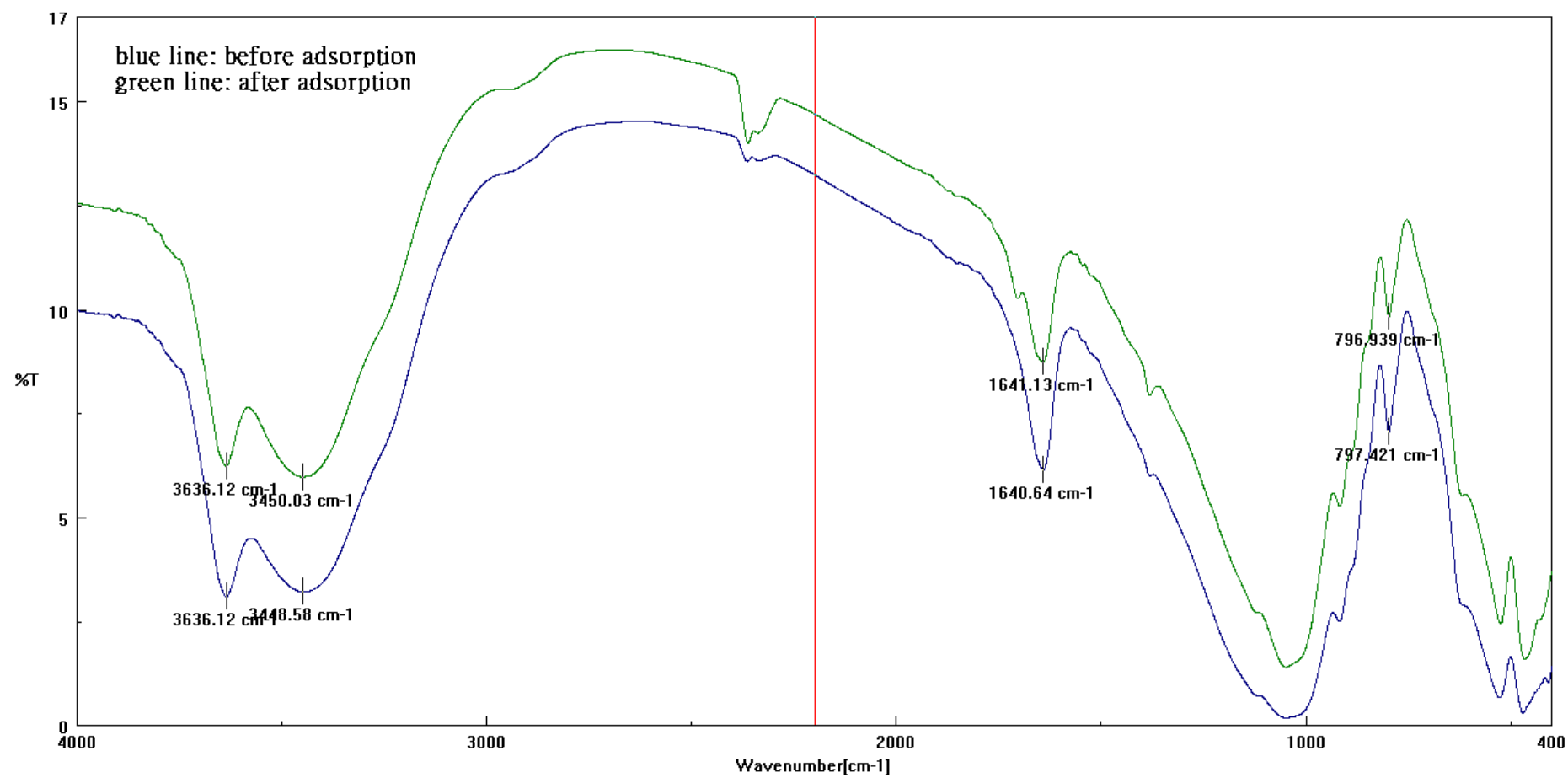


Figure 65.FTIR Spectra of CCB Before And After Adsorption

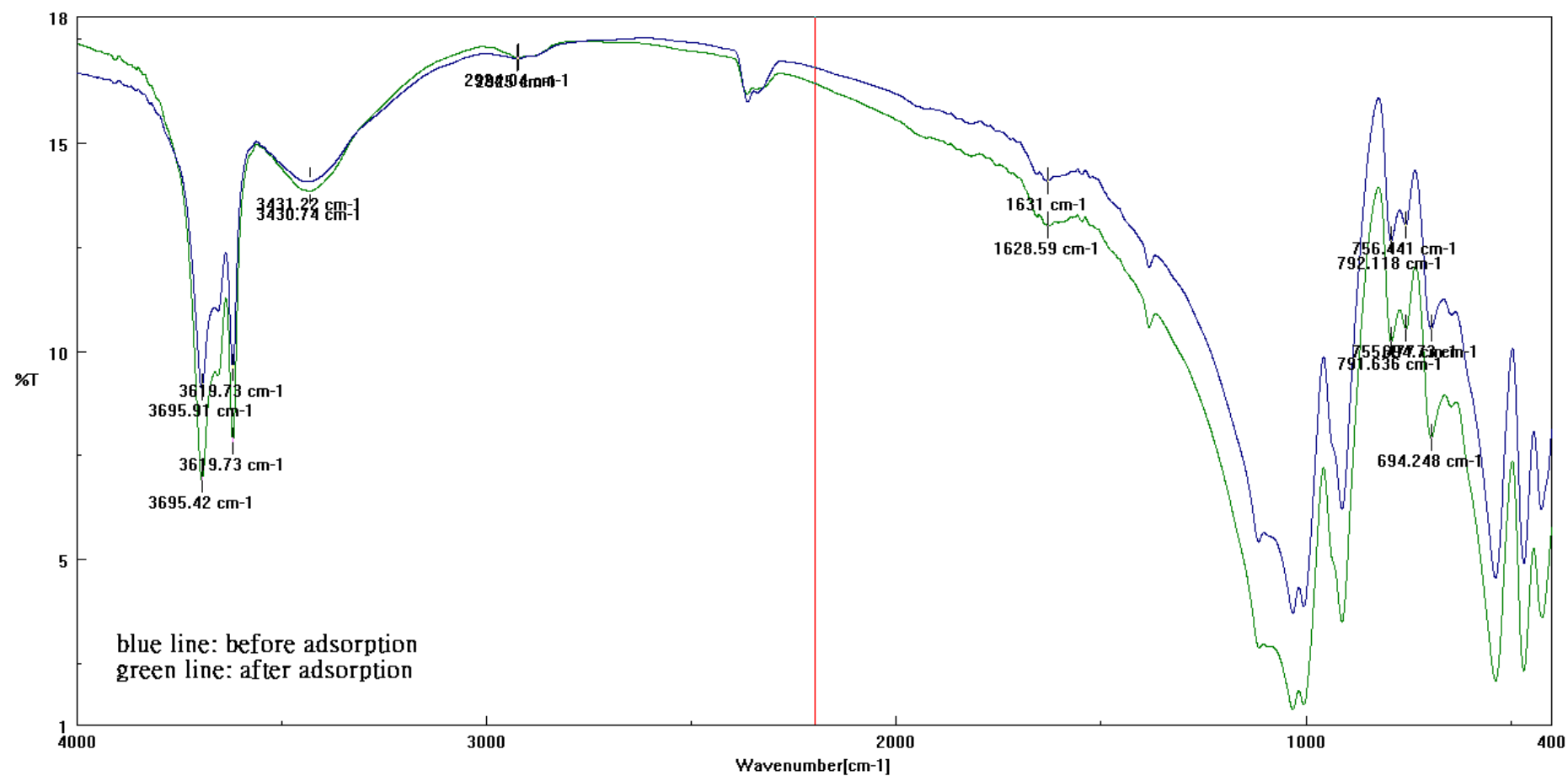


Figure 66. FTIR Spectra of CCK Before And After Adsorption

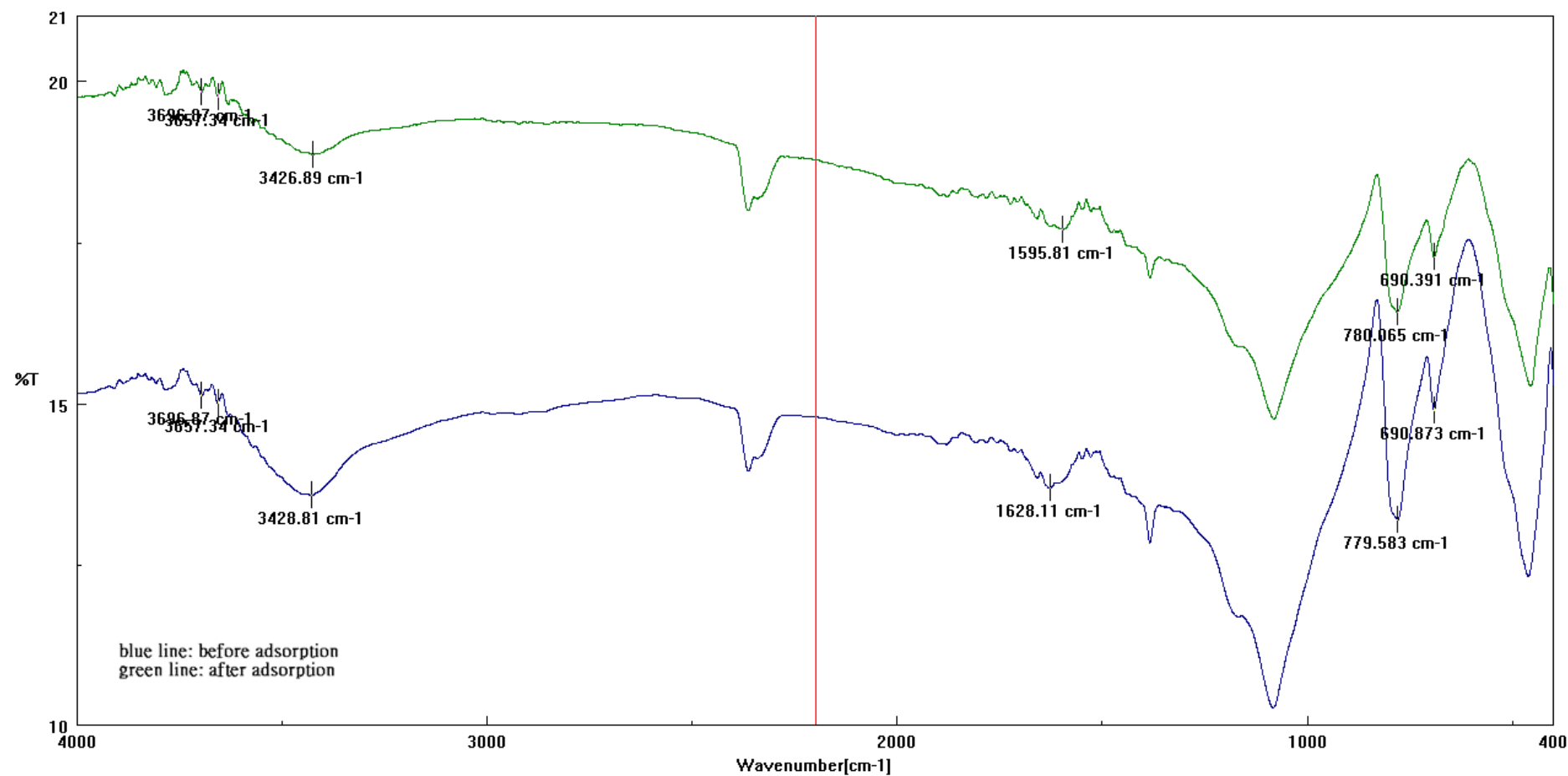


Figure 67. FTIR Spectra of CCS Before And After Adsorption